Title
Bioelectronic Intervention in Cardiovascular Control

Author
Chui, Ray

Publication Date
2017

Peer reviewed|Thesis/dissertation

UNIVERSITY OF CALIFORNIA
Los Angeles

Bioelectronic Intervention in Cardiovascular Control

A dissertation submitted in partial satisfaction of the requirements for the degree
Doctor of Philosophy in Molecular, Cellular and Integrative Physiology

by

Raymond Wai-Keung Chui

2017

ABSTRACT OF THE DISSERTATION

Bioelectronic Intervention in Cardiovascular Control

by

Raymond Wai-Keung Chui
Doctor of Philosophy in Molecular, Cellular and Integrative Physiology
University of California, Los Angeles, 2017
Professor Kalyanam Shivkumar, Chair

The autonomic nervous system (ANS) has a profound influence on cardiac function. Alterations in ANS balance has tremendous impact on the initiation and progression of cardiac pathology. Current standards of care (pharmacology, surgery, devices) have proven efficacy, but well-known limitations as well. Bioelectronic therapy has the potential to provide a reversible, on demand, scalable approach to cardiac control. The hypothesis of this thesis is that imbalances in information processing between different levels of the cardiac neuraxis is a primary determinant in mediating electrical instability of the heart and progression into heart failure. As a corollary, mitigating imposed neural imbalances within the hierarchy for cardiac control is cardioprotective.

To investigate bioelectronic modulation of the parasympathetic control of cardiac pathology, vagal nerve stimulation (VNS) was employed in a guinea pig pressure overload (PO) model of heart failure with preserved ejection fraction (HFpEF). Guinea pigs were subjected to aortic constriction, in the presence or absence of VNS. The effects on disease were assessed in the whole animal (echocardiography) and at the neural (intracellular current clamp recordings of intrinsic cardiac (IC) neurons) and myocyte (protein expression) levels.

To investigate bioelectronic modulation of sympathetic drive to the heart, proof of concept studies involving kilohertz frequency alternating current (KHFAC) and charge-balanced direct current carousel (CBDCC) were employed in an anesthetized porcine model. CBDCC was also used to determine impact on arrhythmia potential in a porcine myocardial infarction (MI) model.

With VNS therapy, PO-induced hemodynamic responses (increased cardiac output, systolic/diastolic left ventricular volumes) were prevented. Enhancements in synaptic efficacy muscarinic sensitivity were also mitigated. Myocyte hypertrophy was prevented using right-sided

VNS. PO-induced hypertrophic myocardium also abnormal energetics, which was modulated with VNS application.

For sympathetic control, KHFAC and CBDCC demonstrated reversible, current-dependent impact on cardiac indices (activation recovery intervals (ARI), heart rate, and contractility). In the MI model, extrasystolic (S1-S2) stimulations induced ventricular arrhythmias in all animals (n=7), whereas right-sided CBDCC application reduced inducibility by 83%. The ventricular effective refractory period (VERP) was prolonged with CBDCC (323±26 ms) compared to baseline (271±32 ms).

In conclusion, the data within this thesis provides validation for a mechanism-based approach to cardiac therapy that combines the potential of bioelectronic therapy with a detailed knowledge of cardiac neuraxis structure/function, addressing a significant unmet need in managing both arrhythmia burden and the progression of heart failure.

The dissertation of Raymond Wai-Keung Chui is approved.

Jeffrey L. Ardell

Yibin Wang

Guy Kember

Kalyanam Shivkumar, Committee Chair

University of California, Los Angeles

2017

DEDICATION

This work is dedicated to my family. Their unwavering love and support have always held me steady. For that, I am eternally grateful.

This work is also dedicated to those who have shared their knowledge, wisdom and insight. By doing so, they have opened my eyes to possibilities in this lifelong journey of learning.

TABLE OF CONTENTS

PREFACE

Chapter 2: A version of this manuscript is published: Beaumont E, Wright GL, Southerland EM, Li Y, **Chui R**, KenKnight BH, Armour JA, Ardell JL. Vagus nerve stimulation mitigates intrinsic cardiac neuronal remodeling and cardiac hypertrophy induced by chronic pressure overload in guinea pig. Am J Physiol Heart Circ Physiol 310: H1349-59, 2016.

Chapter 3: A version of this manuscript is published: Buckley U*, **Chui RW***, Rajendran PS, Vrabec T, Shivkumar K & Ardell JL. Bioelectric neuromodulation of the paravertebral cardiac efferent sympathetic outflow and its effect on ventricular electrical indices. Heart Rhythm 2017 (in press).

Chapter 4: A version of this manuscript currently under review: **Chui RW***, Buckley U*, Rajendran PS, Vrabec T, Shivkumar K & Ardell JL. Bioelectric block of the paravertebral chain stabilizes ventricular electrical function and reduces arrhythmia potential post-myocardial infarction.

* Authors contributed equally.

VITA

Education

University of British Columbia: September 1999 to March 2002, MS

University of British Columbia: September 1993 to April 1998, BS (Hons)

Research and Industry Experience

Neurocardiology Research Center, UCLA: January 2013 to present

Integrated Discovery and Safety Pharmacology, Amgen Inc: December 2006 to present

Safety Pharmacology, Xenon Pharmaceuticals Inc: April 2002 to November 2006

University of British Columbia, Dept. of Pathology: September 1999 to March 2002

Organizational Affiliations

American Heart Association

Safety Pharmacology Society

Publications

1. Buckley U*, Chui RW*, Rajendran PS, Vrabec T, Shivkumar K & Ardell JL. Bioelectric neuromodulation of the paravertebral cardiac efferent sympathetic outflow and its effect on ventricular electrical indices. Heart Rhythm, 2017 (in press).
2. Hamon D, Rajendran PS, Chui RW, Ajijola OA, Irie T, Talebi R, Salavatian S, Vaseghi M, Bradfield JS, Armour JA, Ardell JL, Shivkumar K. Premature ventricular contraction coupling interval variability destabilizes cardiac neuronal and electrophysiological control: insights from simultaneous cardio-neural mapping. Circ Arrhythm Electrophysiol. 10: e004937, 2017.
3. Rajendran PS, Chui RW, Fishbein MC, Hong L, Chang G, Peacock WJ, Yamakawa K, Ardell JL, Shivkumar K, Armour JA. Human cardiac innervation: insights for autonomic neuromodulation (in preparation).
4. Beaumont E, Wright GL, Southerland EM, Li Y, Chui R, KenKnight BH, Armour JA, Ardell JL. Vagus nerve stimulation mitigates intrinsic cardiac neuronal remodeling and cardiac hypertrophy induced by chronic pressure overload in guinea pig. Am J Physiol Heart Circ Physiol 310: H1349-59, 2016.
5. Yagishita D, Chui RW, Yamakawa K, Rajendran PS, Ajijola OA, Nakamura K, So EL, Mahajan A, Shivkumar K, Vaseghi M. Sympathetic nerve stimulation, not circulating

norepinephrine, modulates T-peak to T-end interval by increasing global dispersion of repolarization. Circ Arrhythm Electrophysiol. 8: 174-85, 2015.

6. Derakhchan K, Chui RW, Stevens D, Gu W, Vargas HM. Detection of QTc interval prolongation using jacket telemetry in conscious non-human primates: comparison with implanted telemetry. Br J Pharmacol 171: 509-22, 2014.
7. Chui RW, Derakhchan K, Vargas HM. Comprehensive analysis of cardiac arrhythmias in telemetered cynomolgus monkeys over a 6 month period. J Pharmacol Toxicol Methods. 66: 84-91, 2012.
8. Chowdhury S, Chafeev M, Liu S, Sun J, Raina V, Chui R, Young W, Kwan R, Fu J, Cadieux JA. Discovery of XEN907, a spirooxindole blocker of NaV1.7 for the treatment of pain. Bioorg Med Chem Lett 21: 3676-81, 2011.
9. Qu Y, Fang M, Gao B, Chui RW, Vargas HM. BeKm-1, a peptide inhibitor of human ether-a-go-go-related gene potassium currents, prolongs QTc intervals in isolated rabbit heart. J Pharmacol Exp Ther 337: 2-8, 2011.
10. Chui R, Dorovini-Zis K. Regulation of CCL2 and CCL3 expression in human brain endothelial cells by cytokines and lipopolysaccharide. J Neuroinflamm 7: 1, 2010.
11. Chui RW, Vargas HM. A comparison of three software platforms for automated ECG analysis. J Pharmacol Toxicol Methods 60: 28-38, 2009.
12. Chui RW, Fosdick A, Conner R, Jiang J, Bruenner BA, Vargas HM. Assessment of two external telemetry systems (PhysioJacket and JET) in beagle dogs with telemetry implants. J Pharmacol Toxicol Methods 60: 58-68, 2009.
13. Omari KM, Chui R, Dorovini-Zis K. Induction of beta-chemokine secretion by human brain microvessel endothelial cells via CD40/CD40L interactions. J Neuroimmunol 146: 203-8, 2004.

Book Chapters

1. Rajendran PS, Chui RW, Ajijola OA, Vaseghi M, Armour JA, Ardell JL, Shivkumar K. Neural Control of Cardiac Function in Health and Disease. Dilsizian & Narula (eds): Atlas of Cardiac Innervation. Springer International Publishing, Switzerland, 2017.
2. Chui RW, Rajendran PS, Buckley U, Shivkumar K, Ardell JL. Vagus Nerve Stimulation: Therapeutic Applications for Cardiac Disease. Horch & Kipke (Eds): Neuroprosthetics: Theory and Practice (2nd edition). World Scientific Publishing Co. Pte. Ltd., Singapore, 2017.

CHAPTER 1:

BIOELECTRONIC INTERVENTION IN CARDIOVASCULAR CONTROL

INTRODUCTION

The autonomic nervous system (ANS) plays an important role in all aspects of cardiac function (172). Dogma suggests that reciprocal actions of the sympathetic and parasympathetic arms of the ANS are responsible for cardiac control. However, the data generated over the past few decades suggests a more complex control system (13). Aberrant function of various aspects of this system have been shown to have critical roles in disease initiation and progression (66). Therapeutic approaches, such as pharmacology and surgical intervention at various anatomic locations, have sought to manage symptoms and reverse pathology (172). Despite successes, there are potential liabilities, including off-target pharmacology, hyperalgesia, hyperhidrosis, etc. (75, 142, 183, 203). Neuromodulation, delivered to specific sites within the autonomic nervous system, has the potential to extend beyond current standard of care. Autonomic Modulation Therapy (AMT) is a growing field for site-specific bioelectronic therapeutics for managing the effects of disease and has been evaluated on a number of neural pathways in humans and subject to significant preclinical investigation (35, 101). Depending on the site, electrode/tissue interface and stimulation protocol, electrical intervention has the potential to modulate central neural processing, peripheral neural reflexes and ultimately impact target organ function via modulation of efferent/afferent neural pathways (17, 101, 186, 187, 194). The foundation for this thesis is to understand structure/function of the cardiac nervous system and the mechanisms by which bioelectronic therapy can impact integrated cardiac control in normal and pathological conditions. **This primary hypothesis for this thesis is that imbalances in information processing between different levels of the cardiac neuraxis is a primary determinant in mediating electrical instability of the heart and progression into heart failure. As a corollary, mitigating imposed neural imbalances within the hierarchy for cardiac control is cardioprotective.**

We present herein an experimental approach based on a structure/function understanding of the cardiac nervous system by which electrical stimulation protocols can be applied to specific convergence (nexus) points within that system to mitigate neural imbalances and thereby induce cardioprotection. Within this chapter, our current understanding of the hierarchy for cardiac control will be reviewed as will prior studies with respect to the potential efficacy for cardiac bioelectronic therapeutics. This will be followed by chapters outlining our recent studies utilizing vagus nerve stimulation for preserved ejection heart failure (Chapter 2) and nerve blocking technologies for control of sympathetic projections to the heart, especially in the context of arrhythmia management (Chapters 3 and 4). Chapter 5 will summarize the body of work.

STRUCTURE/FUNCTION OF THE CARDIAC NEURAXIS

Understanding the role of the ANS in cardiac regulation is critical for untangling the complexities of normal physiology and disease development and progression. In order to do this, an appreciation of its organization and anatomy is of utmost importance. Alterations in sympathetic and parasympathetic structure/function/balance have been noted in a number of cardiac diseases and can lead to sudden cardiac death (49, 169). The consequences of an abnormal ANS have been implicated in hypertension, heart failure, cardiac arrhythmias and myocardial infarction (MI), among others (13, 66, 172).

The ANS, consisting of the sympathetic and parasympathetic divisions, modulates cardiac electrical and mechanical function on a beat-to-beat basis (11, 23, 66, 112). Such control reflects neural network interactions mediated by a series of interacting feedback loops from the heart (23) to the insular cortex (77, 138) (Figure 1). Cardiac afferents provide beat-to-beat sensory information about cardiac muscle activity to the cardiac ANS (66). The processing of these afferent neural signals at multiples levels of the hierarchy provides a means to fine-tune regulation of efferent neural signals in normal and altered states (66). Classically, peripheral autonomic ganglia were considered passive relay stations (109), however recent data demonstrates that the cardiac nervous system is an intelligent neural network capable of mult-level reflex processing involving both peripheral and CNS neural circuits (11, 23, 66). These feedback loops include the intrinsic cardiac ganglia, extracardiac intrathoracic ganglia, spinal cord, brainstem and higher centers (11, 23) (Figure 2). The neural circuitry at each level consists of sensory neurons, autonomic motor neurons, and local circuit neurons functioning as neural processors (23). The more peripheral of the control loops (intrinsic cardiac and extracardiac intrathoracic) are primarily concerned with cardio-cardiac reflexes (14, 21, 23, 24). Neural circuits in the CNS (spinal cord, brainstem and above) exert major effects on cardiac function and peripheral blood flow distribution (8, 99, 212). To understand how all these players interact for integrated control of the heart, it is critical that one first evaluates the constituent parts.

PARASYMPATHETIC NERVOUS SYSTEM

The vagus nerve (from the Latin for “wandering”; cranial nerve X), has a role in direct control of cardiac and visceral function (cardiovascular, respiratory and gastrointestinal systems) (109, 155, 191, 202), as well as impacting homeostasis by modulating immune and endocrine function (90, 202). The vagus is bilateral and contains a mix of afferent and efferent

(parasympathetic and sympathetic) projecting axons (140, 156, 168). Vagal preganglionic efferent projections account for 20% of the fibers contained within the cervical vagosympathetic trunk, with the remainder being afferent (4, 61). According to the classification system of Erlanger and Gasser, the vagus nerve contains A-, B- and C-fibers (202). Myelinated A-fibers reflect somatic afferent projections, with the smaller A-fibers transmitting visceral afferent information. Small myelinated B-fibers are primarily postganglionic sympathetic and preganglionic parasympathetic efferent projections. Unmyelinated C-fibers transmit visceral afferent information (36, 159, 202). Afferent axons transduce pain, stretch, pressure, temperature, chemical milieu, and osmolarity from thoracic and visceral organs (26, 36, 202), relaying this information to multiple brain regions (8, 191), from which preganglionic activity is reflexly controlled and projected back to ganglia on cardiac and visceral organs (69, 76, 120, 159). The peripheral autonomic ganglia function as the end-stage processors for controlling organ function (20, 23, 153).

The vagus nerve embryologically represents the nerve of the 4th branchial arch. It arises from the nucleus ambiguous (NA) and dorsal motor nucleus (DMN) of the medulla oblongata (68, 120, 159) as 8 to 10 rootlets, forming a single trunk and exiting the cranium via the jugular foramen. The vagus forms two sensory ganglia, one within the jugular foramen (called the jugular or superior ganglion, giving off the auricular branch of the vagus) and one below (nodose or inferior ganglion) (159). Upon exit from the jugular foramen, the vagus continues down the neck within the carotid sheath. At the level of the nodose, the vagus branches off into the superior laryngeal nerve and pharyngeal branches, which join with branches of the glossopharyngeal nerve and superior cervical ganglion (36, 92, 159). Once the vagus enters the thorax, the right and left nerves differ anatomically, with the right vagus following the origin of the subclavian artery, diverging into the recurrent laryngeal nerve and the main trunk, which travels behind the main bronchus and posterior aspect of the esophagus (36, 92, 159). On the left, the nerve enters the thorax between the left common carotid and subclavian arteries, passing anterior to the aortic arch. The cardiac branches, on the left vagus, arise primarily from the recurrent laryngeal nerve (36, 92, 153, 159). At the heart, preganglionic parasympathetic fibers innervate multiple intrinsic cardiac ganglia, with subsequent postganglionic projections to all four chambers (11, 23). Exiting the thorax through the esophageal hiatus of the diaphragm, the vagus also terminates at various abdominal organs, including the liver, spleen, stomach, pancreas, kidney and intestines (36, 92, 159). Cervical and thoracic projections also contain substantial contributions from sympathetic fibers that arise from interconnections with the

paravertebral sympathetic chain (18, 41, 155). As such, the vagus is a mixed vagosympathetic efferent nerve with major afferent cardio-visceral components (168, 202).

Preganglionic neurons release acetylcholine (Ach) which in turn bind to nicotinic ACh receptors on intrinsic cardiac postganglionic parasympathetic neurons (67, 123, 151). These neurons are contained within ganglia located on atrial and ventricular myocardium, each with preferential spheres of influence (e.g. control of heart rate, speed of cardiac conduction) (11, 46, 154). Histological studies have demonstrated that acetylcholine containing nerves form a complex network innervating the endocardium and epicardium on both ventricles (40, 65). ACh released by postganglionic neurons bind muscarinic (M_2) receptors on cardiac myocytes, inducing decreases in heart rate, speed of electrical conduction and force of cardiac contraction, as well as modulating sympathetic function via sympathetic/parasympathetic interactions (40, 112, 113, 123). In addition to postganglionic parasympathetic neurons, intrinsic cardiac ganglia also contain afferent soma and a major population of local circuit neurons (LCN) (11, 23, 27), which mediate information processing within and between intrathoracic ganglia (23).

Cardiac Parasympathetic Neurons Cardiac parasympathetic preganglionic neurons originate in the NA and DMN and project to postganglionic neurons located in the intrinsic cardiac nervous system (ICNS) (68, 76, 94, 120). The ICNS is a distributed network of neuronal aggregates, termed ganglionated plexi, that are located in atrial and ventricular epicardial tissue (27, 29, 201). ICNS postganglionic soma project axons to all regions of the heart (12, 23, 46). Under physiological conditions, the various pathways are coordinated such that changes in rate are matched by changes in conduction, as a means to minimize the potential for heart block (123, 135, 154). In general, unilateral stimulation of preganglionic inputs leads to relatively equivalent cardiac effects on both sides of the heart and between endo- and epicardium (195). This divergence of control is a result of interplay between different intrinsic cardiac ganglia via interganglionic connections mediated by LCNs (23).

The evoked response to cervical vagosympathetic bioelectronic stimuli reflects the interdependent interaction mediated within neural hierarchy for cardiac control. Low-level cervical VNS results in augmented regional cardiac function, primarily due to afferent mediated withdrawal of central parasympathetic drive (17). Increases in VNS stimulus intensity lead to direct stimulation of descending parasympathetic preganglionic projections to the heart with the expected suppression in cardiac function (16). The point at which afferent mediated withdrawal is balanced against the direct activation of parasympathetic efferent projections is defined at the

neural fulcrum (17). As such, VNS, delivered at the neural fulcrum, engages the cardiac nervous system without major disruptions in cardiac control (17).

Local Circuit Neurons For the cardiac nervous system, LCNs contained within the intrathoracic ganglia are the primary integration points for afferent and efferent processing (23). They are categorized as afferent LCN's and efferent LCN's according to whether they process afferent or efferent (sympathetic and/or parasympathetic) information (23, 32, 150). Convergent LCN's respond to at least one autonomic efferent input and at least one type of sensory input, which can modulate neural activity (23, 32, 150). Importantly, this subclass of neurons are primary targets for neuromodulation therapy (70), including but not limited to spinal cord stimulation and vagal nerve stimulation (15).

Bioelectronic Control of the Parasympathetic Nervous System

In the 1880's, James Leonard Corning created the carotid fork for carotid artery compression to treat epileptic seizures. Later, he would combine carotid compression with transcutaneous electrical stimulation of the cervical vagosympathetic trunk, observing side effects, such as bradycardia, dizziness and syncope (110). Since the late 1930's, a number of groups have evaluated the effect of vagal afferent stimulation on reducing seizures in various animal models (1, 30, 204, 206). Currently, VNS for epilepsy continues to be a standard of care for specific sub-populations of patients (139).

At the current time, a search of active clinical trials (www.clinicaltrials.gov) yields more than 30 VNS studies, treating varied disorders including irritable bowel syndrome, motion sickness, inflammation, arthritis, headache, migraine, diabetes, obesity, appetite suppression, seizure, pain, syncope, heart failure, among others.

VNS Implementation: In general terms, VNS systems can be stratified into implantable vs. transcutaneous devices. For implantable systems, most consist of a wrap-around helical electrode as an interface with the vagosympathetic trunk, connecting to an implantable programmable generator (IPG). Bioelectronic stimulation protocols involves frequency, pulse width, intensity, with a secondary contribution of bipolar orientation (17, 102, 198). The data suggests that optimum stimulus paradigms are target organ specific: e.g. 20-30 Hz is the standard of care for epilepsy (108); cardiovascular indications are well treated in the 5-10 Hz range (88); and VNS efficacy for immune modulation may only require short periods of stimulation (175). Memory is also a significant factor within the neural circuits being impacted

by VNS (98). Finally, while VNS is primarily delivered in an open-loop manner, important strides are being made to close the loop using biomarkers such as heart rate (88).

Emerging technologies for VNS now include non-invasive approaches. These include trans-auricular and trans-cervical methodologies (35). A recent study evaluated respiratory-gated auricular vagal afferent nerve stimulation (RAVANS) in patients with chronic pelvic pain due to endometriosis. This study demonstrated patients experienced reduced pain intensity, temporal summation of mechanical pain and decreased anxiety (131). Bilateral tragus stimulation has been shown to attenuate LV remodeling in canines with healed MI (190) and suppress of atrial fibrillation (AF) in a rapid atrial pacing canine model (200). In patients, Stavrakis et al have shown that auricular stimulation is anti-arrhythmic in patients with paroxysmal AF (174). This latter data initiated a current clinical trial (160).

VNS in Heart Failure: Heart failure (HF) is a complex disorder that manifests itself as impaired ventricular filling or ejection (56), and can be due to issues with the pericardium, various regions of the heart (myocardium, endocardium, valves, coronary vessels) or from certain metabolic abnormalities (196). HF patients can be classified roughly two ways: i) HF with reduced ejection fraction (≤40%, HFrEF); or ii) HF with preserved ejection fraction (≥50%, HFpEF) (196). At the present time, in the United States, it is estimated that HF afflicts 5.1 million people (≥20 years), with projections that the prevalence will increase 46% by 2030, to an estimated 8 million people (71). The costs associated with this are $30.7 billion; that number is balloon to $69.7 billion by 2030 (81). Even with improving care, morbidity and mortality remain high, with median survival times of 1.7 years in men and 3.2 years in women, with the 5-year survival rate being 25% and 38%, for men and women, respectively (83).

Over the course of the past century, it is well known that vagal efferent nerve activity can modulate cardiac function, even in progressive cardiac disease. In mouse models with chronic MI, VNS was able to modulate cardiac redox state, decrease sympathetic drive and suppress free radical production (177). Li et al showed in rat models with chronic MI that 6 weeks of VNS therapy improved pump function and survival (114). Furthermore, short term (e.g. 3 days) VNS delivered 3 weeks after coronary artery ligation in a rat model attenuated cardiac remodeling and improved cardiac excitation-contraction coupling (116). In canine models of HF, VNS improved left ventricular function and various other cardiac indices in response to tachy-pacing (208), intracoronary microembolizations (78), and chronic mitral regurgitation (199). More recent data has suggested that even low level VNS stimulation (inducing minimal HR changes) using

invasive (34) and non-invasive (bilateral transcutaneous stimulation of the auricular branch) (189) methods can reduce disease burden in HF (33, 34).

From a clinical perspective, abnormal autonomic balance has been recognized as a factor in increased mortality in myocardial infarction and heart failure (64). The progression of HF is associated with a shift in the autonomic balance towards increased sympathetic with reduced centrally mediated parasympathetic activity (87, 212). In moderate to severe chronic HF, decreased sensitivity of vagal reflexes is significantly associated with poor prognosis (125). The Autonomic Tone and Reflexes After Myocardial Infarction study (ATRAMI) and the Cardiac Insufficiency Bisprolol Study II (CIBIS II) showed that decreased vagal activity positively correlated with increased mortality (107, 111). By restoring parasympathetic drive with VNS, excessive sympathoexcitation is mitigated and myocytes rendered stress resistant (33, 34, 170, 171). Despite this, results from recent trials of VNS for HF have been equivocal, likely due to stimulation paradigms and patient selection, in part.

CardioFit was a Phase II feasibility study conducted using the CardioFit system, an implantable system, consisting of an asymmetric bipolar stimulating cuff with electrodes for on-phase partial anodal block and a cardiac lead for R wave detection (52, 167). An initial study with 8 patients (left ventricular ejection fraction (LVEF) <35%, New York Heart Association (NYHA) class II-III) showed improvement in NYHA class, quality of life (QOL), left ventricular end-systolic volume and a trend towards reduction of left ventricular end-diastolic volume (167). A subsequent larger study was conducted to assess safety and tolerability involved patients (n=32) with NYHA class II-IV patients and LVEF (23 ±8%) (52, 53). Most patients improved at least one NYHA class at 3 (18/32 patients) and 6 months (19/32 patients), with similar improvements in QOL and 6-minute walk tests. These results suggested that chronic VNS was feasible and warranted further clinical investigation (52, 53).

Increase of Vagal TonE in Heart Failure (INOVATE-HF) evolved from the Cardiofit trial. The primary efficacy endpoint was defined as whether VNS increased the time to first event defined by all-cause mortality or unplanned HF hospitalization. The study consisted of 650 symptomatic HF patients NYHA class III, LVEF <40% (80) and was initiated in February 2011 with an estimated conclusion by December 2016 (clinicaltrials.gov site). In 2015, the independent Data Safety Monitoring Board for the INOVATE-HF trial completed a pre-specified interim analysis of the data and recommended the discontinuation of the INOVATE-HF trial due to statistical futility in the primary efficacy endpoint. Final analysis demonstrated that the death rate of patients from chronic HF was not reduced by VNS (72).

NEural Cardiac TherApy foR Heart Failure (NECTAR-HF) was a double-blind, multi-center randomized control study to evaluate safety and efficacy in patients, with NYHA class II-III symptoms and LVEF ≤ 35% (55). LV end systolic diameter (LVESD), echocardiographic parameters and N-terminal brain natriuretic peptide (NT-proBNP) failed to show significant differences from the control group. However, quality of life, NYHA classification and health surveys showed significant improvement (207). These findings were unexpected based on previous trials and preclinical data. However, off-target effects evoked during the on-phase (20 Hz) stimulation limited current delivery and may have placed these patients at sub-therapeutic levels (207).

Autonomic Neural regulation Therapy to Enhance Myocardial function in Heart Failure (ANTHEM-HF) was an open loop feasibility study to assess safety and efficacy of the bipolar VNS delivered to the right or left cervical vagus. Patients had NYHA class II-III and LVEF ≤ 40% (57). After 6 months of VNS therapy, LVEF (both sides) improved significantly (4.5%), but LVESV was not statistically significant. NYHA, 6-minute walk and QOL all showed significant improvements. There were no statistical differences between right and left VNS (147). 49 patients participated in an extended follow-up (to 1 year) showed maintenance of results from the 6-month time point, with LVESV now achieving significance from baseline (148). In these same patients, VNS reduced peak T-wave alternans levels, HR and non-sustained ventricular tachycardias (VT). HR turbulence slope, high frequency power and HR variability all increased (2). For ANTHEM-HF, the VNS protocol was based on the neural fulcrum approach (17).

VNS Control of Cardiac Arrhythmias: It is estimated that sudden cardiac death (SCD) accounts for 4 to 5 million cases annually, worldwide (49, 210). SCD can be broadly categorized into electrical and nonelectrical in nature. For electrical causes of SCD, the majority is associated with ventricular tachyarrhythmias (including ventricular fibrillation) and, to a lesser degree, bradyarrhythmias (31). Altered autonomic control, superimposed on an abnormal cardiac myocyte substrate, is fundamental to the induction of cardiac arrhythmias (66, 184).

Bioelectronic stimulation, delivered to various elements of the cardiac nervous system, has the potential to increase or decrease atrial arrhythmogenesis (48, 129, 133). Simultaneous sympathetic and parasympathetic nerve stimulation can trigger rapid firing within canine pulmonary veins, frequently a precursor to AF (144). Conversely, VNS has been shown to alter the electrophysiological properties of the rat atrium (193), improving left atrial (LA) function, and suppressing LA fibrosis in a canine tachy-pacing model (106). Though the specific neurotransmitters released during neurally-induced AF remains poorly defined, it is likely that

adrenergic, cholinergic and peptinergic receptors are important players (28, 48, 158). VNS-induced release vasoactive intestinal polypeptide (VIP) is one potential candidate (197). In contrast to arrhythmia control with intrinsic cardiac ganglia ablation, VNS can engage multiple ganglia targets on the heart simultaneously (32, 150). For example, VNS can prevent AF in canines triggered from both PV and non-PV sites (115). A likely mechanism is VNS-mediated anti-adrenergic effects and stabilization of reflex processing within the intrinsic cardiac nervous system (70, 98, 123, 151).

Ventricular arrhythmias, especially ventricular tachycardia, are potentially life threatening. VNS has been demonstrated to impact ventricular function and prevent ventricular arrhythmias in a number of preclinical models. Right and left vagi project to both ventricles in a similar manner, on both the endocardial and epicardial surfaces (195). The anti-fibrillatory effects of VNS have a long-standing clinical history. Einbrodt, in 1859, demonstrated that it was more difficult to induce VF in a dog during vagal stimulation (40, 58). Later studies supported Einbrodt's early findings (73, 128, 163). Cardioprotective properties of VNS were shown to be due in part to modulation of sympathetic-parasympathetic interactions (103). Recent studies have shown that pre-emptive VNS limits infarct size in pigs with transient myocardial ischemia (179) and increase the ventricular fibrillation threshold in canines even in models with enhanced sympathetic drive induced by stellate stimulation (87). VNS can suppress VT/VF in chronic MI, even when animals are subjected to exercise and a second ischemic event (182). In rats with healed MI, VNS suppressed the incidence of premature ventricular contractions (PVC) and increased the high frequency component of HRV (209). Furthermore, even intermittent VNS was efficacious by significantly reducing infarct size and incidence of VF episodes in a porcine model of ischemia-reperfusion injury (171). A follow-up study showed that VNS initiated late in ischemia was still effective in inducing cardioprotection, but was ineffectual if applied after reperfusion (170). VNS-induced remodeling of peripheral neural networks and their link to cardiac mechanical and electrical function (33, 34, 78), as well as changes in myocyte function are important factors in mediating cardioprotection (34, 48, 164, 170, 171). Galanin (82), neuropeptide-Y (82), and nitric oxide (9, 39) are all thought to be involved. A potential link to the α-7 nicotinic anti-inflammatory pathway may also be of importance (43, 145).

In the clinic, VNS can either promote or suppress the potential for cardiac arrhythmias depending on the underlying pathology. Some arrhythmia types are triggered by increased parasympathetic activity, including early repolarization syndrome (104), subgroups of idiopathic VT (95), Brugada (10), and LQT3 (60, 88). Non-invasive VNS (auricular branch) may serve as an effective screening to determine efficacy prior to implant. In healthy humans, trans-

cutaneous VNS shifted autonomic balance towards parasympathetic predominance (50). In patients with coronary artery disease, auricular VNS reduced sympathetic outflow to the heart and improved LV contractility (205). In patients with drug-resistant focal epilepsy, VNS reduces incidence of T-wave alternans and low frequency HRV components, signaling a reduction in electrical instability and a shift towards increased parasympathetic tone (165). In patients with refractory epilepsy, a significant increase in the high frequency component and reduction in low frequency was noted (42). TREAT-AF (transcutaneous electrical vagus nerve stimulation to suppress atrial fibrillation) is a current clinical trial designed to examine the potential of low level tragus stimulation to reduce atrial fibrillation (AF) burden and suppress inflammatory cytokines in patients with paroxysmal AF (160).

SYMPATHETIC NERVOUS SYSTEM

Sympathetic preganglionic neurons innervating the heart originate in the intermediolateral (IML) region between the T1-T4 segments of the spinal cord (188), receiving inputs from glutamatergic neurons of the rostral ventrolateral medulla (RVLM) in the medulla (141). Preganglionic neurons travel through the ventral rami and synapse on postganglionic neurons contained primarily within extracardiac intrathoracic ganglia (paravertebral chain and mediastinum), which include the stellate ganglia (105), superior and middle cervical (19), mediastinal (25) and intrinsic cardiac ganglia (23). Postganglionic fibers from these ganglia innervate the atrial/ventricular myocardium and coronary vasculature (89, 97). Preganglionic neurons release acetylcholine, which binds to nicotinic acetylcholine receptors on postganglionic neurons. Postganglionic neurons release norepinephrine, which binds to alpha- and beta-adrenergic receptors within the cardiac myocardium and vasculature, initiating signal transduction pathways that include G proteins, cyclic adenosine monophosphate and protein kinase A, resulting in changes in chronotropy, dromotropy, inotropy and lusitropy (74). Cardiac “sympathetic” afferent signals are transmitted to the CNS via bipolar neurons with cell bodies in the dorsal root ganglion (DRG), which have peripheral axons projecting to the heart and central axons projecting to the dorsal horn of the spinal cord (26).

Anatomically, within the thorax, as the paravertebral sympathetic chain proceeds cranially, the T1 and inferior cervical ganglia fuse forming the stellate ganglion (SG). The ventral and dorsal ansa subclavia sprout from the stellate, wind around the subclavian artery and converge on the middle cervical ganglia (MCG). The dorsal ansa can be absent on one or both sides due to merging of the stellate and inferior portion of the middle cervical ganglia (89). The SG and the MCG contain most of the postganglionic sympathetic neurons that innervate the heart (84). In

addition to the heart, sympathetic postganglionic fibers contained in the extracardiac intrathoracic ganglia innervate the esophagus, trachea, bronchi, as well as other structures in the head and neck (188). Multiple cardiopulmonary nerves (CPNs) also run lateral to the trachea as they course to the base of the heart (89). Sympathetic CPNs have been found to arise from the stellate ganglia and cervical sympathetic trunk below the level of the cricoid cartilage (89).

Cardiac Sympathetic Neurons As mentioned previously, cardiac sympathetic preganglionic neurons originate in the IML cell column of the T1-T4 segments of the spinal cord and project to postganglionic neurons located in the stellate (105), middle cervical (19), mediastinal ganglia (25) and intrinsic cardiac ganglia (23). Activation of sympathetic projections to the heart results in increases in chronotropy, inotropy, dromotropy and lusitropy (152, 155, 185). There is stratification in sympathetic projections, with unilateral predominance, but with the potential for bilateral control of all regions of the heart (18, 112, 185). Importantly, the intrinsic cardiac ganglia mediate major sympathetic/parasympathetic interactions to compliment the well-recognized pre- and post-junctional interactions mediated at the nerve-cardiac myocyte end-terminus junction (67, 123, 151).

Cardiac Sensory Neurons Cardiac afferent neurons transduce the chemical and/or mechanical milieu of myocardial tissue (26). The cell bodies of cardiac-related afferent neurons are located in the nodose, intrathoracic ganglia and DRG (26). Bipolar neurons in the nodose have peripheral projections to sensory neurites in all regions of the heart and central projections to second-order neurons in the nucleus tractus solitarii (NTS) of the medulla (8, 191), modulating efferent parasympathetic neurons located in the NA and DMN (68, 76, 120, 191). These can also impact sympathetic outflow via the brainstem reticular formation and reticulospinal projections to sympathetic preganglionic fibers within the IML (62, 94). Bipolar neurons in the DRG have peripheral projections to the heart and central projections to the dorsal horn of the spinal cord (62, 94). These second-order neurons modulate the activity of efferent sympathetic neurons in the IML cell column of the spinal cord (94) with major effects mediated by spinal reticular projections to brainstem cardiovascular control sites including the NTS that are reflected back to the spinal cord via reticulo-spinal projections to the IML (8, 62, 63, 191). While the nodose and DRG are the dominant locations of cardiac afferents, afferent neurons have also been identified in the intrinsic cardiac and extracardiac intrathoracic ganglia (14, 22, 23,

26). This afferent input can mediate control of local cardiac reflexes independently of the CNS (11, 23).

Neuromodulation of Cardiac Sympathetic Drive

Remodeling of cardiac and extra-cardiac nerves has been demonstrated in experimental cardiac injury models (7, 44, 45). Electrophysiological changes within and beyond the infarct zone has been reviewed (184). In experimental ischemic heart disease, neural remodeling is heterogeneous and hyperadrenergic (44, 45), with re-innervation occurring after MI, as new nerve sprouts are observed at the border zones (44, 45). This creates a neuronal milieu that may increase arrhythmogenesis and the risk of sudden cardiac death. Additional preclinical data from canines with tachypacing-induced AF demonstrated increased heterogeneous pattern and density of atrial sympathetic innervation (47, 91). These findings were confirmed in human biopsy samples from patients undergoing coronary bypass surgery, who experienced AF (132). Furthermore, in cardiac disease, alterations to the structure, neurotransmitter profile and cellular function at the level of intrathoracic ganglia, brainstem and higher centers have also been characterized (172). While beyond the scope of this introductory chapter, such changes in central-mediated reflexes are a major factor in setting up the imbalance in neural processing with the cardiac nervous system that underlies the progression of cardiac disease (13, 66, 172).

From a clinical treatment perspective, pharmacological approaches can reduce arrhythmia burden, but can also be pro-arrhythmic when there are ischemic challenges (149). Implantable cardioverter defibrillators (ICDs) are effective in reactively treating ventricular arrhythmias but are not preventative (149). Furthermore, ICD shocks are known to decrease the quality of life, correlate with poor prognosis and increase mortality (127). Catheter ablation is an effective treatment in patients with ventricular arrhythmias, but subsets of individuals remain unresponsive to all the aforementioned approaches (178). For these patients, surgical approaches aimed at attenuating sympathetic drive, such as thoracic epidural anesthesia (acutely) and bilateral cardiac stellate decentralization (BCSD, chronically), have shown efficacy for reducing arrhythmic events (38, 166, 183). Both therapeutic approaches are predicated on reducing conflict between central and peripheral aspects of the cardiac nervous system.

Thoracic Epidural Anesthesia/Stellate Ganglion Blockade: For patients with sympathetically triggered arrhythmias, short term relief can be obtained via high thoracic epidural anesthesia (TEA) or left stellate ganglion block. Percutaneous administration of local anesthetics to the T1-T5 spinal segments can block both afferent and efferent sympathetic signaling of the left and

right spinal roots. This has been demonstrated in patients with ventricular tachycardia refractory to pharmacology/ablation (38, 118) and patients undergoing lung surgery by reducing postoperative supra-ventricular tachyarrhythmias (136). These anti-arrhythmic properties are mediated by increasing repolarization and prolongation of refractory periods (124). In patients with ischemic cardiac disease, TEA can reduce pain and preserve coronary perfusion, particularly in stenotic vessels (134, 137).

LSG block is also an acute anti-arrhythmic procedure mediated by percutaneous administration of local anesthetics, which, similar to TEA, reduces sympathetic drive to the heart (117, 130, 143). The non-specific nature of LSG block by local anesthetics typically attenuates conduction to not only the heart, but the head, neck and diaphragm as well. This would preclude bilateral application, unless patient is ventilated (172).

Cardiac Sympathetic Decentralization: Cardiac sympathetic decentralization (CSD) involves surgical resection of the caudal half of the stellate ganglion and T2-T4 thoracic ganglia (5, 183). Though this approach was first used a century ago, CSD has re-emerged as a viable treatment for recurrent ventricular tachycardia and channelopathies in the past 50 years (54, 59, 126, 192, 211). The underlying mechanism behind this approach is the reduction in norepinephrine release in the ventricles, mitigating arrhythmic potential by decreasing repolarization heterogeneity and increasing ventricular fibrillation threshold (79, 166). This, in effect, eliminates conflicts between central and peripheral reflex data, resulting in a more stable myocardium. In patients with structural heart disease and refractory VT, unilateral or bilateral CSD is emerging as a viable option, as approximately 30-50% experience recurrent arrhythmias and ICD shocks despite pharmacological/ablation interventions (5, 38, 183).

BCSD, while effective in ventricular arrhythmia management (183), is permanent and often accompanied by undesired off-target effects including hyperalgesia and hyperhidrosis (75, 142, 203). Thus, a major unmet need is to impact neural control of cardiac function with a targeted, rapid, reversible and scalable modality that is safe for autonomic nerves and that ultimately can be deployed chronically. Bioelectronic therapy has the potential to impact multiple levels of the cardiac neuraxis and reduce disease pathology, via both direct and indirect control.

Bioelectronic Block: The first report of electrical inhibition of action potential conduction was the use of direct current (DC) by Pfluger in 1858 (reviewed in (101)). Since then, there have been numerous different strategies employed to enable nerve block, including DC, monophasic high frequency, neurotransmitter depletion, kilohertz frequency alternating current (KHFAC),

and radiofrequency (RF) ablation (101). The two most promising approaches are KHFAC (101) and DC (186, 187).

Preclinically, KHFAC has demonstrated rapid efficacy and reversibility in a number of models using somatic nerves (101). Clinically, the first demonstration of KHFAC conduction block was on the musculocutaneous nerve (101). Since then, a number of studies have been completed, including vagal block for obesity control (VBLOC, Enteromedics, (162)), sciatic nerve block for amputee pain relief (173), and thoracic spinal cord for back pain (Nevro Corp, (181)). While KHFAC is efficient in long-term suppression of axon nerve activity, an onset response is evoked when first initiated and that response can last up to many seconds (100, 101). The onset response results from asynchronous fiber stimulation before block is established in these same axons (37, 93). This onset response is a potentially significant barrier for clinical applications of KHFAC (Figure 3). Particularly for sympathetic nerves, this would translate into an abrupt sympatho-excitation, which could have catastrophic consequences when applied against a pathologic cardiac electrophysiological substrate (6, 66, 184).

Direct current likewise has the capability to block nerve conduction (186, 187) and has demonstrated efficacy in studies on the sciatic (146), saphenous (119) and sural nerves (3), dorsal roots (121), vagus (51, 85, 86, 176) and phrenic nerves (161). DC can be delivered in a charge-balanced mode (CBDC), consisting of a cathodic current phase necessary for nerve block, followed by an anodic current recharge phase, with the net current delivery to the tissue being zero (186) (Figure 4). To prevent nerve activation in transition phases (baseline-block-recharge-baseline), current ramps are used instead of step changes (96, 146). These current ramps mitigate the potential for onset sympatho-excitation with DC application.

CBDC control of nerves fulfills the need for rapid onset and scalability, but from a single node it is limited by duration, due to the potential creation of toxic reactants at the electrode-nerve interface (122, 157, 186, 187). This potential can be mitigated in part by using interfaces with high effective surface area electrodes and by the CBDC waveform (186) (Figure 4). Even with such measures, from a single node, CBDC can be safely applied for ~10 seconds during the blocking phase and then only with a 10% duty cycle (e.g. block 10% of time) (186). This would limit its potential utility in cardiac arrhythmia management (66, 172, 184). This temporal design constraint can be overcome by adding CBDC nodes in series and interlacing the stimulation waveforms (186). By such approaches, the duty cycle for CBDC can be increased up to 100% and functional blocking phase increased to minutes (186). This approach is referred to as CBDC carousel (CBDCC) and has been validated in a rat sciatic nerve preparation (Figure 5).

Usage of bioelectronic methodologies to manage sympathetic drive to the heart is unexplored at this stage, however the potentials could revolutionize cardiac therapy. Usage of KHFAC could have potential limitations due to onset sympatho-excitation, which could promote arrhythmogenesis. The CBDCC approach may mitigate this limitation.

THESIS OBJECTIVES

It is well known that alterations in sympathetic/parasympathetic balance can have adverse effects on the heart. This manifests itself in disease initiation and progression. The overall hypothesis of this thesis is that imbalances in information processing between different levels of the cardiac neuraxis is a primary determinant in mediating electrical instability of the heart and progression into heart failure. Having a clear understanding of the structure/function of the cardiac neuraxis enables us to employ a more intelligent approach to applying therapeutic methodologies. In addition, mitigating alterations in autonomic balance and the potential impact on central/peripheral interactions is cardioprotective. A mechanism-based approach to cardiac therapy that marries the potential of bioelectronic therapy (reversible, on demand, scalable, etc.) with an intimate knowledge of cardiac neuraxis structure/function addresses a significant unmet need for patients.

The objectives of this thesis are to evaluate the potential for using bioelectronic methodologies to impact acute/chronic disease initiation and progression:

1. HFpEF is the most common form of HF in patients > 65, yet standard of care is suboptimal and specific mechanisms of pathophysiology are poorly defined (180). Heart failure results in a shift in autonomic balance towards sympatho-excitation with a corresponding reduction in parasympathetic control. We hypothesize that VNS will mitigate the maladaptive pathology associated with pressure overload, doing so by reverse remodeling of the ICNS and by rendering myocytes stress-resistant. For this objective, chronic pressure overload will be induced in a guinea pig model with and without reactive VNS.
2. Excessive sympatho-excitation is a primary determinant of the arrhythmogenic potential of the diseased heart. Objective two focuses on defining critical aspects of axonal modulation therapy (AMT) using either KHFAC or CBDCC with respect to modulating sympathetic drive to the heart. For this objective, we will evaluate the efficacy of AMT applied to the T1-T2 paravertebral chain to alter baseline and evoked cardiac response to activation of primary preganglionic sympathetic projections to the heart. These

studies are conducted in the anesthetized porcine model and with high density mapping of cardiac electrical function.

3. For the final objective, we hypothesize that disruption of central/peripheral neural network processing within the cardiac nervous system is a primary determinant of increased proarrhythmic potential in the infarcted heart. As a corollary, reducing this conflict should reduce the arrhythmia potential. Using a bioelectronic approach, we propose to reverse this imbalance in autonomic control and thereby stabilize the heart, thus decreasing the arrhythmia burden. For this objective, chronic myocardial infarction will be induced in porcine models and the efficacy of acute AMT to reduce the arrhythmia burden will be assessed in terminal experiments.

FIGURES

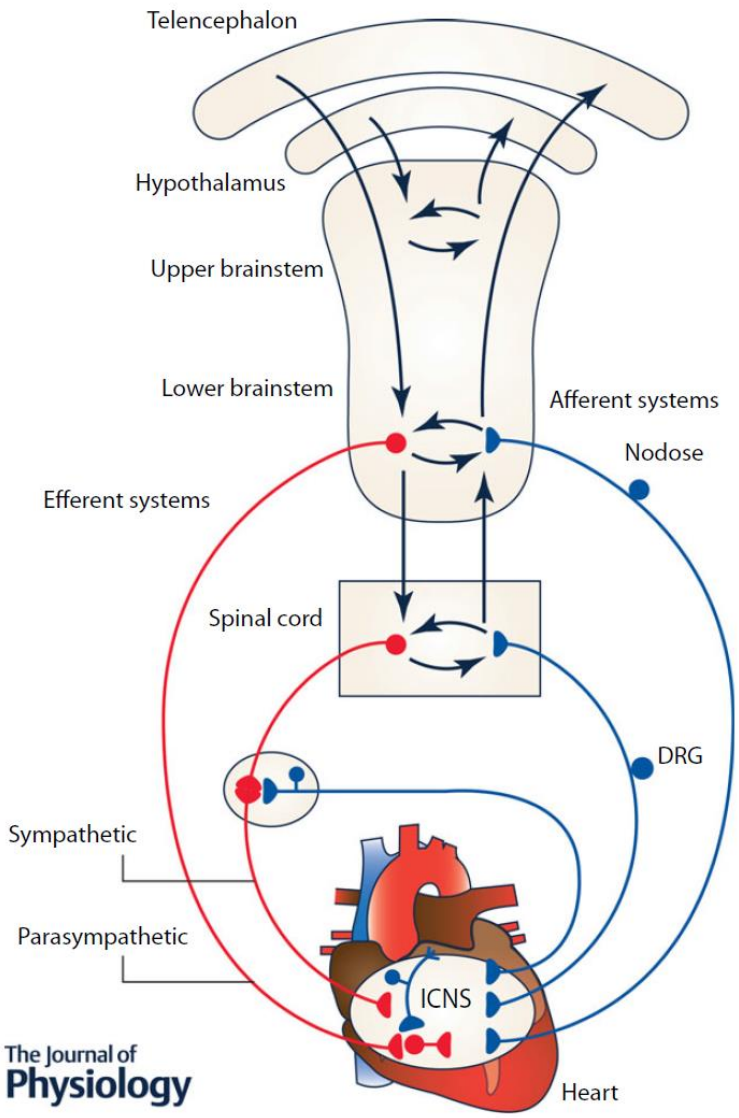

Figure 1: Schematic showing cardiac neurotransmission pathways. Red lines denote efferent and blue lines denote afferent pathways. DRG: dorsal root ganglion; ICNS: intrinsic cardiac nervous system. (172, 188).

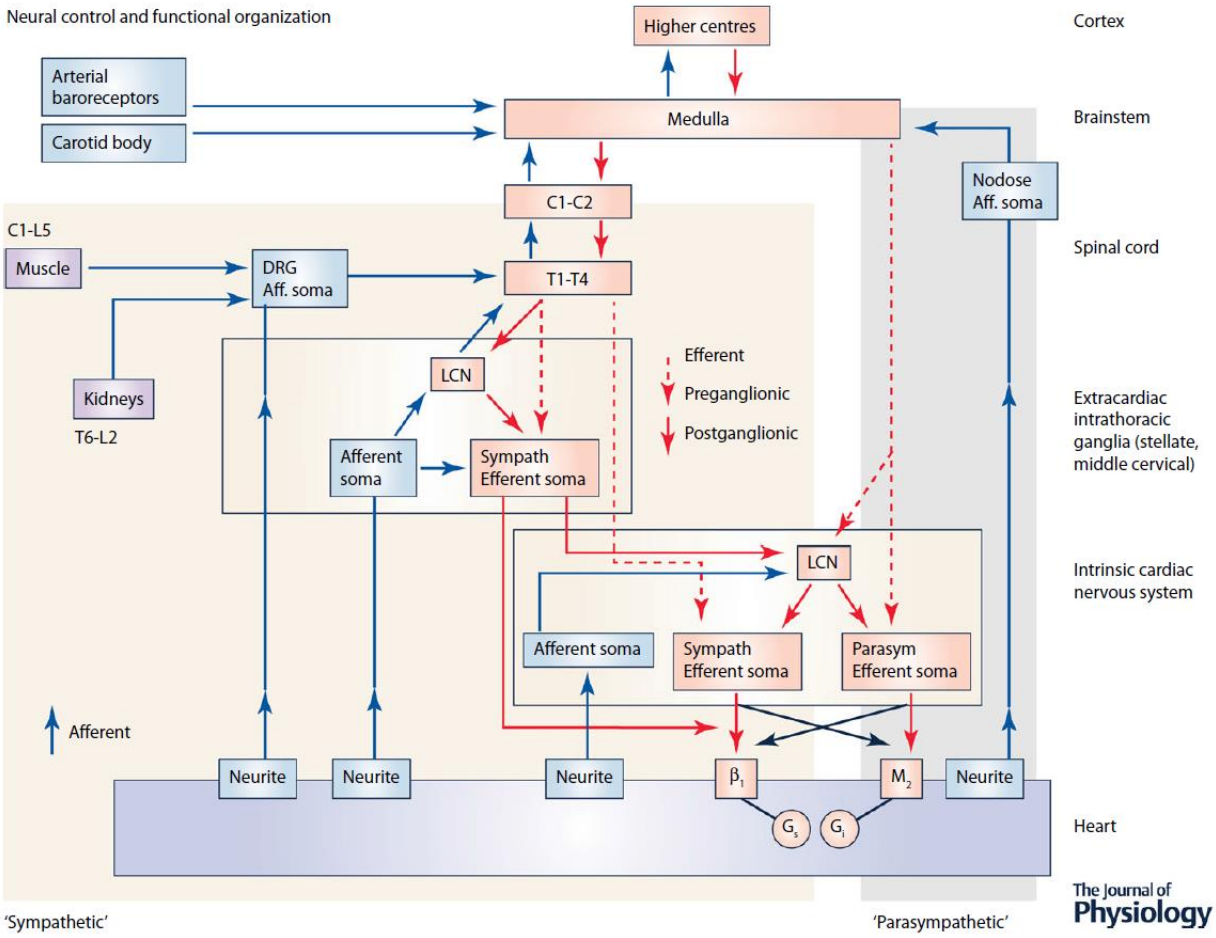

Figure 2: Schematic illustrating the functional organization of the cardiac neuraxis. Afferent projections are shown with blue lines and efferent projections are shown with red lines (dashed: preganglionic; solid: postganglionic). Abbreviations: DRG – dorsal root ganglion; LCN – local circuit neurons; β_1 – β_1-adrenergic receptor; M_2 –muscarinic acetylcholine receptor M2; G_s – G_s alpha subunit; G_i – G_i alpha subunit (172).

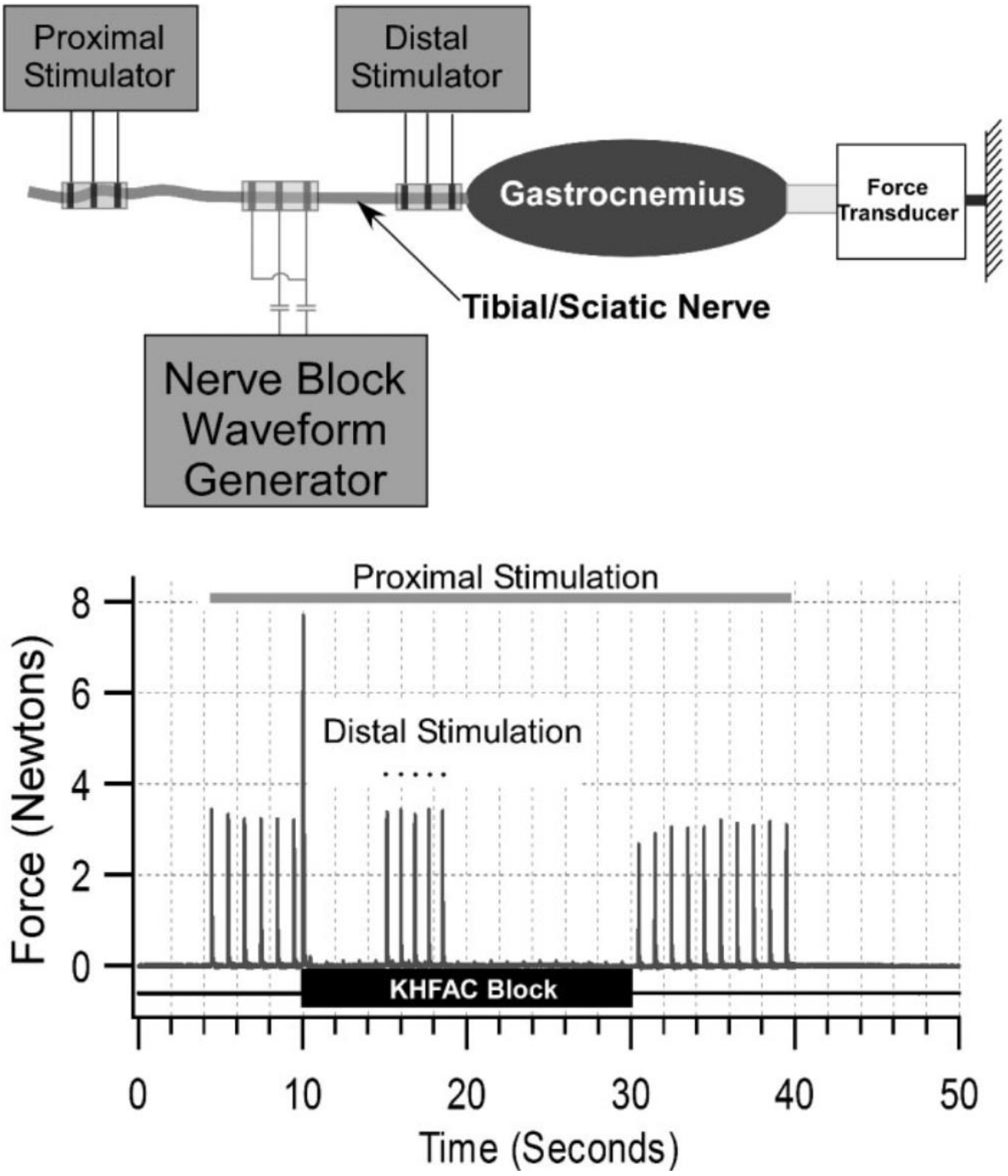

Figure 3: Typical KHFAC response in rat sciatic nerve preparation. Top panel illustrates a typical experimental setup. Bottom panel shows complete suppression of nerve conduction is achieved after a brief increase on motor contraction (onset sympatho-excitation) at KHFAC block (black bar). Proximal stimulation is shown with grey bar. Distal stimulation shows a responsive neuromuscular junction, demonstrating the local nature of the conduction block (101).

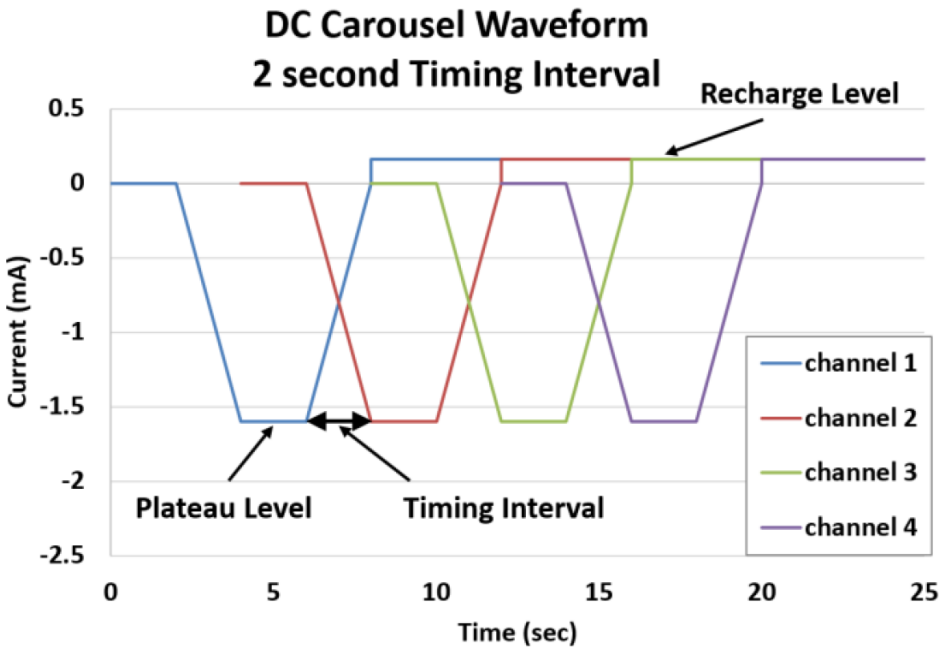

Figure 4: Schematic demonstrating a CBDCC waveform with interlaced waveforms from 4 channels (186).

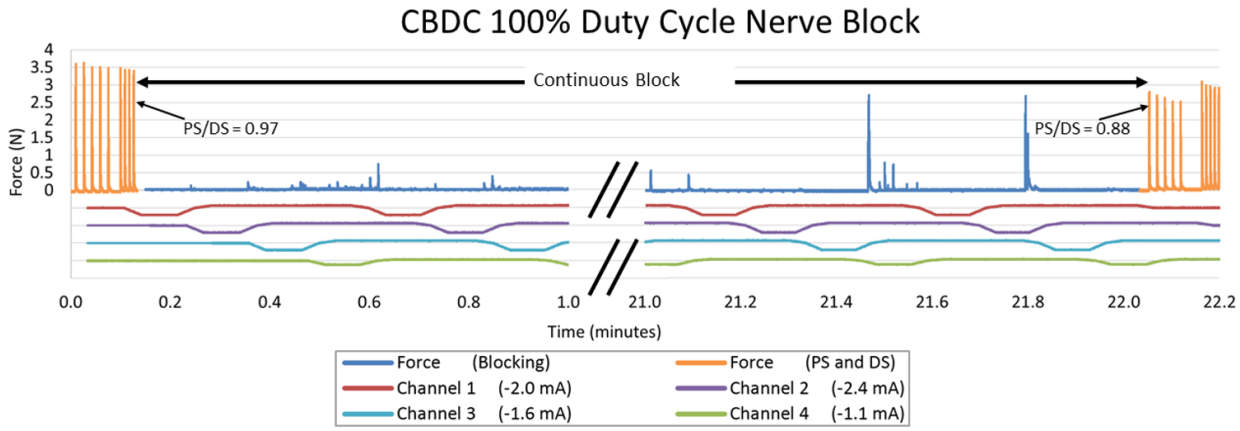

Figure 5: Continuous CBDCC block of the rat sciatic nerve. 100% duty cycle block was employed using sequential cycling of four contacts, for a total continuous duration of up to 22 mins (45 cycles). Force output is shown in blue. The ratio of proximal and distal stimulations (PS/DS) was calculated to determine if nerve conduction was affected by block. As in figure 3, the proximal stimulation point assesses block efficacy, whereas distal stimulation point bypasses block position (186).

REFERENCES

1. Aalbers M, Vles J, Klinkenberg S, Hoogland G, Majoie M, and Rijkers K. Animal models for vagus nerve stimulation in epilepsy. *Experimental neurology* 230: 167-175, 2011.
2. Abdala AP, McBryde FD, Marina N, Hendy EB, Engelman ZJ, Fudim M, Sobotka PA, Gourine AV, and Paton JF. Hypertension is critically dependent on the carotid body input in the spontaneously hypertensive rat. *J Physiol*590: 4269-4277, 2012.
3. Accornero N, Bini G, Lenzi GL, and Manfredi M. Selective Activation of peripheral nerve fibre groups of different diameter by triangular shaped stimulus pulses. *J Physiol* 273: 539-560, 1977.
4. Agostini E, Chinnock JE, De Burgh Daly M, and Murray JG. Functional and histological studies of the vagus nerve and its branches to the heart, lungs and abdominal viscera in the cat. *J Physiol*135: 182-205, 1957.
5. Ajijola OA, Lellouche N, Bourke T, Tung R, Ahn S, Mahajan A, and Shivkumar K. Bilateral cardiac sympathetic denervation for the management of electrical storm. *Journal of the American College of Cardiology* 59: 91-92, 2012.
6. Ajijola OA, Yagishita D, Patel KJ, Vaseghi M, Zhou W, Yamakawa K, So E, Lux RL, Mahajan A, and Shivkumar K. Focal myocardial infarction induces global remodeling of cardiac sympathetic innervation: neural remodeling in a spatial context. *Am J Physiol Heart Circ Physiol*305: H1031-1040, 2013.
7. Ajijola OA, Yagishita D, Reddy NK, Yamakawa K, Vaseghi M, Downs AM, Hoover DB, Ardell JL, and Shivkumar K. Remodeling of stellate ganglion neurons after spatially targeted myocardial infarction: Neuropeptide and morphologic changes. *Heart Rhythm* 12: 1027-1035, 2015.
8. Andresen MC, Kunze DL, and Mendelowitz D. Central Nervous System Regulation of the Heart. In: *Basic and Clincial Neurocardiology*, edited by Armour JA and Ardell JL. New York: Oxford University Press, 2004, p. 187-219.
9. Annoni EM, Xie X, Lee SW, Libbus I, KenKnight BH, Osborn JW, and Tolkacheva EG. Intermittent electrical stimulation of the right cervical vagus nerve in salt-sensitive hypertensive rats: effects on blood pressure, arrhythmias, and ventricular electrophysiology. *Physiological reports* 3, 2015.
10. Antzelevitch C. Brugada syndrome. *Pacing and clinical electrophysiology : PACE* 29: 1130-1159, 2006.

11. Ardell JL. Intrathoracic neuronal regulation of cardiac function In: *Basic and Clinical Neurocardiology*, edited by Armour JA and Ardell JL. New York: Oxford University Press, 2004, p. 118-152.
12. Ardell JL. Structure and function of mammalian intrinsic cardiac neurons. In: *Neurocardiology*, edited by Armour JA and Ardell JL. New York: Oxford University Press, 1994, p. 95-114.
13. Ardell JL, Andresen MC, Armour JA, Billman GE, Chen PS, Foreman RD, Herring N, O'Leary DS, Sabbah HN, Schultz HD, Sunagawa K, and Zucker IH. Translational neurocardiology: preclinical models and cardioneural integrative aspects. *J Physiol* 594: 3877-3909, 2016.
14. Ardell JL, Butler CK, Smith FM, Hopkins DA, and Armour JA. Activity of in vivo atrial and ventricular neurons in chronically decentralized canine hearts. *Am J Physiol* 260: H713-721, 1991.
15. Ardell JL, Cardinal R, Beaumont E, Vermeulen M, Smith FM, and Armour JA. Chronic spinal cord stimulation modifies intrinsic cardiac synaptic efficacy in the suppression of atrial fibrillation. *Autonomic neuroscience : basic & clinical* 186: 38-44, 2014.
16. Ardell JL, Ragendran PS, Nier HA, KenKnight BH, and Armour JA. Central-Peripheral Neural Network Interactions Evoked by Vagus Nerve Stimulation: Functional Consequences on Control of Cardiac Function. *Am J Physiol Heart Circ Physiol*: ajpheart.00557.02015, 2015.
17. Ardell JL, Rajendran PS, Nier HA, KenKnight BH, and Armour JA. Central-peripheral neural network interactions evoked by vagus nerve stimulation: functional consequences on control of cardiac function. *Am J Physiol Heart Circ Physiol*309: H1740-1752, 2015.
18. Ardell JL, Randall WC, Cannon WJ, Schmacht DC, and Tasdemiroglu E. Differential sympathetic regulation of automatic, conductile, and contractile tissue in dog heart. *Am J Physiol* 255: H1050-1059, 1988.
19. Armour JA. Activity of in situ middle cervical ganglion neurons in dogs, using extracellular recording techniques. *Canadian journal of physiology and pharmacology* 63: 704-716, 1985.
20. Armour JA. Functional anatomy of intrathoracic neurons innervating the atria and ventricles. *Heart Rhythm* 7: 994-996, 2010.
21. Armour JA. Instant to instant reflex cardiac regulation. *Cardiology* 61: 309-328, 1976.

22. Armour JA. Neuronal activity recorded extracellularly in chronically decentralized in situ canine middle cervical ganglia. *Canadian journal of physiology and pharmacology* 64: 1038-1046, 1986.
23. Armour JA. Potential clinical relevance of the 'little brain' on the mammalian heart. *Experimental physiology* 93: 165-176, 2008.
24. Armour JA. Synaptic transmission in the chronically decentralized middle cervical and stellate ganglia of the dog. *Canadian journal of physiology and pharmacology* 61: 1149-1155, 1983.
25. Armour JA and Janes RD. Neuronal activity recorded extracellularly from in situ canine mediastinal ganglia. *Canadian journal of physiology and pharmacology* 66: 119-127, 1988.
26. Armour JA and Kember G. Cardiac sensory neurons. In: *Basic and Clinical Neurocardiology*, edited by Armour JA and Ardell JL. New York: Oxford University Press, 2004, p. 79-117.
27. Armour JA, Murphy DA, Yuan BX, Macdonald S, and Hopkins DA. Gross and microscopic anatomy of the human intrinsic cardiac nervous system. *The Anatomical record* 247: 289-298, 1997.
28. Armour JA, Richer LP, Page P, Vinet A, Kus T, Vermeulen M, Nadeau R, and Cardinal R. Origin and pharmacological response of atrial tachyarrhythmias induced by activation of mediastinal nerves in canines. *Autonomic neuroscience : basic & clinical* 118: 68-78, 2005.
29. Arora RC, Waldmann M, Hopkins DA, and Armour JA. Porcine intrinsic cardiac ganglia. *The anatomical record Part A, Discoveries in molecular, cellular, and evolutionary biology* 271: 249-258, 2003.
30. Bailey P and Bremer F. A sensory cortical representation of the vagus nerve. *Journal of neurophysiology*: 405-412, 1938.
31. Bayes de Luna A, Coumel P, and Leclercq JF. Ambulatory sudden cardiac death: mechanisms of production of fatal arrhythmia on the basis of data from 157 cases. *American heart journal* 117: 151-159, 1989.
32. Beaumont E, Salavatian S, Southerland EM, Vinet A, Jacquemet V, Armour JA, and Ardell JL. Network interactions within the canine intrinsic cardiac nervous system: implications for reflex control of regional cardiac function. *J Physiol*591: 4515-4533, 2013.

33. Beaumont E, Southerland EM, Hardwick JC, Wright GL, Ryan S, Li Y, KenKnight BH, Armour JA, and Ardell JL. Vagus nerve stimulation mitigates intrinsic cardiac neuronal and adverse myocyte remodeling postmyocardial infarction. *Am J Physiol Heart Circ Physiol*309: H1198-1206, 2015.
34. Beaumont E, Wright GL, Southerland EM, Li Y, Chui RW, KenKnight BH, Armour JA, and Ardell JL. Vagus nerve stimulation mitigates intrinsic cardiac neuronal remodeling and cardiac hypertrophy induced by chronic pressure overload in guinea pig. *American journal of physiology Heart and circulatory physiology*: ajpheart 00939 02015, 2016.
35. Ben-Menachem E, Revesz D, Simon BJ, and Silberstein S. Surgically implanted and non-invasive vagus nerve stimulation: a review of efficacy, safety and tolerability. *European journal of neurology : the official journal of the European Federation of Neurological Societies* 22: 1260-1268, 2015.
36. Berthoud HR and Neuhuber WL. Functional and chemical anatomy of the afferent vagal system. *Autonomic neuroscience : basic & clinical* 85: 1-17, 2000.
37. Bhadra N and Kilgore KL. High-frequency electrical conduction block of mammalian peripheral motor nerve. *Muscle & nerve* 32: 782-790, 2005.
38. Bourke T, Vaseghi M, Michowitz Y, Sankhla V, Shah M, Swapna N, Boyle NG, Mahajan A, Narasimhan C, Lokhandwala Y, and Shivkumar K. Neuraxial modulation for refractory ventricular arrhythmias: value of thoracic epidural anesthesia and surgical left cardiac sympathetic denervation. *Circulation* 121: 2255-2262, 2010.
39. Brack KE, Patel VH, Coote JH, and Ng GA. Nitric oxide mediates the vagal protective effect on ventricular fibrillation via effects on action potential duration restitution in the rabbit heart. *J Physiol*583: 695-704, 2007.
40. Brack KE, Winter J, and Ng GA. Mechanisms underlying the autonomic modulation of ventricular fibrillation initiation--tentative prophylactic properties of vagus nerve stimulation on malignant arrhythmias in heart failure. *Heart failure reviews* 18: 389-408, 2013.
41. Buckley U, Yamakawa K, Takamiya T, Armour JA, Shivkumar K, and Ardell JL. Targeted Stellate Decentralization: Implications for Sympathetic Control of Ventricular Electrophysiology. *Heart rhythm : the official journal of the Heart Rhythm Society*, 2015.
42. Cadeddu C, Deidda M, Mercuro G, Tuveri A, Muroni A, Nocco S, Puligheddu M, Maleci A, and Marrosu F. Cardiovascular modulation during vagus nerve stimulation therapy in patients with refractory epilepsy. *Epilepsy research* 92: 145-152, 2010.

43. Calvillo L, Vanoli E, Andreoli E, Besana A, Omodeo E, Gnecchi M, Zerbi P, Vago G, Busca G, and Schwartz PJ. Vagal stimulation, through its nicotinic action, limits infarct size and the inflammatory response to myocardial ischemia and reperfusion. *Journal of cardiovascular pharmacology* 58: 500-507, 2011.
44. Cao JM, Chen LS, KenKnight BH, Ohara T, Lee MH, Tsai J, Lai WW, Karagueuzian HS, Wolf PL, Fishbein MC, and Chen PS. Nerve sprouting and sudden cardiac death. *Circ Res* 86: 816-821, 2000.
45. Cao JM, Fishbein MC, Han JB, Lai WW, Lai AC, Wu TJ, Czer L, Wolf PL, Denton TA, Shintaku IP, Chen PS, and Chen LS. Relationship between regional cardiac hyperinnervation and ventricular arrhythmia. *Circulation* 101: 1960-1969, 2000.
46. Cardinal R, Page P, Vermeulen M, Ardell JL, and Armour JA. Spatially divergent cardiac responses to nicotinic stimulation of ganglionated plexus neurons in the canine heart. *Autonomic neuroscience : basic & clinical* 145: 55-62, 2009.
47. Chang CM, Wu TJ, Zhou S, Doshi RN, Lee MH, Ohara T, Fishbein MC, Karagueuzian HS, Chen PS, and Chen LS. Nerve sprouting and sympathetic hyperinnervation in a canine model of atrial fibrillation produced by prolonged right atrial pacing. *Circulation* 103: 22-25, 2001.
48. Chen PS, Chen LS, Fishbein MC, Lin SF, and Nattel S. Role of the autonomic nervous system in atrial fibrillation: pathophysiology and therapy. *Circ Res* 114: 1500-1515, 2014.
49. Chugh SS, Reinier K, Teodorescu C, Evanado A, Kehr E, Al Samara M, Mariani R, Gunson K, and Jui J. Epidemiology of sudden cardiac death: clinical and research implications. *Progress in cardiovascular diseases* 51: 213-228, 2008.
50. Clancy JA, Mary DA, Witte KK, Greenwood JP, Deuchars SA, and Deuchars J. Non-invasive vagus nerve stimulation in healthy humans reduces sympathetic nerve activity. *Brain stimulation* 7: 871-877, 2014.
51. Coleridge HM, Coleridge JC, Dangel A, Kidd C, Luck JC, and Sleight P. Impulses in slowly conducting vagal fibers from afferent endings in the veins, atria, and arteries of dogs and cats. *Circ Res* 33: 87-97, 1973.
52. De Ferrari GM. Vagal stimulation in heart failure. *Journal of cardiovascular translational research* 7: 310-320, 2014.
53. De Ferrari GM, Crijns HJ, Borggrefe M, Milasinovic G, Smid J, Zabel M, Gavazzi A, Sanzo A, Dennert R, Kuschyk J, Raspopovic S, Klein H, Swedberg K, Schwartz PJ, and CardioFit Multicenter Trial I. Chronic vagus nerve stimulation: a new and promising therapeutic approach for chronic heart failure. *Eur Heart J* 32: 847-855, 2011.

54. De Ferrari GM, Dusi V, Spazzolini C, Bos JM, Abrams DJ, Berul CI, Crotti L, Davis AM, Eldar M, Kharlap M, Khoury A, Krahn AD, Leenhardt A, Moir CR, Odero A, Olde Nordkamp L, Paul T, Roses INF, Shkolnikova M, Till J, Wilde AA, Ackerman MJ, and Schwartz PJ. Clinical Management of Catecholaminergic Polymorphic Ventricular Tachycardia: The Role of Left Cardiac Sympathetic Denervation. *Circulation* 131: 2185-2193, 2015.
55. De Ferrari GM, Tuinenburg AE, Ruble S, Brugada J, Klein H, Butter C, Wright DJ, Schubert B, Solomon S, Meyer S, Stein K, Ramuzat A, and Zannad F. Rationale and study design of the NEuroCardiac TherApy foR Heart Failure Study: NECTAR-HF. *European journal of heart failure* 16: 692-699, 2014.
56. Del Rio R, Marcus NJ, and Schultz HD. Carotid chemoreceptor ablation improves survival in heart failure: rescuing autonomic control of cardiorespiratory function. *Journal of the American College of Cardiology* 62: 2422-2430, 2013.
57. Dicarlo L, Libbus I, Amurthur B, Kenknight BH, and Anand IS. Autonomic regulation therapy for the improvement of left ventricular function and heart failure symptoms: the ANTHEM-HF study. *Journal of cardiac failure* 19: 655-660, 2013.
58. Einbrodt. Ueber Herzreizung und ihr Verhaeltnis zum Blutdruck. *Akademie der Wissenschaften (Vienna) Sitzungsberichte* 38: 345, 1859.
59. Estes EH, Jr. and Izlar HL, Jr. Recurrent ventricular tachycardia. A case successfully treated by bilateral cardiac sympathectomy. *Am J Med* 31: 493-497, 1961.
60. Flaim SN and McCulloch AD. Acetylcholine-induced shortening of the epicardial action potential duration may increase repolarization gradients and LQT3 arrhythmic risk. *Journal of electrocardiology* 40: S66-69, 2007.
61. Foley JO and DuBois FS. Quantitative studies of the vagus nerve in the cat. I. The ratio of sensory to motor fibers. *The Journal of comparative neurology* 67: 49-67, 1937.
62. Foreman RD. Mechanisms of cardiac pain. *Annual review of physiology* 61: 143-167, 1999.
63. Foreman RD and Linderoth B. Neural mechanisms of spinal cord stimulation. *International review of neurobiology* 107: 87-119, 2012.
64. Frenneaux MP. Autonomic changes in patients with heart failure and in post-myocardial infarction patients. *Heart* 90: 1248-1255, 2004.
65. Fudim M, Groom KL, Laffer CL, Netterville JL, Robertson D, and Elijovich F. Effects of carotid body tumor resection on the blood pressure of essential hypertensive patients. *Journal of the American Society of Hypertension : JASH* 9: 435-442, 2015.

66. Fukuda K, Kanazawa H, Aizawa Y, Ardell JL, and Shivkumar K. Cardiac innervation and sudden cardiac death. *Circ Res* 116: 2005-2019, 2015.
67. Furukawa Y, Hoyano Y, and Chiba S. Parasympathetic inhibition of sympathetic effects on sinus rate in anesthetized dogs. *Am J Physiol* 271: H44-50, 1996.
68. Geis GS and Wurster RD. Cardiac responses during stimulation of the dorsal motor nucleus and nucleus ambiguus in the cat. *Circ Res* 46: 606-611, 1980.
69. Geis GS and Wurster RD. Horseradish peroxidase localization of cardiac vagal preganglionic somata. *Brain research* 182: 19-30, 1980.
70. Gibbons DD, Southerland EM, Hoover DB, Beaumont E, Armour JA, and Ardell JL. Neuromodulation targets intrinsic cardiac neurons to attenuate neuronally mediated atrial arrhythmias. *Am J Physiol Reg Integr Comp Physiol* 302: R357-364, 2012.
71. Go AS, Mozaffarian D, Roger VL, Benjamin EJ, Berry JD, Blaha MJ, Dai S, Ford ES, Fox CS, Franco S, Fullerton HJ, Gillespie C, Hailpern SM, Heit JA, Howard VJ, Huffman MD, Judd SE, Kissela BM, Kittner SJ, Lackland DT, Lichtman JH, Lisabeth LD, Mackey RH, Magid DJ, Marcus GM, Marelli A, Matchar DB, McGuire DK, Mohler ER, 3rd, Moy CS, Mussolino ME, Neumar RW, Nichol G, Pandey DK, Paynter NP, Reeves MJ, Sorlie PD, Stein J, Towfighi A, Turan TN, Virani SS, Wong ND, Woo D, Turner MB, American Heart Association Statistics C, and Stroke Statistics S. Heart disease and stroke statistics--2014 update: a report from the American Heart Association. *Circulation* 129: e28-e292, 2014.
72. Gold MR, Van Veldhuisen DJ, Hauptman PJ, Borggrefe M, Kubo SH, Lieberman RA, Milasinovic G, Berman BJ, Djordjevic S, Neelagaru S, Schwartz PJ, Starling RC, and Mann DL. Vagus Nerve Stimulation for the Treatment of Heart Failure: The INOVATE-HF Trial. *Journal of the American College of Cardiology* 68: 149-158, 2016.
73. Goldstein RE, Karsh RB, Smith ER, Orlando M, Norman D, Farnham G, Redwood DR, and Epstein SE. Influence of atropine and of vagally mediated bradycardia on the occurrence of ventricular arrhythmias following acute coronary occlusion in closed-chest dogs. *Circulation* 47: 1180-1190, 1973.
74. Gordan R, Gwathmey JK, and Xie LH. Autonomic and endocrine control of cardiovascular function. *World J Cardiol* 7: 204-214, 2015.
75. Gossot D, Kabiri H, Caliandro R, Debrosse D, Girard P, and Grunenwald D. Early complications of thoracic endoscopic sympathectomy: a prospective study of 940 procedures. *The Annals of thoracic surgery* 71: 1116-1119, 2001.

76. Gray AL, Johnson TA, Lauenstein JM, Newton SS, Ardell JL, and Massari VJ. Parasympathetic control of the heart. III. Neuropeptide Y-immunoreactive nerve terminals synapse on three populations of negative chronotropic vagal preganglionic neurons. *Journal of applied physiology* 96: 2279-2287, 2004.
77. Gray MA, Taggart P, Sutton PM, Groves D, Holdright DR, Bradbury D, Brull D, and Critchley HD. A cortical potential reflecting cardiac function. *Proc Natl Acad Sci U S A* 104: 6818-6823, 2007.
78. Hamann JJ, Ruble SB, Stolen C, Wang M, Gupta RC, Rastogi S, and Sabbah HN. Vagus nerve stimulation improves left ventricular function in a canine model of chronic heart failure. *European journal of heart failure* 15: 1319-1326, 2013.
79. Han J and Moe GK. NONUNIFORM RECOVERY OF EXCITABILITY IN VENTRICULAR MUSCLE. *Circ Res* 14: 44-60, 1964.
80. Hauptman PJ, Schwartz PJ, Gold MR, Borggrefe M, Van Veldhuisen DJ, Starling RC, and Mann DL. Rationale and study design of the increase of vagal tone in heart failure study: INOVATE-HF. *American heart journal* 163: 954-962 e951, 2012.
81. Heidenreich PA, Albert NM, Allen LA, Bluemke DA, Butler J, Fonarow GC, Ikonomidis JS, Khavjou O, Konstam MA, Maddox TM, Nichol G, Pham M, Pina IL, Trogdon JG, American Heart Association Advocacy Coordinating C, Council on Arteriosclerosis T, Vascular B, Council on Cardiovascular R, Intervention, Council on Clinical C, Council on E, Prevention, and Stroke C. Forecasting the impact of heart failure in the United States: a policy statement from the American Heart Association. *Circulation Heart failure* 6: 606-619, 2013.
82. Herring N, Cranley J, Lokale MN, Li D, Shanks J, Alston EN, Girard BM, Carter E, Parsons RL, Habecker BA, and Paterson DJ. The cardiac sympathetic co-transmitter galanin reduces acetylcholine release and vagal bradycardia: implications for neural control of cardiac excitability. *Journal of molecular and cellular cardiology* 52: 667-676, 2012.
83. Ho KK, Pinsky JL, Kannel WB, and Levy D. The epidemiology of heart failure: the Framingham Study. *Journal of the American College of Cardiology* 22: 6A-13A, 1993.
84. Hopkins DA and Armour JA. Localization of sympathetic postganglionic and parasympathetic preganglionic neurons which innervate different regions of the dog heart. *J Comp Neurol* 229: 186-198, 1984.
85. Hopp FA and Seagard JL. Respiratory responses to selective blockade of carotid sinus baroreceptors in the dog. *Am J Physiol* 275: R10-18, 1998.

86. Hopp FA, Zuperku EJ, Coon RL, and Kampine JP. Effect of anodal blockade of myelinated fibers on vagal C-fiber afferents. *Am J Physiol* 239: R454-462, 1980.
87. Huang J, Qian J, Yao W, Wang N, Zhang Z, Cao C, Song B, and Zhang Z. Vagus nerve stimulation reverses ventricular electrophysiological changes induced by hypersympathetic nerve activity. *Experimental physiology* 100: 239-248, 2015.
88. Huang WA, Shivkumar K, and Vaseghi M. Device-based autonomic modulation in arrhythmia patients: the role of vagal nerve stimulation. *Current treatment options in cardiovascular medicine* 17: 379, 2015.
89. Janes RD, Brandys JC, Hopkins DA, Johnstone DE, Murphy DA, and Armour JA. Anatomy of human extrinsic cardiac nerves and ganglia. *Am J Cardiol* 57: 299-309, 1986.
90. Janig W. Autonomic nervous system and inflammation. *Autonomic neuroscience : basic & clinical* 182: 1-3, 2014.
91. Jayachandran JV, Sih HJ, Winkle W, Zipes DP, Hutchins GD, and Olgin JE. Atrial fibrillation produced by prolonged rapid atrial pacing is associated with heterogeneous changes in atrial sympathetic innervation. *Circulation* 101: 1185-1191, 2000.
92. Jinkins JR. *Atlas of neuroradiologic embryology, anatomy, and variants*. Philadelphia: Lippincott Williams & Wilkins, 2000.
93. Joseph L and Butera RJ. High-frequency stimulation selectively blocks different types of fibers in frog sciatic nerve. *IEEE transactions on neural systems and rehabilitation engineering : a publication of the IEEE Engineering in Medicine and Biology Society* 19: 550-557, 2011.
94. Jänig W. *The Integrative Action of the Autonomic Nervous System: Neurobiology of Homeostasis*. New York: Cambridge University Press, 2006.
95. Kasanuki H, Ohnishi S, Ohtuka M, Matsuda N, Nirei T, Isogai R, Shoda M, Toyoshima Y, and Hosoda S. Idiopathic ventricular fibrillation induced with vagal activity in patients without obvious heart disease. *Circulation* 95: 2277-2285, 1997.
96. Kato M and Fukushima K. Effect of differential blocking of motor axons on antidromic activation of Renshaw cells in the cat. *Experimental brain research* 20: 135-143, 1974.
97. Kawashima T. Anatomy of the cardiac nervous system with clinical and comparative morphological implications. *Anat Sci Int* 86: 30-49, 2011.
98. Kember G, Ardell JL, Armour JA, and Zamir M. Vagal nerve stimulation therapy: what is being stimulated? *PloS one* 9: e114498, 2014.

99. Kember G, Armour JA, and Zamir M. Neural control hierarchy of the heart has not evolved to deal with myocardial ischemia. *Physiological genomics* 45: 638-644, 2013.
100. Kilgore KL and Bhadra N. Nerve conduction block utilising high-frequency alternating current. *Medical & biological engineering & computing* 42: 394-406, 2004.
101. Kilgore KL and Bhadra N. Reversible nerve conduction block using kilohertz frequency alternating current. *Neuromodulation : journal of the International Neuromodulation Society* 17: 242-254; discussion 254-245, 2014.
102. Koh A, Gutbrod SR, Meyers JD, Lu C, Webb RC, Shin G, Li Y, Kang SK, Huang Y, Efimov IR, and Rogers JA. Ultrathin Injectable Sensors of Temperature, Thermal Conductivity, and Heat Capacity for Cardiac Ablation Monitoring. *Advanced healthcare materials*, 2015.
103. Kolman BS, Verrier RL, and Lown B. The effect of vagus nerve stimulation upon vulnerability of the canine ventricle: role of sympathetic-parasympathetic interactions. *Circulation* 52: 578-585, 1975.
104. Koncz I, Gurabi Z, Patocskai B, Panama BK, Szel T, Hu D, Barajas-Martinez H, and Antzelevitch C. Mechanisms underlying the development of the electrocardiographic and arrhythmic manifestations of early repolarization syndrome. *Journal of molecular and cellular cardiology* 68: 20-28, 2014.
105. Kuntz A. *The Autonomic Nervous System*. Philadelphia: Lea & Febiger, 1934.
106. Kusunose K, Zhang Y, Mazgalev TN, Van Wagoner DR, Thomas JD, and Popovic ZB. Impact of vagal nerve stimulation on left atrial structure and function in a canine high-rate pacing model. *Circulation Heart failure* 7: 320-326, 2014.
107. La Rovere MT, Bigger JT, Jr., Marcus FI, Mortara A, and Schwartz PJ. Baroreflex sensitivity and heart-rate variability in prediction of total cardiac mortality after myocardial infarction. ATRAMI (Autonomic Tone and Reflexes After Myocardial Infarction) Investigators. *Lancet* 351: 478-484, 1998.
108. Labiner DM and Ahern GL. Vagus nerve stimulation therapy in depression and epilepsy: therapeutic parameter settings. *Acta neurologica Scandinavica* 115: 23-33, 2007.
109. Langley G. *The Autonomic Nervous System*. Cambridge, UK: Cambridge University Press, 1921.
110. Lanska DJ. J.L. Corning and vagal nerve stimulation for seizures in the 1880s. *Neurology* 58: 452-459, 2002.

111. Lechat P, Hulot JS, Escolano S, Mallet A, Leizorovicz A, Werhlen-Grandjean M, Pochmalicki G, and Dargie H. Heart rate and cardiac rhythm relationships with bisoprolol benefit in chronic heart failure in CIBIS II Trial. *Circulation* 103: 1428-1433, 2001.
112. Levy MN. Sympathetic-parasympathetic interactions in the heart. *Circ Res* 29: 437-445, 1971.
113. Levy MN and Martin PJ. Neural control of the heart. In: *Handbook of Physiology: Section 2: The Cardiovascular System, Volume 1: The Heart*, edited by Berne RM. Bethesda: The American Physiological Society, 1979, p. 581-620.
114. Li M, Zheng C, Sato T, Kawada T, Sugimachi M, and Sunagawa K. Vagal nerve stimulation markedly improves long-term survival after chronic heart failure in rats. *Circulation* 109: 120-124, 2004.
115. Li S, Scherlag BJ, Yu L, Sheng X, Zhang Y, Ali R, Dong Y, Ghias M, and Po SS. Low-level vagosympathetic stimulation: a paradox and potential new modality for the treatment of focal atrial fibrillation. *Circulation Arrhythmia and electrophysiology* 2: 645-651, 2009.
116. Li Y, Xuan YH, Liu SS, Dong J, Luo JY, and Sun ZJ. Shortterm vagal nerve stimulation improves left ventricular function following chronic heart failure in rats. *Molecular medicine reports* 12: 1709-1716, 2015.
117. Loyalka P, Hariharan R, Gholkar G, Gregoric ID, Tamerisa R, Nathan S, and Kar B. Left stellate ganglion block for continuous ventricular arrhythmias during percutaneous left ventricular assist device support. *Tex Heart Inst J* 38: 409-411, 2011.
118. Mahajan A, Moore J, Cesario DA, and Shivkumar K. Use of thoracic epidural anesthesia for management of electrical storm: a case report. *Heart Rhythm* 2: 1359-1362, 2005.
119. Manfredi M. Differential block of conduction of larger fibers in peripheral nerve by direct current. *Arch Ital Biol* 108: 52-71, 1970.
120. Massari VJ, Johnson TA, and Gatti PJ. Cardiotopic organization of the nucleus ambiguus? An anatomical and physiological analysis of neurons regulating atrioventricular conduction. *Brain research* 679: 227-240, 1995.
121. McCloskey DI and Mitchell JH. Reflex cardiovascular and respiratory responses originating in exercising muscle. *J Physiol* 224: 173-186, 1972.
122. McCreery DB, Agnew WF, Yuen TG, and Bullara LA. Comparison of neural damage induced by electrical stimulation with faradaic and capacitor electrodes. *Annals of biomedical engineering* 16: 463-481, 1988.

123. McGuirt AS, Schmacht DC, and Ardell JL. Autonomic interactions for control of atrial rate are maintained after SA nodal parasympathectomy. *Am J Physiol* 272: H2525-2533, 1997.
124. Meissner A, Eckardt L, Kirchhof P, Weber T, Rolf N, Breithardt G, Van Aken H, and Haverkamp W. Effects of thoracic epidural anesthesia with and without autonomic nervous system blockade on cardiac monophasic action potentials and effective refractoriness in awake dogs. *Anesthesiology* 95: 132-138; discussion 136A, 2001.
125. Mortara A, La Rovere MT, Pinna GD, Parziale P, Maestri R, Capomolla S, Opasich C, Cobelli F, and Tavazzi L. Depressed arterial baroreflex sensitivity and not reduced heart rate variability identifies patients with chronic heart failure and nonsustained ventricular tachycardia: the effect of high ventricular filling pressure. *American heart journal* 134: 879-888, 1997.
126. Moss AJ and McDonald J. Unilateral cervicothoracic sympathetic ganglionectomy for the treatment of long QT interval syndrome. *N Engl J Med* 285: 903-904, 1971.
127. Moss AJ, Schuger C, Beck CA, Brown MW, Cannom DS, Daubert JP, Estes NA, 3rd, Greenberg H, Hall WJ, Huang DT, Kautzner J, Klein H, McNitt S, Olshansky B, Shoda M, Wilber D, and Zareba W. Reduction in inappropriate therapy and mortality through ICD programming. *N Engl J Med* 367: 2275-2283, 2012.
128. Myers RW, Pearlman AS, Hyman RM, Goldstein RA, Kent KM, Goldstein RE, and Epstein SE. Beneficial effects of vagal stimulation and bradycardia during experimental acute myocardial ischemia. *Circulation* 49: 943-947, 1974.
129. Nadeau R, Cardinal R, Armour JA, Kus T, Richer LP, Vermeulen M, Yin Y, and Page P. Cervical vagosympathetic and mediastinal nerves activation effects on atrial arrhythmia formation. *Anadolu kardiyoloji dergisi : AKD = the Anatolian journal of cardiology* 7 Suppl 1: 34-36, 2007.
130. Nademanee K, Taylor R, Bailey WE, Rieders DE, and Kosar EM. Treating electrical storm : sympathetic blockade versus advanced cardiac life support-guided therapy. *Circulation* 102: 742-747, 2000.
131. Napadow V, Edwards RR, Cahalan CM, Mensing G, Greenbaum S, Valovska A, Li A, Kim J, Maeda Y, Park K, and Wasan AD. Evoked pain analgesia in chronic pelvic pain patients using respiratory-gated auricular vagal afferent nerve stimulation. *Pain medicine* 13: 777-789, 2012.
132. Nguyen BL, Fishbein MC, Chen LS, Chen PS, and Masroor S. Histopathological substrate for chronic atrial fibrillation in humans. *Heart Rhythm* 6: 454-460, 2009.

133. Niewinski P, Janczak D, Rucinski A, Tubek S, Engelman ZJ, Jazwiec P, Banasiak W, Sobotka PA, Hart EC, Paton JF, and Ponikowski P. Dissociation between blood pressure and heart rate response to hypoxia after bilateral carotid body removal in men with systolic heart failure. *Experimental physiology* 99: 552-561, 2014.
134. Nygard E, Kofoed KF, Freiberg J, Holm S, Aldershvile J, Eliasen K, and Kelbaek H. Effects of high thoracic epidural analgesia on myocardial blood flow in patients with ischemic heart disease. *Circulation* 111: 2165-2170, 2005.
135. O'Toole MF, Ardell JL, and Randall WC. Functional interdependence of discrete vagal projections to SA and AV nodes. *Am J Physiol* 251: H398-404, 1986.
136. Oka T, Ozawa Y, and Ohkubo Y. Thoracic epidural bupivacaine attenuates supraventricular tachyarrhythmias after pulmonary resection. *Anesth Analg* 93: 253-259, 251st contents page, 2001.
137. Olausson K, Magnusdottir H, Lurje L, Wennerblom B, Emanuelsson H, and Ricksten SE. Anti-ischemic and anti-anginal effects of thoracic epidural anesthesia versus those of conventional medical therapy in the treatment of severe refractory unstable angina pectoris. *Circulation* 96: 2178-2182, 1997.
138. Oppenheimer SM and Lima J. Neurology and the heart. *J Neurol Neurosurg Psychiatry* 64: 289-297, 1998.
139. Orosz I, McCormick D, Zamponi N, Varadkar S, Feucht M, Parain D, Griens R, Vallee L, Boon P, Rittey C, Jayewardene AK, Bunker M, Arzimanoglou A, and Lagae L. Vagus nerve stimulation for drug-resistant epilepsy: a European long-term study up to 24 months in 347 children. *Epilepsia* 55: 1576-1584, 2014.
140. Paintal AS. Vagal Afferent Fibres. *Ergebnisse der Physiologie, biologischen Chemie und experimentellen Pharmakologie* 52: 74-156, 1963.
141. Palma JA and Benarroch EE. Neural control of the heart: recent concepts and clinical correlations. *Neurology* 83: 261-271, 2014.
142. Panhofer P, Gleiss A, Eilenberg WH, Jakesz R, Bischof G, and Neumayer C. Long-term outcomes after endothoracic sympathetic block at the T4 ganglion for upper limb hyperhidrosis. *Br J Surg* 100: 1471-1477, 2013.
143. Patel RA, Priore DL, Szeto WY, and Slevin KA. Left stellate ganglion blockade for the management of drug-resistant electrical storm. *Pain Med* 12: 1196-1198, 2011.
144. Patterson E, Po SS, Scherlag BJ, and Lazzara R. Triggered firing in pulmonary veins initiated by in vitro autonomic nerve stimulation. *Heart Rhythm* 2: 624-631, 2005.

145. Pavlov VA and Tracey KJ. The cholinergic anti-inflammatory pathway. *Brain, behavior, and immunity* 19: 493-499, 2005.
146. Petruska JC, Hubscher CH, and Johnson RD. Anodally focused polarization of peripheral nerve allows discrimination of myelinated and unmyelinated fiber input to brainstem nuclei. *Experimental brain research* 121: 379-390, 1998.
147. Premchand RK, Sharma K, Mittal S, Monteiro R, Dixit S, Libbus I, DiCarlo LA, Ardell JL, Rector TS, Amurthur B, KenKnight BH, and Anand IS. Autonomic Regulation Therapy via Left or Right Cervical Vagus Nerve Stimulation in Patients with Chronic Heart Failure: Results of the ANTHEM-HF Trial. *Journal of cardiac failure* 20: 808-816, 2014.
148. Premchand RK, Sharma K, Mittal S, Monteiro R, Dixit S, Libbus I, DiCarlo LA, Ardell JL, Rector TS, Amurthur B, KenKnight BH, and Anand IS. Extended Follow-Up of Patients with Heart Failure Receiving Autonomic Regulation Therapy in the ANTHEM-HF Study. *Journal of cardiac failure*, 2015.
149. Priori SG, Blomstrom-Lundqvist C, Mazzanti A, Blom N, Borggrefe M, Camm J, Elliott PM, Fitzsimons D, Hatala R, Hindricks G, Kirchhof P, Kjeldsen K, Kuck KH, Hernandez-Madrid A, Nikolaou N, Norekval TM, Spaulding C, and Van Veldhuisen DJ. 2015 ESC Guidelines for the management of patients with ventricular arrhythmias and the prevention of sudden cardiac death: The Task Force for the Management of Patients with Ventricular Arrhythmias and the Prevention of Sudden Cardiac Death of the European Society of Cardiology (ESC)Endorsed by: Association for European Paediatric and Congenital Cardiology (AEPC). *Europace* 17: 1601-1687, 2015.
150. Rajendran PS, Nakamura K, Ajijola OA, Vaseghi M, Armour JA, Ardell JL, and Shivkumar K. Myocardial infarction induces structural and functional remodelling of the intrinsic cardiac nervous system. *J Physiol-London* 594: 321-341, 2016.
151. Randall DC, Brown DR, McGuirt AS, Thompson GW, Armour JA, and Ardell JL. Interactions within the intrinsic cardiac nervous system contribute to chronotropic regulation. *Am J Physiol Reg Integr Comp Physiol* 285: R1066-1075, 2003.
152. Randall WC. Efferent Sympathetic Innervation of the Heart. In: *Neurocardiology*, edited by Armour JA and Ardell JL. New York: Oxford University Press, 1994, p. 77-94.
153. Randall WC, Ardell JL, and Becker DM. Differential responses accompanying sequential stimulation and ablation of vagal branches to dog heart. *Am J Physiol* 249: H133-140, 1985.

154. Randall WC, Ardell JL, O'Toole MF, and Wurster RD. Differential autonomic control of SAN and AVN regions of the canine heart: structure and function. *Progress in clinical and biological research* 275: 15-31, 1988.
155. Randall WC and Armour JA. Regional vagosympathetic control of the heart. *Am J Physiol* 227: 444-452, 1974.
156. Randall WC, Priola DV, and Pace JB. Responses of individucal cardiac chambers to stimulation of the cervical vagosympathetic trunk in atropinized dogs. *Circ Res* 20: 534-544, 1967.
157. Ravid E and Prochazka A. Controlled nerve ablation with direct current: parameters and mechanisms. *IEEE transactions on neural systems and rehabilitation engineering : a publication of the IEEE Engineering in Medicine and Biology Society* 22: 1172-1185, 2014.
158. Richer LP, Vinet A, Kus T, Cardinal R, Ardell JL, and Armour JA. Alpha-adrenoceptor blockade modifies neurally induced atrial arrhythmias. *Am J Physiol Reg Integr Comp Physiol* 295: R1175-1180, 2008.
159. Ruffoli R, Giorgi FS, Pizzanelli C, Murri L, Paparelli A, and Fornai F. The chemical neuroanatomy of vagus nerve stimulation. *Journal of chemical neuroanatomy* 42: 288-296, 2011.
160. S S. Transcutaneous Electrical Vagus Nerve Stimulation to Suppress Atrial Fibrillation (ID NCT02548754), 2017.
161. Sant'Ambrogio G, Decandia M, and Provini L. Diaphragmatic contribution to respiration in the rabbit. *J Appl Physiol* 21: 843-847, 1966.
162. Sarr MG, Billington CJ, Brancatisano R, Brancatisano A, Toouli J, Kow L, Nguyen NT, Blackstone R, Maher JW, Shikora S, Reeds DN, Eagon JC, Wolfe BM, O'Rourke RW, Fujioka K, Takata M, Swain JM, Morton JM, Ikramuddin S, Schweitzer M, Chand B, and Rosenthal R. The EMPOWER study: randomized, prospective, double-blind, multicenter trial of vagal blockade to induce weight loss in morbid obesity. *Obes Surg* 22: 1771-1782, 2012.
163. Scherlag BJ, Helfant RH, Haft JI, and Damato AN. Electrophysiology underlying ventricular arrhythmias due to coronary ligation. *Am J Physiol* 219: 1665-1671, 1970.
164. Scherlag BJ, Nakagawa H, Jackman WM, Lazzara R, and Po SS. Non-pharmacological, non-ablative approaches for the treatment of atrial fibrillation: experimental evidence and potential clinical implications. *Journal of cardiovascular translational research* 4: 35-41, 2011.

165. Schomer AC, Nearing BD, Schachter SC, and Verrier RL. Vagus nerve stimulation reduces cardiac electrical instability assessed by quantitative T-wave alternans analysis in patients with drug-resistant focal epilepsy. *Epilepsia* 55: 1996-2002, 2014.
166. Schwartz PJ. Cardiac sympathetic denervation to prevent life-threatening arrhythmias. *Nature reviews Cardiology* 11: 346-353, 2014.
167. Schwartz PJ, De Ferrari GM, Sanzo A, Landolina M, Rordorf R, Raineri C, Campana C, Revera M, Ajmone-Marsan N, Tavazzi L, and Odero A. Long term vagal stimulation in patients with advanced heart failure: first experience in man. *European journal of heart failure* 10: 884-891, 2008.
168. Seki A, Green HR, Lee TD, Hong L, Tan J, Vinters HV, Chen PS, and Fishbein MC. Sympathetic nerve fibers in human cervical and thoracic vagus nerves. *Heart Rhythm* 11: 1411-1417, 2014.
169. Shen MJ and Zipes DP. Role of the autonomic nervous system in modulating cardiac arrhythmias. *Circ Res* 114: 1004-1021, 2014.
170. Shinlapawittayatorn K, Chinda K, Palee S, Surinkaew S, Kumfu S, Kumphune S, Chattipakorn S, KenKnight BH, and Chattipakorn N. Vagus nerve stimulation initiated late during ischemia, but not reperfusion, exerts cardioprotection via amelioration of cardiac mitochondrial dysfunction. *Heart Rhythm* 11: 2278-2287, 2014.
171. Shinlapawittayatorn K, Chinda K, Palee S, Surinkaew S, Thunsiri K, Weerateerangkul P, Chattipakorn S, KenKnight BH, and Chattipakorn N. Low-amplitude, left vagus nerve stimulation significantly attenuates ventricular dysfunction and infarct size through prevention of mitochondrial dysfunction during acute ischemia-reperfusion injury. *Heart Rhythm* 10: 1700-1707, 2013.
172. Shivkumar K, Ajijola OA, Anand I, Armour JA, Chen PS, Esler M, De Ferrari GM, Fishbein MC, Goldberger JJ, Harper RM, Joyner MJ, Khalsa SS, Kumar R, Lane R, Mahajan A, Po S, Schwartz PJ, Somers VK, Valderrabano M, Vaseghi M, and Zipes DP. Clinical neurocardiology defining the value of neuroscience-based cardiovascular therapeutics. *J Physiol*594: 3911-3954, 2016.
173. Soin A, Shah NS, and Fang ZP. High-frequency electrical nerve block for postamputation pain: a pilot study. *Neuromodulation* 18: 197-205; discussion 205-196, 2015.
174. Stavrakis S, Humphrey MB, Scherlag BJ, Hu Y, Jackman WM, Nakagawa H, Lockwood D, Lazzara R, and Po SS. Low-level transcutaneous electrical vagus nerve stimulation

suppresses atrial fibrillation. *Journal of the American College of Cardiology* 65: 867-875, 2015.

175. Sundman E and Olofsson PS. Neural control of the immune system. *Advances in physiology education* 38: 135-139, 2014.
176. Thoren P, Shepherd JT, and Donald DE. Anodal block of medullated cardiopulmonary vagal afferents in cats. *Journal of applied physiology: respiratory, environmental and exercise physiology* 42: 461-465, 1977.
177. Tsutsumi T, Ide T, Yamato M, Kudou W, Andou M, Hirooka Y, Utsumi H, Tsutsui H, and Sunagawa K. Modulation of the myocardial redox state by vagal nerve stimulation after experimental myocardial infarction. *Cardiovascular research* 77: 713-721, 2008.
178. Tung R, Vaseghi M, Frankel DS, Vergara P, Di Biase L, Nagashima K, Yu R, Vangala S, Tseng CH, Choi EK, Khurshid S, Patel M, Mathuria N, Nakahara S, Tzou WS, Sauer WH, Vakil K, Tedrow U, Burkhardt JD, Tholakanahalli VN, Saliaris A, Dickfeld T, Weiss JP, Bunch TJ, Reddy M, Kanmanthareddy A, Callans DJ, Lakkireddy D, Natale A, Marchlinski F, Stevenson WG, Della Bella P, and Shivkumar K. Freedom from recurrent ventricular tachycardia after catheter ablation is associated with improved survival in patients with structural heart disease: An International VT Ablation Center Collaborative Group study. *Heart Rhythm* 12: 1997-2007, 2015.
179. Uitterdijk A, Yetgin T, te Lintel Hekkert M, Sneep S, Krabbendam-Peters I, van Beusekom HM, Fischer TM, Cornelussen RN, Manintveld OC, Merkus D, and Duncker DJ. Vagal nerve stimulation started just prior to reperfusion limits infarct size and no-reflow. *Basic research in cardiology* 110: 508, 2015.
180. Upadhya B and Kitzman DW. Management of Heart Failure with Preserved Ejection Fraction: Current Challenges and Future Directions. *Am J Cardiovasc Drugs*, 2017.
181. Van Buyten JP, Al-Kaisy A, Smet I, Palmisani S, and Smith T. High-frequency spinal cord stimulation for the treatment of chronic back pain patients: results of a prospective multicenter European clinical study. *Neuromodulation : journal of the International Neuromodulation Society* 16: 59-65; discussion 65-56, 2013.
182. Vanoli E, De Ferrari GM, Stramba-Badiale M, Hull SS, Jr., Foreman RD, and Schwartz PJ. Vagal stimulation and prevention of sudden death in conscious dogs with a healed myocardial infarction. *Circ Res* 68: 1471-1481, 1991.
183. Vaseghi M, Gima J, Kanaan C, Ajijola OA, Marmureanu A, Mahajan A, and Shivkumar K. Cardiac sympathetic denervation in patients with refractory ventricular arrhythmias or electrical storm: intermediate and long-term follow-up. *Heart Rhythm* 11: 360-366, 2014.

184. Vaseghi M and Shivkumar K. The role of the autonomic nervous system in sudden cardiac death. *Progress in cardiovascular diseases* 50: 404-419, 2008.
185. Vaseghi M, Yamakawa K, Sinha A, So EL, Zhou W, Ajijola OA, Lux RL, Laks M, Shivkumar K, and Mahajan A. Modulation of regional dispersion of repolarization and T-peak to T-end interval by the right and left stellate ganglia. *Am J Physiol Heart Circ Physiol*305: H1020-1030, 2013.
186. Vrabec T, Bhadra N, Acker G, and Kilgore K. Continuous Direct Current Nerve Block Using Multi Contact High Capacitance Electrodes. *IEEE Trans Neural Syst Rehabil Eng*, 2016.
187. Vrabec T, Bhadra N, Wainright J, Franke M, and Kilgore K. Characterization of high capacitance electrodes for the application of direct current electrical nerve block. *Med Biol Eng Comput* 54: 191-203, 2016.
188. W J. *The Integrative Action of the Autonomic Nervous System: Neurobiology of Homeostasis* New York: Cambridge University Press, 2006.
189. Wang Z, Yu L, Chen M, Wang S, and Jiang H. Transcutaneous electrical stimulation of auricular branch of vagus nerve: a noninvasive therapeutic approach for post-ischemic heart failure. *International journal of cardiology* 177: 676-677, 2014.
190. Wang Z, Yu L, Wang S, Huang B, Liao K, Saren G, Tan T, and Jiang H. Chronic intermittent low-level transcutaneous electrical stimulation of auricular branch of vagus nerve improves left ventricular remodeling in conscious dogs with healed myocardial infarction. *Circulation Heart failure* 7: 1014-1021, 2014.
191. Waxman SG. *Clinical neuroanatomy*. New York: McGraw-Hill Education/Medical, 2013.
192. Wilde AA, Bhuiyan ZA, Crotti L, Facchini M, De Ferrari GM, Paul T, Ferrandi C, Koolbergen DR, Odero A, and Schwartz PJ. Left cardiac sympathetic denervation for catecholaminergic polymorphic ventricular tachycardia. *N Engl J Med* 358: 2024-2029, 2008.
193. Xueyi X, Lee SW, Johnson C, Ippolito J, KenKnight BH, and Tolkacheva EG. Intermittent vagal nerve stimulation alters the electrophysiological properties of atrium in the myocardial infarction rat model. *Conference proceedings : Annual International Conference of the IEEE Engineering in Medicine and Biology Society IEEE Engineering in Medicine and Biology Society Annual Conference* 2014: 1575-1578, 2014.
194. Yamakawa K, Rajendran PS, Takamiya T, Yagishita D, So EL, Mahajan A, Shivkumar K, and Vaseghi M. Vagal nerve stimulation activates vagal afferent fibers that reduce

cardiac efferent parasympathetic effects. *Am J Physiol Heart Circ Physiol*309: H1579-1590, 2015.

195. Yamakawa K, So EL, Rajendran PS, Hoang JD, Makkar N, Mahajan A, Shivkumar K, and Vaseghi M. Electrophysiological effects of right and left vagal nerve stimulation on the ventricular myocardium. *Am J Physiol Heart Circ Physiol*307: H722-731, 2014.
196. Yancy CW, Jessup M, Bozkurt B, Butler J, Casey DE, Jr., Drazner MH, Fonarow GC, Geraci SA, Horwich T, Januzzi JL, Johnson MR, Kasper EK, Levy WC, Masoudi FA, McBride PE, McMurray JJ, Mitchell JE, Peterson PN, Riegel B, Sam F, Stevenson LW, Tang WH, Tsai EJ, Wilkoff BL, American College of Cardiology F, and American Heart Association Task Force on Practice G. 2013 ACCF/AHA guideline for the management of heart failure: a report of the American College of Cardiology Foundation/American Heart Association Task Force on Practice Guidelines. *Journal of the American College of Cardiology* 62: e147-239, 2013.
197. Yang D, Xi Y, Ai T, Wu G, Sun J, Razavi M, Delapasse S, Shurail M, Gao L, Mathuria N, Elayda M, and Cheng J. Vagal stimulation promotes atrial electrical remodeling induced by rapid atrial pacing in dogs: evidence of a noncholinergic effect. *Pacing and clinical electrophysiology : PACE* 34: 1092-1099, 2011.
198. Yoo PB, Liu H, Hincapie JG, Ruble SB, Hamann JJ, and Grill WM. Modulation of heart rate by temporally patterned vagus nerve stimulation in the anesthetized dog. *Physiological reports* 4, 2016.
199. Yu H, Tang M, Yu J, Zhou X, Zeng L, and Zhang S. Chronic vagus nerve stimulation improves left ventricular function in a canine model of chronic mitral regurgitation. *Journal of translational medicine* 12: 302, 2014.
200. Yu L, Scherlag BJ, Li S, Fan Y, Dyer J, Male S, Varma V, Sha Y, Stavrakis S, and Po SS. Low-level transcutaneous electrical stimulation of the auricular branch of the vagus nerve: a noninvasive approach to treat the initial phase of atrial fibrillation. *Heart Rhythm* 10: 428-435, 2013.
201. Yuan BX, Ardell JL, Hopkins DA, Losier AM, and Armour JA. Gross and microscopic anatomy of the canine intrinsic cardiac nervous system. *The Anatomical record* 239: 75-87, 1994.
202. Yuan H and Silberstein SD. Vagus Nerve and Vagus Nerve Stimulation, a Comprehensive Review: Part I. *Headache*, 2015.

203. Yuncu G, Turk F, Ozturk G, and Atinkaya C. Comparison of only T3 and T3-T4 sympathectomy for axillary hyperhidrosis regarding treatment effect and compensatory sweating. *Interactive cardiovascular and thoracic surgery* 17: 263-267, 2013.
204. Zabara J. Inhibition of experimental seizures in canines by repetitive vagal stimulation. *Epilepsia* 33: 1005-1012, 1992.
205. Zamotrinsky AV, Kondratiev B, and de Jong JW. Vagal neurostimulation in patients with coronary artery disease. *Autonomic neuroscience : basic & clinical* 88: 109-116, 2001.
206. Zanchetti A, Wang SC, and Moruzzi G. The effect of vagal afferent stimulation on the EEG pattern of the cat. *Electroencephalography and clinical neurophysiology* 4: 357-361, 1952.
207. Zannad F, De Ferrari GM, Tuinenburg AE, Wright D, Brugada J, Butter C, Klein H, Stolen C, Meyer S, Stein KM, Ramuzat A, Schubert B, Daum D, Neuzil P, Botman C, Castel MA, D'Onofrio A, Solomon SD, Wold N, and Ruble SB. Chronic vagal stimulation for the treatment of low ejection fraction heart failure: results of the NEural Cardiac TherApy foR Heart Failure (NECTAR-HF) randomized controlled trial. *Eur Heart J* 36: 425-433, 2015.
208. Zhang Y, Popovic ZB, Bibevski S, Fakhry I, Sica DA, Van Wagoner DR, and Mazgalev TN. Chronic vagus nerve stimulation improves autonomic control and attenuates systemic inflammation and heart failure progression in a canine high-rate pacing model. *Circulation Heart failure* 2: 692-699, 2009.
209. Zheng C, Li M, Inagaki M, Kawada T, Sunagawa K, and Sugimachi M. Vagal stimulation markedly suppresses arrhythmias in conscious rats with chronic heart failure after myocardial infarction. *Conference proceedings : Annual International Conference of the IEEE Engineering in Medicine and Biology Society IEEE Engineering in Medicine and Biology Society Annual Conference* 7: 7072-7075, 2005.
210. Zheng ZJ, Croft JB, Giles WH, and Mensah GA. Sudden cardiac death in the United States, 1989 to 1998. *Circulation* 104: 2158-2163, 2001.
211. Zipes DP, Festoff B, Schaal SF, Cox C, Sealy WC, and Wallace AG. Treatment of ventricular arrhythmia by permanent atrial pacemaker and cardiac sympathectomy. *Ann Intern Med* 68: 591-597, 1968.
212. Zucker IH, Patel KP, and Schultz HD. Neurohumoral stimulation. *Heart failure clinics* 8: 87-99, 2012.

CHAPTER 2:

VAGUS NERVE STIMULATION MITIGATES INTRINSIC CARDIAC NEURONAL REMODELING AND CARDIAC HYPERTROPHY INDUCED BY CHRONIC PRESSURE OVERLOAD IN GUINEA PIG

INTRODUCTION

Autonomic control of the heart is mediated by complex interactions occurring throughout the peripheral and central components of the cardiac neuroaxis (11, 27, 62). Neural activity within the intrathoracic autonomic ganglia is influenced by afferent and preganglionic efferent inputs as processed by local circuit neurons with subsequent modulation of post-ganglionic efferent outflows to all regions of the heart (11, 14). Consequently, the cardiac neuroaxis can be considered as a potential target for bioelectric neuromodulation strategies to treat select cardiac pathologies (19, 21, 23, 49, 61). In that regard, we have demonstrated that select pathologies are associated with time dependent changes in its intrinsic cardiac component (30, 32, 37). For example, for states of chronic pressure overload (PO), myocyte hypertrophy results in altered neural control associated with enhanced numbers of nitric oxide synthase immunoreactive IC neurons along with increased density of mast cells in the intrinsic cardiac nervous system (ICNS) (30). The neurohumoral remodeling associated with PO is further indicated by the effects of chronic beta blockade (e.g. timolol) that inhibits the synergism between angiotensin II and norepinephrine to increase IC neuronal excitability and to likewise reduce synaptic efficacy within the intrinsic cardiac neuronal network (34). The therapeutic efficiency of pharmacological (beta-adrenergic, ACE inhibitors and angiotensin receptor blockers) and bioelectric manipulations of intrinsic cardiac nervous system are pronounced, especially during dynamic states of disease progression (15, 33, 34).

Alterations in sensory transduction are central to the reflex adaptations that occur in the cardiac nervous system in response to cardiac pathology (3, 13, 58). Alterations in sensory inputs arising from cardiac and cardiovascular afferent neurons transducing PO are reflected in central-mediated reflex sympatho-excitation coupled with a corresponding reduction in central neuronal drive of cardiac parasympathetic efferent neurons (38, 62). Bioelectric therapy directed at the cervical vagus has the potential to impact multiple levels of the hierarchy for cardiac control via it activation of ascending (afferent) and descending (efferent) axons (8, 43, 59). Bioelectric activation of afferent fibers impacts central drive for both sympathetic and parasympathetic nervous systems (5, 8). Electrical activation of preganglionic parasympathetic fibers can impact sympathetic-parasympathetic interactions mediated within intrinsic cardiac ganglia (14, 28, 46, 51) and at the end-effectors of the heart (43, 44, 53). It is the dynamic interplay between central and peripheral reflex control that ultimately determines functional neural regulation of regional cardiac function (11).

Since central parasympathetic outflow is reduced as a compensatory response to chronic cardiac insults (25, 27, 62), we hypothesize that restoration of biomimetic levels of

"central" parasympathetic drive via cervical VNS mitigates adverse remodeling of the intrinsic cardiac nervous system (ICNS) evoked in reflex response to PO. We propose that cardiac myocytes are rendered 'stress resistant' due in part to attenuation of excessive sympathetic drive to intrinsic cardiac neurons and cardiac end-effectors. We further propose that VNS will stabilize peripheral reflex processing by limiting adverse remodeling of synaptic efficacy within the ICNS. Finally, we propose that VNS imparts changes in myocyte metabolic function in response to alterations in neural inputs. To mechanistically evaluate this hypothesis, we studied intrinsic cardiac neuronal and cardiac function in response to chronic PO of the left ventricle in order to determine how VNS impacts: i) passive and active membrane properties of the ICNS such that ii) cardiac hemodynamics are maintained even in the face of a sustained afterload stressor.

MATERIALS AND METHODS

All procedures were approved by the Institutional Animal Care and Use Committee of East Tennessee State University and were in accordance with the Guide for the Care and Use of Laboratory Animals, Eighth Edition, National Academy Press, Washington DC, 2010. Implantation of VNS systems: 48 male Hartley guinea pigs (Charles River), weighing between 500 and 650 g (9 week-old), were implanted with bipolar vagus nerve stimulation (VNS) electrodes connected to a pulse generator. Under aseptic conditions, animals were pretreated with atropine (0.1mg/kg, SQ) and ketamine (80mg/kg, IP). Thereafter, anesthesia was induced with 3% isoflurane via an induction chamber (VetEquip Inc., Pleasanton, CA). Upon removal from the induction chamber, 2.5% isoflurane was delivered via a conical nose cone (VetEquip Inc.) until responses to hind limb toe pinch stimuli were absent. Following endotracheal intubation, mechanical ventilation was initiated and maintained with a positive pressure ventilator (SAR-830/P ventilator, IITC Inc., Woodland Hills, CA) using 100% O2. Anesthesia was maintained with isoflurane (1-3%). Core body temperature was maintained at 38.5˚C via a circulating water heating pad. Buprenorphine (0.05 mg/kg, SQ) was administered preoperatively.

Following anesthesia induction, a midline neck incision was made in the ventral neck. Either the right or left vagus nerve and the adjacent carotid arteries were identified, isolated and a bipolar VNS electrode (PerennialFlex, Cyberonics, Inc.) positioned around that artery-nerve complex. The leads were secured in place and tunneled to a subcutaneous pocket created over the dorsal aspect of the back where the implantable VNS pulse generator (Demipulse, Model 103, Cyberonics, Inc.) was positioned. The incisions were closed in layers. Subsequent post-

operative care included Buprenorphine (0.05 mg/kg, sc, prn) and Cefazolin (30mg/kg, im) administered for seven days. The pulse generator remained inactive during the recovery period (~2 weeks duration).

Animal Identification: At the time of VNS system implant, an AVID® microchip (AVID® MicroChip I.D. Systems, Folsom, LA) was placed into the interscapular subcutaneous space using a 12 gauge needle. A MiniTracker™ (AVID® MicroChip I.D. Systems, Folsom, LA) scanner was passed over the implant site to detect the unique identification number chosen for each animal.

Induction of Chronic Pressure Overload: Two weeks following the VNS stimulator implant, pressure overload (PO) was induced. Using the same anesthetic regimen detailed above for VNS implant under aseptic surgical techniques, a left thoracotomy was performed in the 2nd-3rd intercostal space to expose the descending thoracic aorta. Uniform constriction of the thoracic aorta was produced by tying a 3-0 surgical ligature around a metal tube (1-2mm external diameter and approximately 1 cm length made from 18 gauge needle) placed adjacent to the descending aorta. Following suture placement, to produce the aortic constriction, the metal tube was removed. After placing a flexible chest tube into the chest cavity and closing the rib space, local musculature and subcutaneous tissues were closed with absorbable sutures; the skin was closed with non-absorbable sutures. Once the chest was closed, residual air was withdrawn via the chest tube, it was removed and spontaneous ventilation was reinstituted. Post-operative care included Buprenorphine (0.05 mg/kg, sc) given as needed and Cefazolin (30mg/kg, im) administered once per day for the next seven days. Animals were maintained for (on average) 50 days post-PO induction. In this group of PO animal, 17 animals with PO induction demonstrated clinical signs of pulmonary congestion within a few days; these animals were euthanized within 0-2 days of PO onset. As such, these animals were not included in subsequent data accumulation.

Neuromodulation therapy: In 19 of these animals, active VNS therapy was initiated 10 days following PO induction. Of these, 10 were treated with right-sided VNS and 9 with left-sided VNS. These groups are designated RCV-PO and LCV-PO respectively. The parameters chosen for VNS therapy were close to the neural fulcrum where we have demonstrated that any effects on heart rate are minimized by the combined effects on VNS on afferent and efferent axonal stimulation within the cervical vagosympathetic complex (8, 15). Continuous cyclic VNS therapy

was delivered at a pulse frequency of 20 Hz, 250μsec pulse duration and a 22.5% duty cycle (14s on phase and 48s off-phase). The average current intensity was 1.13±0.04 mA for RCV and 1.17±0.06 mA for LCV. The intensity of stimulation elicited by VNS therapy was limited in the guinea pig over time by its effects on animal water and/or food intakes. In those animals that did not exhibit bradycardia, attempts to further increase stimulus intensity resulted in loss of body weight. Twelve of the animals had VNS system implant that remained inactive throughout the 50 day chronic PO induction (sham treatment control group). Time-matched controls (n=9) were also evaluated concurrently with the PO models.

Cardiac indices: Following sedation with isoflurane (1-2% via nose cone), short-axis echocardiograms were used to determine left ventricular internal diameters at end-systole and end-diastole (LVIDs and LVIDd), along with estimated left ventricular volume such that stroke volume could be estimated. Using those data and heart rate data, cardiac output was derived in each animal in the initial and final stages of each experiment. As such, these indices were determined prior to PO and/or VNS implant as well as at 50 days post PO just prior to the terminal experiment.

Following completion of echo, the isoflurane dose was increased to 2.5% until responses to hind limb toe pinch stimuli were absent. Following endotracheal intubation, mechanical ventilation was initiated and maintained with a positive pressure ventilator (SAR-830/P ventilator, IITC Inc., Woodland Hills, CA) using 100% O2. The right carotid artery was isolated and a 2Fr pressure/volume catheter connected to a MPVS single segment system (Millar Instruments, Houston, TX) was inserted into it and advanced to the left ventricle. From this catheter, indices of LV performance including systolic pressure (LVSP), end diastolic pressure (LVEDP) and rate of change of LV developed pressure (LV +dp/dt and LV –dp/dt) were determined along with basal heart rate.

Terminal Experiments: Following echocardiographic and LV hemodynamic analyses, animals were euthanized via CO2 inhalation. The heart and lungs were removed rapidly and placed into ice-cold Krebs Ringer solution (mM: NaCl 121, KCl 5.9, CaCl2 2.5, MgCl2 1.2, NaH2PO4 1.2, NaHCO3 25, glucose 8, aerated with 95% O2/ 5% CO2 for a pH of 7.4). Hearts were weighed. The lungs were dried at 37 ºC and weighed (dry lungs). The intrinsic cardiac nerve plexus located in the epicardium of dorsal atrial walls was dissected free of other tissues and placed in a tissue bath so that tissues could be continuously superfused (6-8 mL/min) with 35-37°C Krebs Ringer.

Preparation of guinea pig heart homogenates and western blots: The ventricles from time matched control, PO, LCV-PO and RCV-PO guinea pigs were removed and, following brief washing in ice-cold PBS to remove blood, the left ventricle was removed, flash frozen, and ground into a fine powder using a liquid nitrogen-jacketed mortar and pestle. The frozen heart powder was homogenized in RIPA buffer composed of 50 mM Tris·HCl, pH 7.4 (Calbiochem, Darmstadt, Germany), 1% Triton X-100 (Fisher, Fair Lawn, NJ), 1% w/v sodium deoxycholate (Fisher, Fair Lawn, NJ), 0.1% w/v SDS (EMD, Billerica, MA), and 1 mM EDTA (Fisher, Fair Lawn, NJ) with 1:100 v/v protease inhibitor cocktail mix (Sigma, St. Louis, MO). These homogenates were incubated on ice for 1 h and then centrifuged at 12,000 rpm at 4°C for 10 min. Thereafter, the supernatant was collected so that the following assays of tissues could be performed.

Protein quantification of lysates was performed on ventricular homogenates using the Pierce BCA protein assay kit (Thermoscientific, Rockford, IL), according to the manufacture protocol. Protein samples were subjected to SDS-PAGE using Pierce Tris-HEPES-SDS precast 4-20% polyacrylamide mini gels (Thermoscientific, Rockford, IL). Proteins were transferred to PVDF membranes (Bio-Rad Laboratories, Hercules, CA) and Ponceau S (Sigma, St. Louis, MO) staining was used to ensure complete transfer and equal protein loading. Membranes were blocked in 5% nonfat dry milk (Bio-Rad Laboratories, Hercules, CA) in TBS with 0.1% Tween 20 (TBS-T) for 1 h at room temperature.

Phospho-BAD (p-BAD) and BAD were exposed to ventricular tissues incubated with rabbit monoclonal primary antibodies diluted 1:1000 in TBS-T (Cell signaling, Danvers, MA). BAX, Bcl-XL, Phospho-Akt (p-Akt). Glycogen synthase (GS) and Phospho-Glycogen synthase (p-GS) were incubated with rabbit polyclonal primary antibodies diluted 1:1000 in TBS-T (Cell signaling, Danvers, MA). Membranes were incubated in primary antibody at 4 °C overnight. After incubation in primary antibody, the membranes were washed for 10 min ×3 in TBS-T before incubation with 1:3000 goat anti-rabbit horseradish peroxidase-conjugated secondary antibodies (EMD Millipore, Temecula, CA) for all of primary antibodies as above at room temperature for 1h. Membranes were washed 3X in TBS-T for 10 min. Pierce supersignal west pico chemiluminescence substrate (Thermoscientific, Rockford, IL) was used for signal detection in the G-Box imaging system (Syngene, Frederick, MD). Densitometry of the protein bands was obtained via ImageJ (National Institutes of Health, Bethesda, MD).

Deoxynucleotide Transferase-Mediated Nick-End Labeling (TUNEL) Assay: Ventricular tissue sections were deparaffinized gradually in xylene and ethanol, followed by fixation in 4%

paraformaldehyde and paraffin embedding (Fisher, Fair Lawn, NJ). Apoptotic guinea pig cardiomyocytes in ventricular tissues were labeled by TUNEL assay using CardioTACS In Situ Detection Kit (R&D Systems, Minneapolis, MN), following manufacturer's instructions. Thereafter, TUNEL-positive stained cardiomyocytes were counted throughout random fields of tissue (×20) (Nikon Eclipse TE2000s). NIH ImageJ software was used for myocyte size determinations of paraffin sections stained with Masson's Trichrome using standard procedures.

Neuronal electrophysiological methods: Neuronal transmembrane properties. Intracellular voltage recordings from intrinsic cardiac neurons derived from explanted intrinsic cardiac ganglia placed in 35-37°C Krebs Ringer solution were obtained by impaling cells with 3 M KCL-filled glass micro-pipettes (40-80 MΩ) using an Axoclamp 2B amplifier (Molecular Devices). Data were collected, digitized and analyzed using pClamp 10.2 (Molecular Devices). Individual neurons were used for data analysis if their RMP was – 40 mV or less and produced action potentials with an overshoot of at least 20 mV. Input resistance was determined using 0.1 and 0.2 nA pulses (500 msec). Neuronal soma excitability was monitored by observing the response to a series of long depolarizing current pulses (0.1-0.6 nA, 500 msec). The number of evoked action potentials (AP) versus stimulus intensity was determined to assess relative changes in excitability. Afterhyperpolarization (AHP) durations were analyzed to determine the time needed to reach 50% of the amplitude from the peak of the AHP to the resting membrane potential.

For each cell, following characterization of the basic electrophysiological properties, induced changes in the number of evoked AP's by depolarizing pulses were again assessed immediately following a 1-2 sec application of norepinephrine (NE, Sigma, 10-3 M) or bethanechol (a muscarinic agonist, Sigma, 10-3 M). Drugs were applied by local pressure ejection (6-9 psi, Picospritzer, General Valve Corp) through small tip diameter (5-10 μm) glass micropipettes positioned 50-100 μm from the individual neuron. For multiple tests of responses in the same cell, the cells were allowed to wash (via the circulating Krebs solution) for several minutes between applications, until the responses returned to control levels.

Neuronal electrophysiological methods: Neuronal synaptic efficacy. To activate synaptic inputs to investigated neurons, a bipolar concentric electrode was placed on nerve bundles connected to the ganglion containing the neuron of interest. Orthodromic responses to fiber tract stimulation (0.1 – 10 V, 1 msec duration) were assessed by studying i) the ability of axonal activation to generate an excitatory post synaptic potential (EPSP) and/or ii) the presence of a time delay between the stimulus artifact and a neuronal response. Suprathreshold stimuli

leading to action potentials were then applied in 2 sec trains at varying frequencies (5, 10, 20 and 30 Hz). The number of action potentials produced by the neuron of interest at each stimulus frequency was assessed.

Statistical Analysis: Cardiac indices recorded in the control, PO and different therapy states were analyzed via ANOVA to compare changes induced among different animal groups compared to baseline conditions, as well as among groups. All pairwise post-hoc multiple comparisons were made with the Holm-Sidak method. As neuronal activity was not normally distributed when analyzed using a Shapiro-Wilk test, a non-parametric Friedman test was utilized at the ordinal level, followed by post-hoc Wilcoxon signed-rank tests with a Bonferroni correction to determine differences in neural data obtained in the different study groups. The data depicting heart rate and LV pressure indices (Table 1), tissue weights (Table 2), along with neuronal transmembrane properties (Table 3), synaptic properties (Figure 3) as well as myocyte structure (Figure 5) and function (Figures 6-8) were found to be continuous and normally distributed by using a Shapiro-Wilk test. These data were analyzed using a simple or a mixed model ANOVA, followed by a Newman–Keuls post-hoc analysis. Results with $p<0.05$ were considered statistically significant. Statistical analyses were conducted using Sigma Plot 12 software.

RESULTS

Hemodynamic indices. Paired echocardiographic assessments, from baseline vs time of termination (51.5 ± 0.5 days post PO induction), demonstrated that LV diameters and volumes (systolic and diastolic) increased significantly in the untreated PO states (Fig. 1). PO likewise was associated with significantly increased LV stroke volume and cardiac output. These PO-induced cardiac changes were minimized by the application of chronic VNS, be it RCV or LCV. In these three chronic PO groups, LV pressure measurement, taken at termination, further indicted that left side VNS therapy differentially increased left ventricular chamber systolic pressure and ± dp/dt relative to either sham VNS or RCV VNS (Table 1).

In support of echocardiographic data, measurement of LV myocyte cross-sectional area confirmed the PO-induced hypertrophy (Fig 2). Note the doubling in myocyte size in the sham VNS group, a response that was mitigated by RCV, but not LCV. In contrast to the myocyte cross-sectional area, no significant differences were found in heart (wet) and lung weights (wet and dry), as a percentage of body weight, among treated groups (Table 2).

Intrinsic cardiac neuronal transmembrane properties: The transmembrane potentials of intrinsic cardiac neurons derived from controls and PO animals, as well as those subjected to right (RCV-PO) vs left (LCV-PO) VNS (including time matched sham VNS; PO) are summarized in Table 3. There were no significant differences identified in the amplitude of after-hyperpolarization (AHP) or neuronal input resistances among groups. However, cellular resting membrane potentials increased (became more negative) in neurons derived from PO animals subjected to RCV therapy compared to controls or animals subjected to PO. AHP half-decay time also increased with right-sided VNS therapy in the presence of PO, as compared to data obtained in the other groups.

Functional excitability of soma, as assessed by measuring the number of action potentials evoked in response to intracellular depolarizing current injection steps, was not significantly altered by PO alone or in response to chronic VNS (Fig. 3). Across all groups, changes in IC neuronal sensitivity elicited by local norepinephrine (NE) application was less than that elicited by bethanechol. Soma excitability to muscarinic agonists was blunted by the presence of chronic RCV or LCV (Fig. 3, lower panels).

Intrinsic cardiac neuronal synaptic efficacy: Input synaptic efficacy was evaluated by measuring intrinsic cardiac neuronal responsiveness during stimulation of axon bundles associated with the ganglia containing these neurons of interest (Fig. 4). Using supra-threshold trains of stimuli (delivered for 2 sec at 5, 10, 20 and 30 Hz), output frequencies of neurons derived from PO animals were significantly greater than those measured in controls (Fig. 5; Control). While, right-sided VNS was effective in restoring this index to control values (Fig. 5; PO+RCV), left-sided VNS only showed a tendency to reduce that index.

Cardiomyocytes: Chronic PO alters cardiomyocyte structure and function (Figs 1 and 2). One aspect of this remodeling can involve changes in energy utilization (54). Glycogen synthase protein levels were significantly depressed in PO tissue (Fig 6). Moreover the ratio of the inactive phosphorylated form of glycogen synthase (pGS) to the unphosphorylated form was increased with PO. These changes are consistent with greater mobilization/utilization of glucose in the PO tissue. The changes in GS expression, induced by PO, were significantly mitigated by LCV but not RCV.

Apoptosis contributes to the transition from hyper-dynamic hypertrophied myocardium to chronic heart failure and the potential for sudden cardiac death (27, 38). The levels of phosphorylated Akt (pAkt), the active anti-apoptotic form of the kinase, were significantly

reduced in PO tissue (Fig 7E). Chronic LCV significantly blunted this effect of PO on pAkt levels compared to PO-sham VNS. BAX and BCL-xL levels were examined and not found to change significantly among the experimental groups (not shown). Bcl-2-associated death promoter (BAD) protein levels were elevated in PO tissue. BAD phosphorylation status was not found to significantly differ among the experimental groups (Fig 7B). However, VNS led to significant reductions in gross BAD protein levels (Fig 7C). While circumstantial, these findings suggested that VNS may exert anti-apoptotic effects upon the stressed myocardium. This led us to evaluate the occurrence of apoptosis within the myocardium. PO tissue was found to contain significantly more apoptotic nuclei compared to control unstressed tissue (Fig 8). However, VNS was found to be without significant effect upon the numbers of myocytes undergoing apoptosis in response to PO stress.

DISCUSSION

A critical bench mark for any interventional therapy applied in progressive cardiovascular pathology is ultimately its efficacy to preserve cardiac function, often in the presence of a sustained stressor. Aortic banding provides a model of chronic pressure overload stress that remains throughout (30, 38). From an echocardiographic perspective, the time point that was evaluated herein reflected a hyperdynamic state characterized by a 34% increase of cardiac output with a corresponding increase in both systolic and diastolic left ventricular volumes. From a histomorphometric perspective, myocyte cross-section area doubled with PO. From an autonomic perspective, withdrawal of central parasympathetic drive coupled with reflex mediated sympatho-excitation and concurrent activation of Angiotensin II contributed to the adverse remodeling (24, 33, 34, 38). This neurohumoral interplay represents an emerging target for therapeutics (19, 24, 25). This study demonstrated that chronic vagus nerve stimulation (VNS) therapy directly targets the intrinsic cardiac nervous system, when appropriately applied, such that left ventricular functional deterioration during the evolution of chronic LV pressure overload is mitigated. Our data further indicate that mitigation of adverse PO-induced remodeling involves both myocyte and neural dependent mechanisms.

VNS and cardioprotection: PO-induced heart failure is accompanied by changes in the ventricular metabolic profile, affecting among other things a shift to greater reliance on glucose that is associated with downregulation of fatty acid oxidation (54). We found that the ratio of the inactive phosphorylated form of glycogen synthase to the unphosphorylated form increased during the evolution of chronic PO. To our knowledge, this is the first report of GS expression

and phosphorylation status being changed by PO. These changes are consistent with greater mobilization/utilization of glucose in the PO ventricle (54). Furthermore, changes in ventricular GS expression were mitigated by LCV, but not by RCV. Autonomic neural regulation of glucose and fatty acid metabolism is widely appreciated in liver and skeletal muscle (47) in the context of "rest and digest". For instance, stimulation of the vagus nerve causes a large increase in the activity of liver GS (52). Direct neural sympathetic effects include stimulation of glycogenolysis in both skeletal muscle and liver (47). It is thus surprising that an almost total dearth of information exists concerning autonomic effects upon myocardial metabolism. Our data indicate that direct neural control of heart metabolism may be profound and that VNS therapy holds the promise of exploiting metabolic regulation to effect better outcomes in intractable pathologies. While further investigation of this issue is warranted, findings concerning ventricular GS changes indicate a reordering of myocardial metabolism in response to VNS such that the heart becomes more resistant to the pathologic stress associated with PO.

Apoptosis and matrix reorganization contributes to the transition from hyper-dynamic hypertrophied myocardium to heart failure (24, 29, 38). We have recently reported the efficacy of VNS to minimize the pro-apoptotic Bcl-2-associated X (BAX) in guinea pigs with chronic myocardial infarction (MI) (15). By analogy, in the PO model reported herein, the levels of phosphorylated Akt (pAkt), the active anti-apoptotic form of the kinase, were significantly reduced. Importantly, chronic LCV significantly blunted this effect of PO on pAkt levels compared to PO-sham VNS. However, while chronic PO was associated with significantly more apoptotic nuclei compare to normal, VNS did not reduce this maladaptive response to PO stress. The difference in part may reflect differences mediated by eccentric ventricular stressor (e.g. MI) compared to the concentric stress imposed by PO (29, 38, 62). It should be further recognized that many of the proteins evaluated sub-serve dual roles in both apoptotic and hypertrophic cardiac responses (45). Taken together, these data suggest that modulation of cardiac myocyte proteins by VNS relates primarily to the hypertrophic response rather than being dependent upon programmed cell death.

VNS and the autonomic neuraxis-cardiac interface: Neural control of regional cardiac function is dependent upon the dynamic interplay between peripheral and central reflexes (11, 12). The peripheral reflexes involve those contained within the intrinsic cardiac nervous system and within extracardiac autonomic ganglia, including the mediastinal, middle cervical and stellate ganglia (11, 12). Central reflex components of the cardiac nervous system include the spinal, cord, brainstem and higher centers (5, 22, 35). Each of these processing nodes contain

afferent, efferent and neural processing neurons, the later referred to as local circuit neurons (11). Coordination within these networks allows for effective control of regional cardiac function and the distribution of blood flow throughout the body at baseline and in response to stress (11, 39, 41). Stressors that lead to imbalances within these autonomic networks can lead to disruptions in autonomic outflows which in turn can contribute to adverse remodeling of heart mechanical function and the potential for arrhythmias including sudden cardiac death (25, 27, 40). The autonomic imbalances, primarily afferent driven, in turn are associated with adverse neural remodeling in neural circuits from those on the heart up to and including higher centers up to the insular cortex (3, 30, 37, 42, 50). Autonomic regulation therapy, of which VNS is one modality, is predicated on targeting specific processing centers to stabilize excessive reflex responses and thereby to moderate efferent outputs (7, 19, 26, 56).

The intrinsic cardiac nervous system (ICNS) is the most proximal reflex processor of the cardiac nervous system (11). It is primarily associated with short-loop coordination of regional cardiac electrical and mechanical function (11). It consists of aggregates on ganglionated plexi that have specific spheres of influence (6, 20). That being said, the separate aggregates maintain a degree of coordination imposed by local circuit intra- and inter-ganglionic projections, common shared afferent inputs and by descending efferent projections (6, 13, 14, 57). These efferent projections include both sympathetic and parasympathetic efferent axons, with i) direct connections to post-ganglionic soma and ii) multi-synaptic inputs onto the local circuit (processing) neurons of the ICNS (14, 55, 57). It is now recognized that major interactions between sympathetic and parasympathetic efferent neuronal control is exerted both at the level of the ICNS and at the end-terminus of efferent projections to the heart (28, 44, 46, 51). At least in larger animals, vagus projections to the ventricles are widespread and bilateral (9, 60). In contrast, those of the sympathetic tend to be more unilateral (2, 10). This difference in efferent distribution may explain in part the different efficacy of right vs left VNS to impact the cardioneural remodeling induced by PO. Regardless, the anti-adrenergic effects of VNS are likely a major contributor to the preservation of cardiac function in the setting of ischemic and non-ischemic cardiac pathologies.

Cardiac pathologies remodel multiple levels of the neural hierarchy for cardiac control. With respect to heart failure, autonomic regulation is deranged and this is usually reflected in sympatho-excitation with a corresponding decrease in central parasympathetic drive (25, 62). Alterations in neurotransmitter interactions at IC soma in conjunction with alterations in synaptic processing within the ICNS are a reflection of these adaptions (17, 30, 33, 34). This results in changes in passive and active membrane properties that underlie overall network function. The

restoration of synaptic efficacy of IC neurons to “normal” is a reflection of the restraining effects that VNS can exert in peripheral networks. Several potential ionic mechanisms could underlie these observed neuronal responses. Indeed, several muscarinic receptor-mediated changes in ion currents have been described in intrinsic cardiac neurons, including inhibition of the M current, regulation of the delayed rectifier potassium current, inhibition of calcium currents and enhanced intracellular calcium release (1, 4, 16, 48). The downward shift in the modulator effects on IC excitability exerted by muscarinic receptors may reflect in part some of these changes. Defining the specific neuro-mediators and neuro-modulators involved in cardiac disease induced neural remodeling and mechanistically how these are impacted by autonomic regulation therapy remains largely undefined and is a critical area for future studies.

It is also critical to note that the majority of axons in a cervical vagus are afferent in nature, project directly to neurons in the nucleus tractus solitarius of the medulla (5, 18). By activating such afferent axons with VNS therapy, centrally mediated reflexes target both sympathetic and the parasympathetic efferent neurons controlling the heart (8, 59). Recent data indicate that low level VNS can exert afferent mediated withdrawal of centrally-derived parasympathetic efferent activity (59). Further increases in stimulus intensity recruits parasympathetic preganglionic axons with the expected suppression of regional cardiac electrical and mechanical indices (8, 44). We propose that the optimum therapeutic parameters for cervical VNS therapy are at the point at which afferent and efferent fibers are activated in a balanced manner. That is, when afferent mediated decreases in central mediated parasympathetic drive is counteracted by direct activation of the cardiac parasympathetic efferent projections to the ICNS and heart. At this point, the net result is a null HR response. We have defined this as the neural fulcrum (8) and the studies presented herein utilized this concept to establish the adequacy of the VNS protocol.

Limitations: While we were able to demonstrate functional manifestations of VNS-mediated changes in ICNS function, we did not attempt to histologically detect changes to neuronal somata. Further, we did not characterize the phenotype of the IC neurons being recorded from, nor by the techniques utilized could we distinguish between post-ganglionic soma and interneurons contained within the intrinsic cardiac nervous system (14, 36, 48, 50). At least in the guinea pig model, the IC neurons recorded with sharp electrodes are known to be primarily cholinergic in nature (31). Future studies should consider the possible contribution of cardiac disease induced changes in IC neural phenotypes and network interactions that contribute to autonomic dysautonomia associated with ischemic and non-ischemic heart disease.

With respect to VNS therapy, we evaluated only one frequency (20 Hz) at a stimulus intensity where afferent and efferent evoked responses balanced each other such that little or no heart rate changes were evoked (8). As such, VNS was able to engage the cardiac nervous system while minimizing the potential for rebound effects occurring during the off-phase that accompanies an intermittent VNS protocol. Future studies should evaluate other VNS stimulus paradigms (duty cycle, frequency, intensity and pulse width). VNS, as applied herein, non-selectively activates vagal afferent fibers arising from thoracic and visceral structures (8, 18, 19). Future studies should consider the effects of cardiac vs. non-cardiac related afferents in mediating central reflex effects. Finally, VNS was delivered early in the disease process. As such, future studies should also evaluate the efficacy of late onset VNS and evaluate the potential of VNS to reverse remodel an already established hypertrophic state and in even later stages when the hyper-dynamic compensated state is transitioning to decompensated heart failure.

Significance and perspectives: Vagus nerve stimulation (VNS) represents an emerging neuromodulation therapy for treating heart failure. Electrical stimulation of the cervical vagosympathetic truck activates both ascending and descending axonal projections therein, thus having the potential to impact both central and peripheral aspects of the cardiac neuroaxis to modulate cardiomyocytes. The results of this study indicate that, in animal models, the deleterious consequences of long-term PO on cardiac structure/function can be attenuated by chronic VNS therapy. This therapy does so, in part, by directly and reflexly targeting intrinsic cardiac neurons to modify their autonomic outflow and specifically to counteract the sympatho-excitation induced by PO. VNS, via modulation of the neural-myocyte interface, likewise can render a state of cardioprotection in the stressed heart. This protection in part, likely reflects induced changes in cardiomyocyte energy pathways.

FIGURES

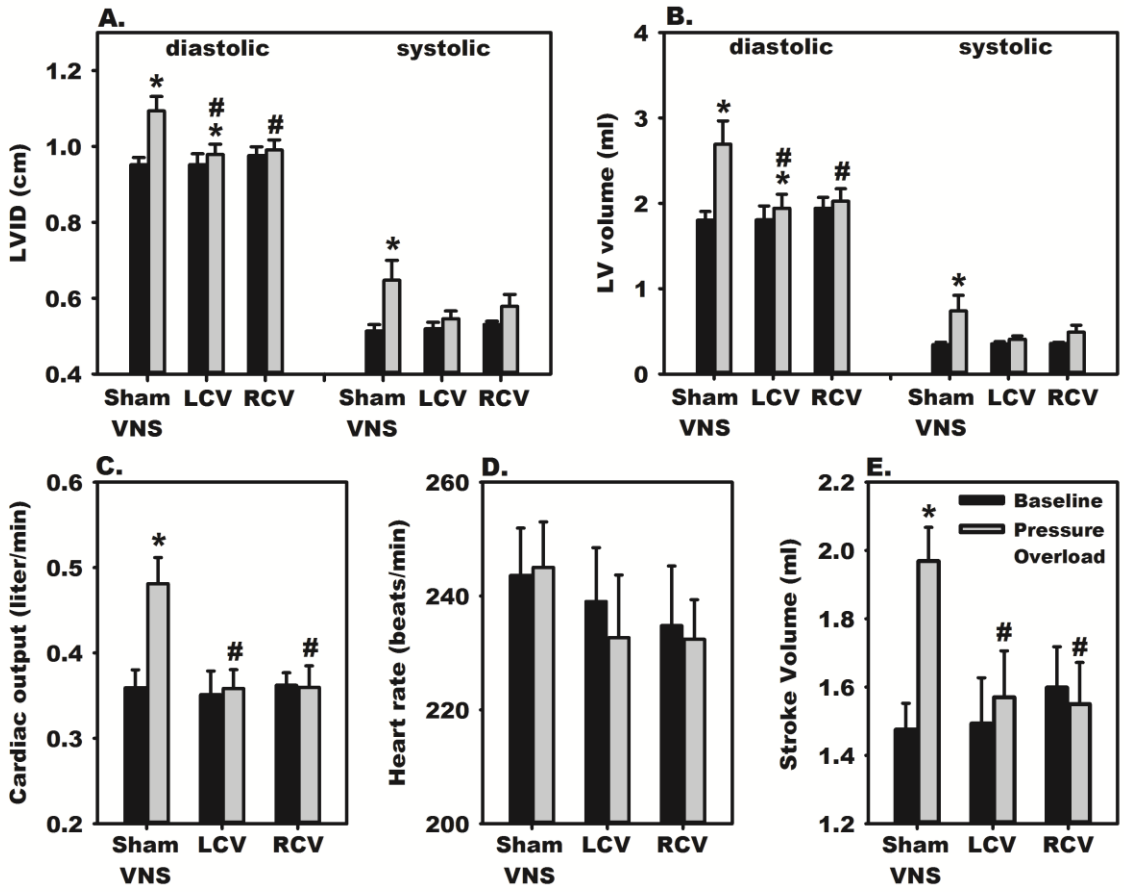

Figure 1: VNS mitigates PO-induced hypertrophy and the hyper-dynamic cardiac behavior. Echocardiographic indices were determined via a short-axis view at baseline (before) and again at 50 days post-PO induction. Sham treatment group had VNS system implant, but without active stimulation. For VNS treatment groups, right (RCV) or left (LCV) cervical vagus stimulation started 10 days post-PO induction and was maintained until termination. # $p<0.05$ baseline vs PO.

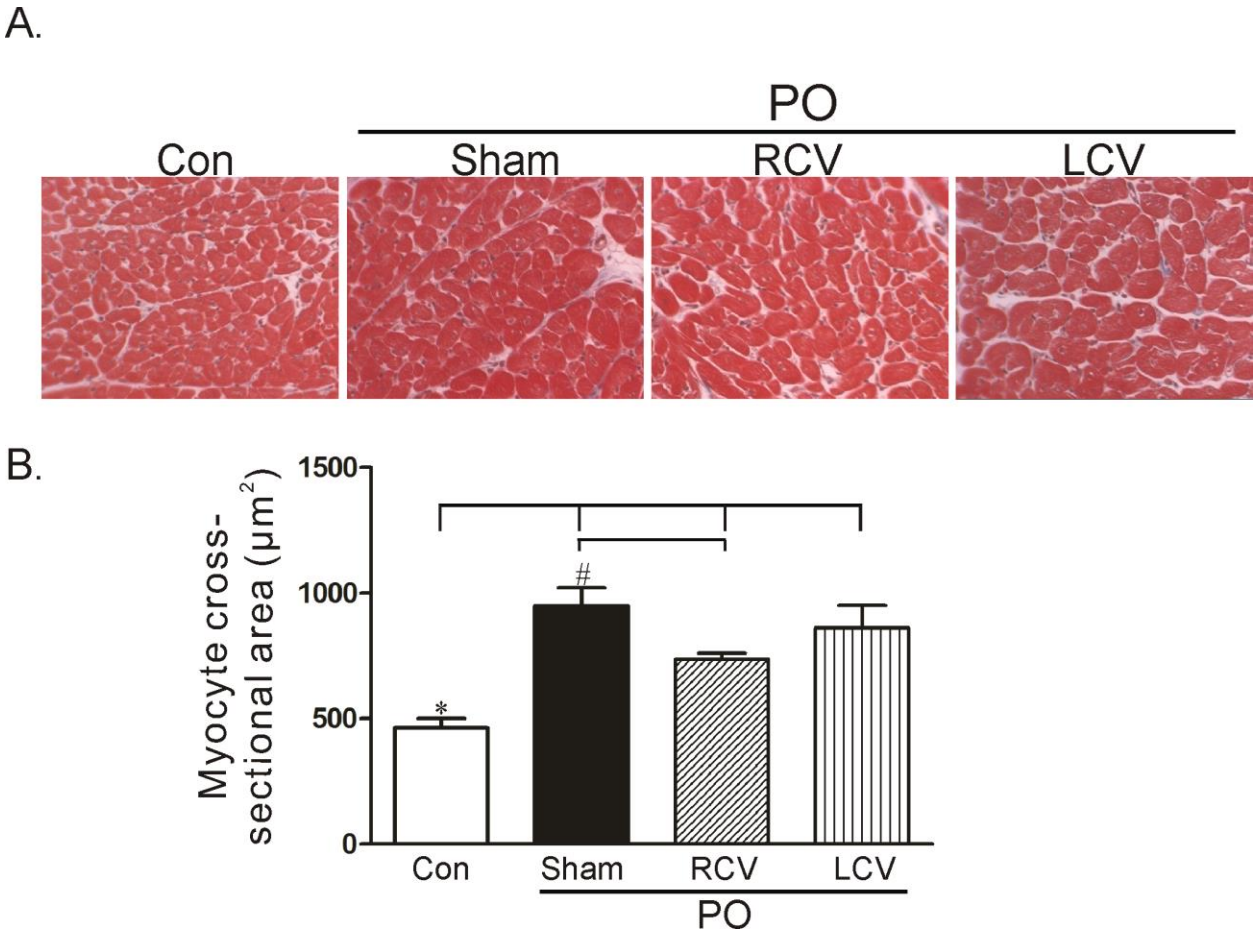

Figure 2: Myocyte hypertrophy associated with PO is significantly reduced by RCV. A: Shows representative Masson's TriChrome stained sections of left ventricular tissue from control and PO hearts. B: The histomorphometric quantification of myocyte cross-sectional areas of the experimental tissues is shown. PO leads to greater myocyte cross-sectional area (*P<0.05). RCV-treated PO tissue had a significant reduction (#P<0.05) in hypertrophy as compared to Sham VNS PO treated tissue.

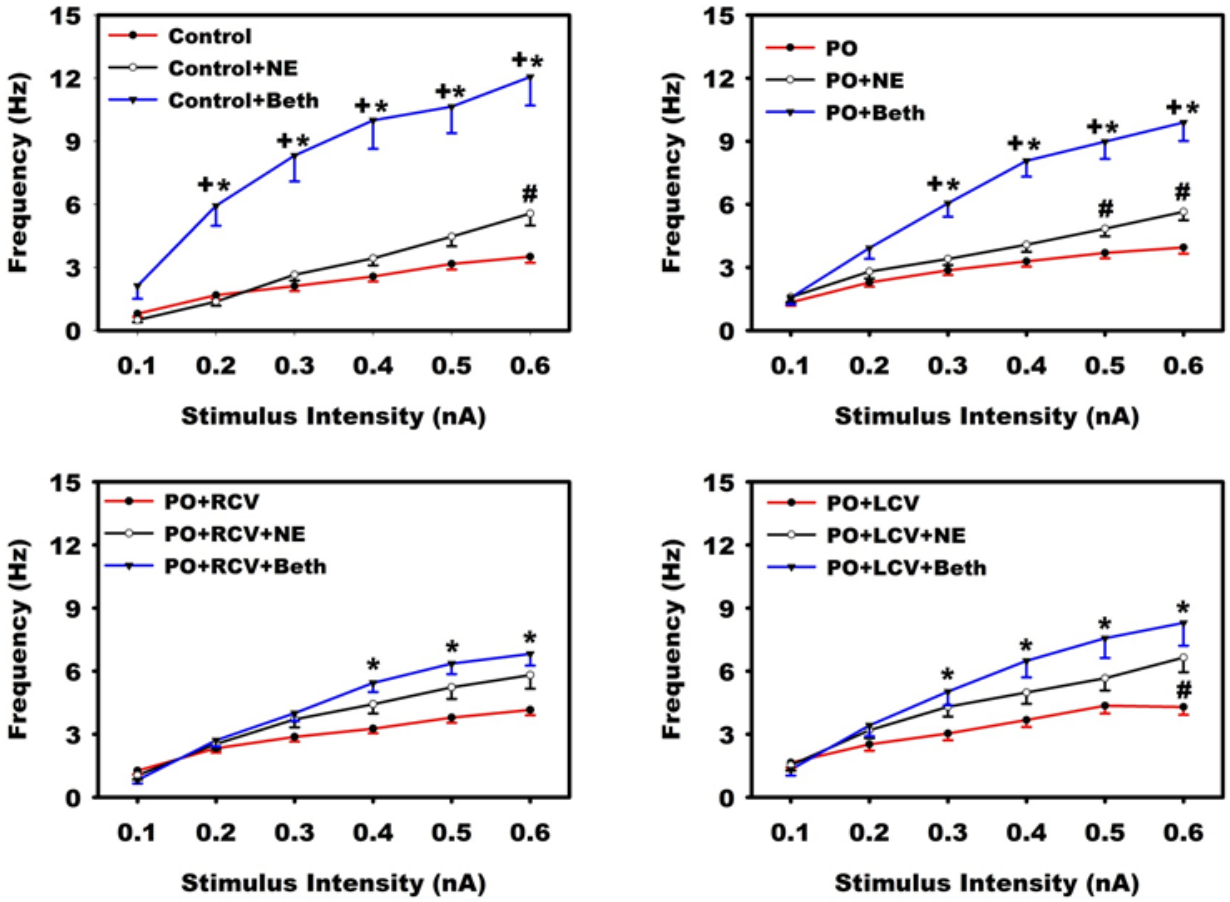

Figure 3: The muscarinic enhancement of neuronal excitability is mitigated with VNS. Evoked action potential frequencies in response to increasing intracellular stimulus intensities were evaluated concurrent with brief (1 s) local exposure to exogenous norepinephrine (NE) or bethanechol (beth) in IC soma derived from control animals and animals following PO with and without chronic VNS (right or left cervical vagus; RCV, LCV). Animals were evaluated 50 days post-PO induction. RCV or LCV started 10 days post-PO induction and maintained to termination. A non-parametric Friedman test was used to evaluate difference among groups followed by Wilcoxon signed-rank post-hoc tests using a Bonferroni correction. Points represent the mean ± SEM from ~60 cells for each condition. * $p<0.05$ baseline (control, PO, PO+RCV or PO+LCV) vs. Beth; + $p<0.05$ NE vs. Beth; # baseline (control, PO, PO+RCV or PO+LCV) vs. NE.

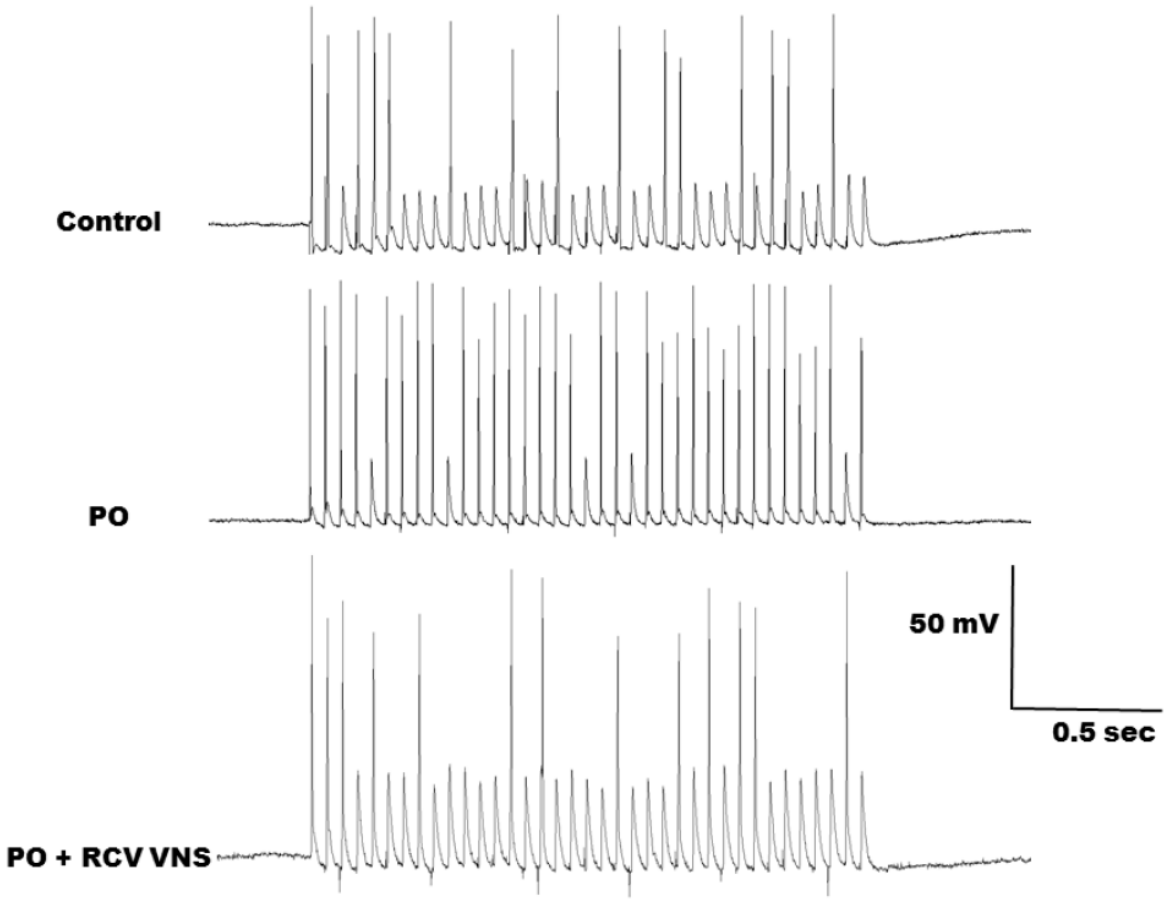

Figure 4: Representative responses of IC neurons to local bioelectric stimulation of primary nerve inputs. Neurons were derived control, PO and PO+RCV VNS animal models (top to bottom traces). Nerve fiber stimulation was at 20 Hz for 2 sec.

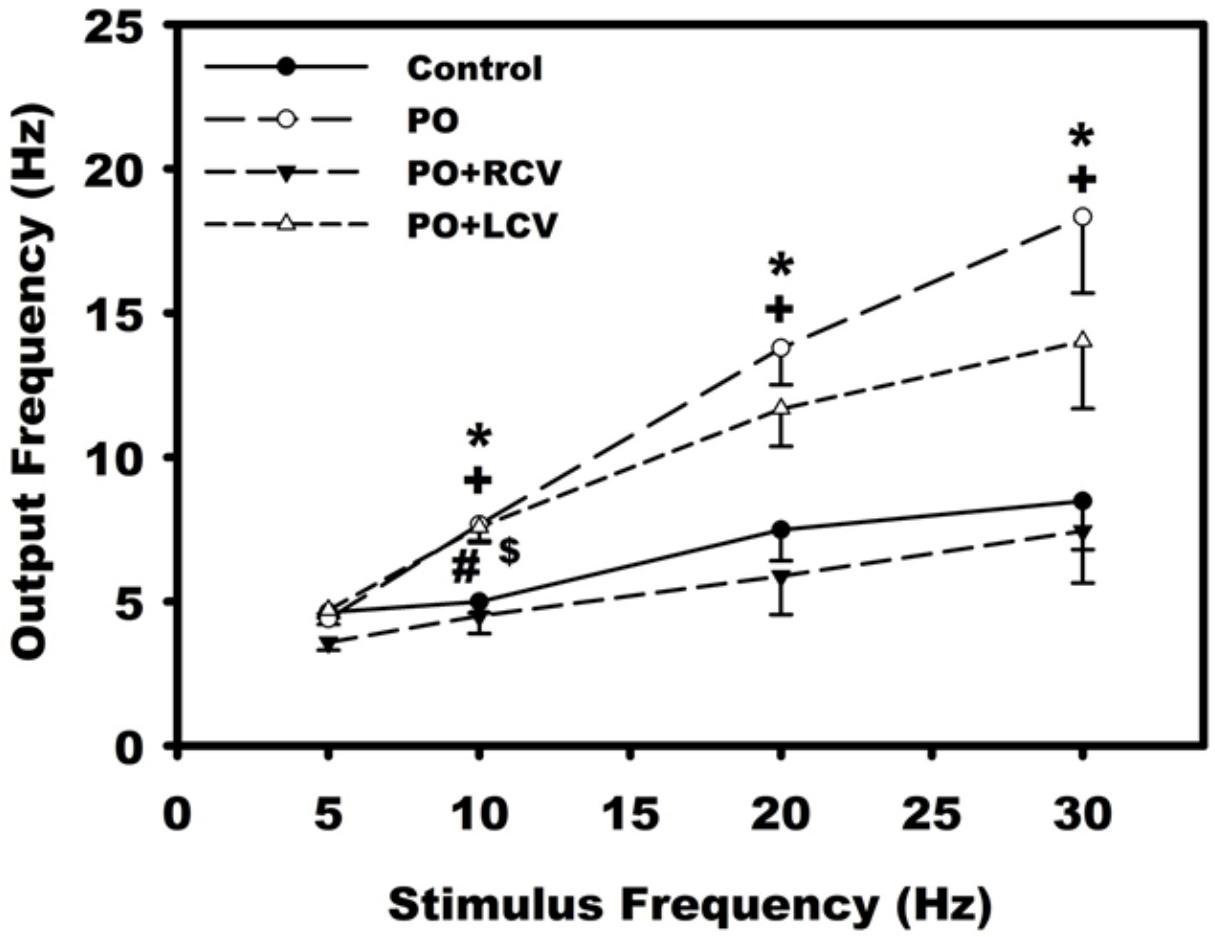

Figure 5: Chronic VNS reduces synaptic efficacy of IC neurons. Nerve fibers synapsing with the intrinsic cardiac neurons were stimulated via an extracellular concentric electrode (0.1-10 V, 2 msec) for 2 sec at frequencies of 5, 10, 20 and 30 Hz. Graph shows average data derived from ~30 cells for each condition. An ANOVA analysis indicated significant differences between treatments and was followed by Newman-Keuls post-hoc analysis. Points are the mean ± SEM. * $p < 0.05$, control vs. PO, # $p<0.05$, control vs. LCV-PO, + $p<0.05$, PO vs. RCV-PO and $ $p<0.05$, LCV-PO vs. RCV-PO.

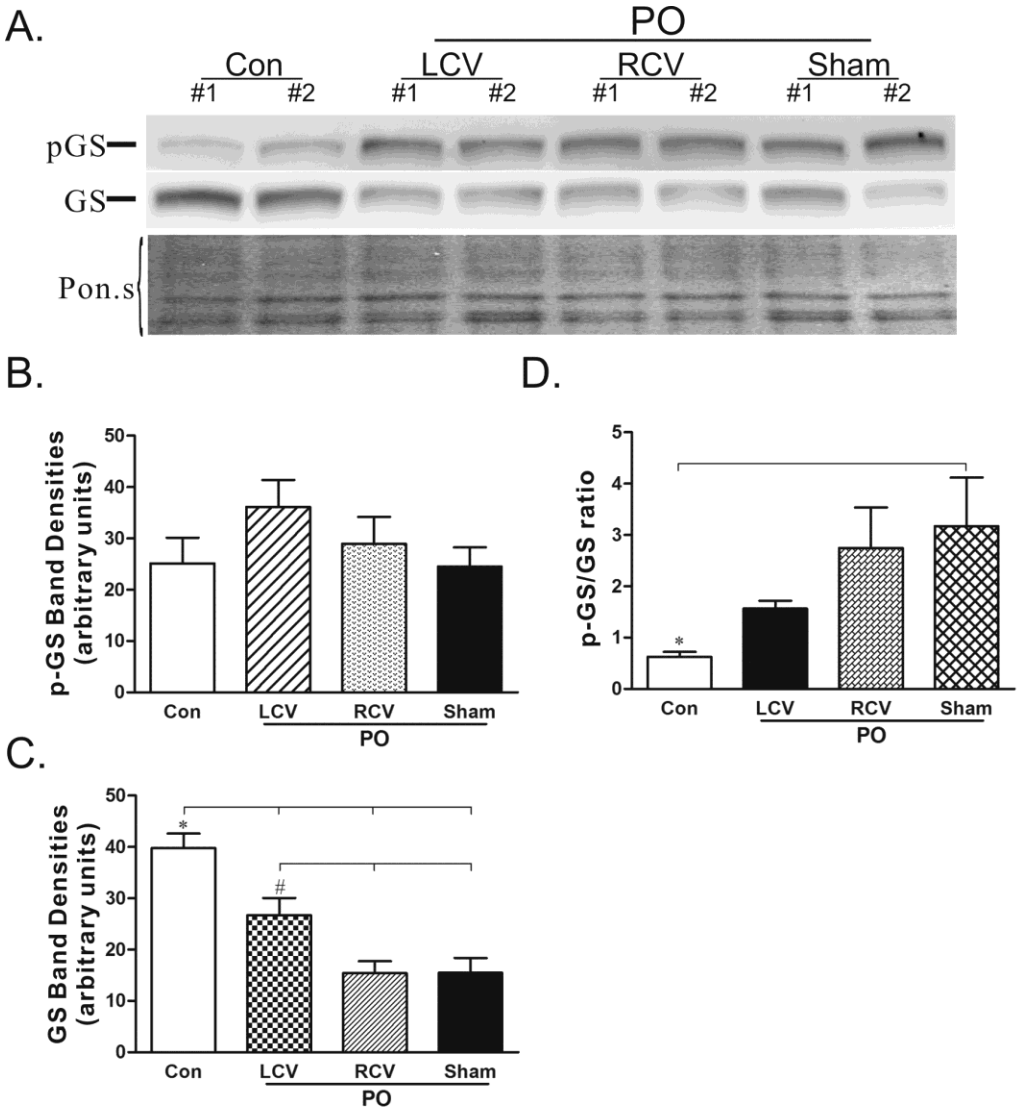

Figure 6: Glycogen synthase (GS) protein levels are significantly reduced and shifted to the inactive phosphorylated form (pGS) in PO; effects that are opposed by left vagus stimulation. A: Representative western blots showing phosphorylated and total glycogen synthase protein levels in Control (n=7), pressure overloaded (PO, n=7), pressure overloaded with right vagus stimulation (PO-RCV, n=7), and pressure overloaded with left vagus stimulation (PO-LCV, n=3) heart extracts. B and C: densitometry analysis of phosphorylated and total glycogen synthase protein band intensities for all the westerns performed. The blot stained with Ponceau S (Pon. S) is shown as a protein-loading control. ANOVA analysis indicated significant differences among the treatments and was followed by Newman-Keuls post hoc analysis. *P<0.05 vs. Con. #P<0.05 vs. PO-LCV. D: the ratio of the pGS/GS band intensities. *P<0.05 vs. Con.

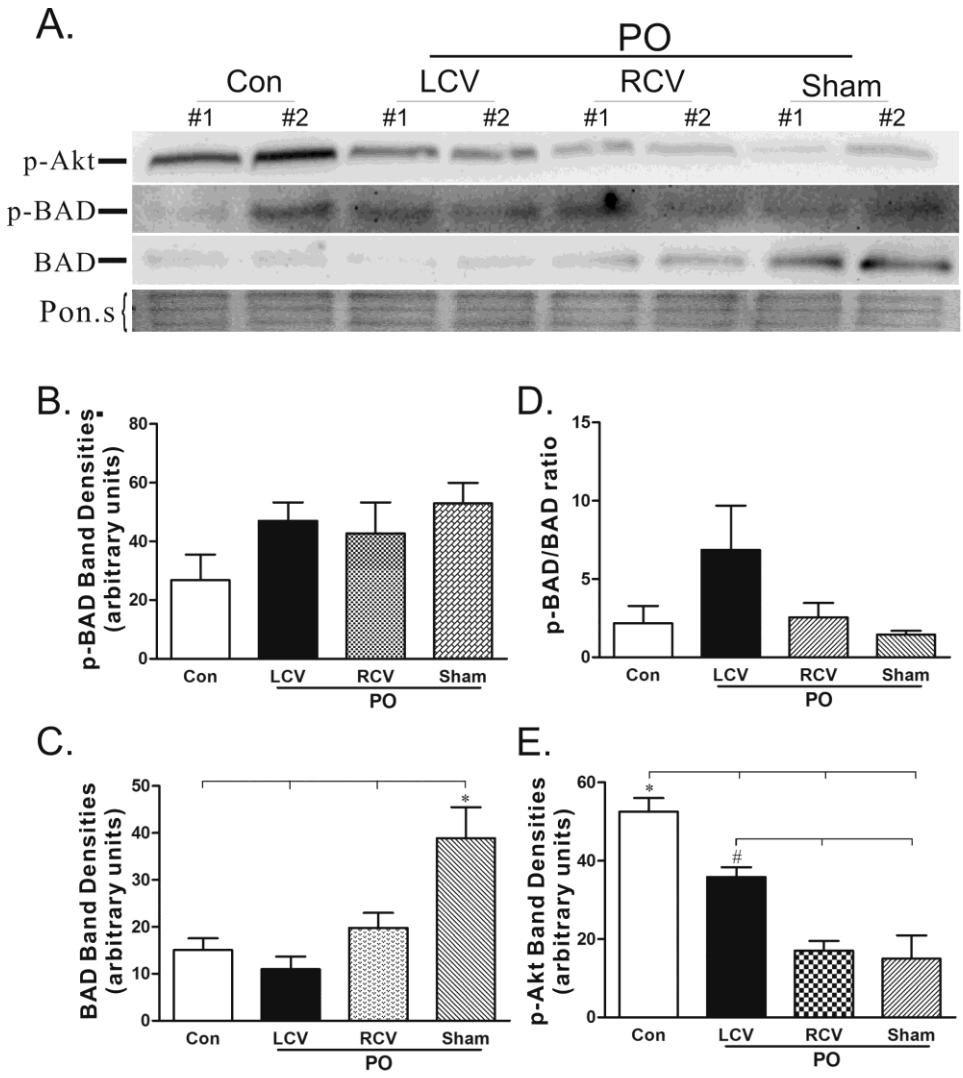

Figure 7: Pressure-overload lead to decreased phospho-Akt (pAkt; active form) and a significant elevation of pro-apoptotic BAD protein level in the pressure overload heart. LCV partially restores pAKT and BAD protein levels to control values. A: shows representative western blots probed for phosphorylated Akt and BAD proteins in Control, PO-LCV, PO-RCV, and PO (n=5) heart extracts. In addition, total BAD protein levels are shown. B and C: densitometry analysis of phosphorylated and total Bad protein band intensity of all western blots (*P<0.05 vs. PO). D: No significant difference in the ratio of the pBAD/BAD was observed. E: densitometry analysis of pAkt protein level in Control, PO, PO-RCV and PO-LCV heart extracts (n=4). Ponceau S (Pon. S) staining is shown as a protein-loading control. ANOVA analysis indicated significant differences among the treatments and was followed by Newman-Keuls post hoc analysis.

A.

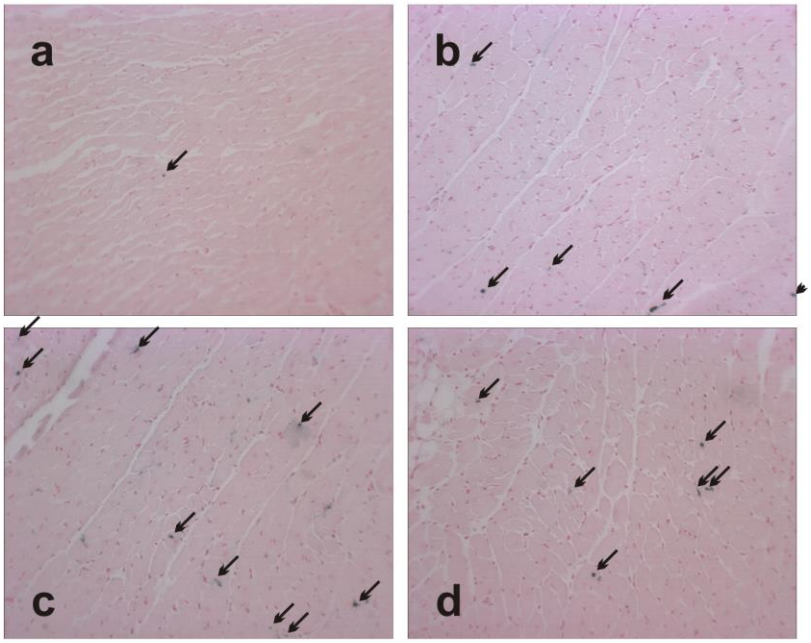

B.

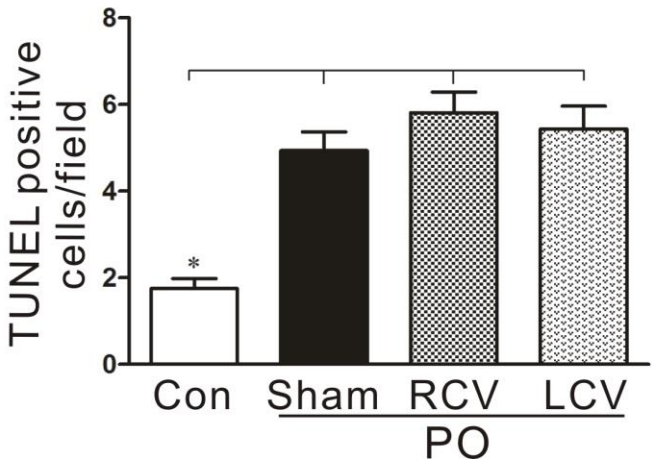

Figure 8: Moderate increases in the number of apoptotic myocytes with PO are unaffected by RCV or LCV therapies. Top panel: Shows representative DNA end-labeled TACS Blue LabelTM stained sections of left ventricular tissue from control and PO hearts. a) Control, b) PO sham heart, c) PO-RCV and d) PO-LCV treated hearts. Arrows indicate blue stained nuclei indicative of DNA fragmentation, a hallmark of apoptosis. Bottom panel: Quantification of number of apoptotic cells found in the experimental groups shown in images.

TABLES

Table 1: Cardiac hemodynamics at termination: among group comparisons

Chronic PO Treatment	LVSP (mmHg)	LVEDP (mmHg)	LV +dp/dt (mmHg/s)	LV –dp/dt (mmHg/s)	Heart Rate (beats/min)	n
Sham VNS	49.3±3.4	3.1±1.2	1211±100	-1265±126	198.0±7.2	12
LCV VNS	61.1±4.6**#**	0.9±1.1	1912±206***#**	-1839±164***#**	215.7±8.8**#**	9
RCV VNS	44.2±2.7	2.5±0.5	1058±187	-1054±133	177.1±12.9	8

p≤**0.05 LCV vs. RCV**; *** p≤0.05 from Sham VNS**

Table 2. Analysis of heart and lung weight in Controls, PO, LCV-PO and RCV-PO.

	Controls (n=8)	PO (n=12)	LCV-PO (n=9)	RCV-PO (n=10)
Age at termination, wk	28.2 ± 1.1	27.3 ± 1.8	26.5 ± 2.8	25.6 ± 1.9
Postoperative recovery, wk	--------	7.3 ± 0.5	7.3 ± 0.3	7.5 ± 0.5
Body weight (wt), g	1011 ± 56	1030 ± 77	969 ± 94	946 ± 86
Heart weight, % of body wt	0.65 ± 0.08	0.57 ± 0.05	0.59 ± 0.08	0.60 ± 0.07
Wet lung weight, % body wt	0.50 ± 0.08	0.41 ± 0.07	0.48 ± 0.17	0.42 ± 0.05
Dry lung weight, % of body wt	0.09 ± 0.01	0.08 ± 0.03	0.09 ± 0.05	0.09 ± 0.01

Values are means ± SD. PO, pressure overload; LCV, left cervical vagus; RCV, right cervical vagus. No significant effect (p<0.05) was found between groups using an ANOVA.

Table 3. Soma properties of intrinsic cardiac neurons derived from controls, PO, RCV-PO and LCV-PO animals.

Property	Controls (n=66)	PO (n=131)	RCV-PO (n=113)	LCV-PO (n=78)
Resting membrane potential (mV)	-49.64 ± 0.83	-49.82 ± 0.68	**-56.58 ± 0.80 ***	-52.23 ± 0.81
Input resistance (MΩ)	73.5 ± 6.0	67.9 ± 5.0	73.1 ± 6.6	65.3 ± 5.2
AHP amplitude (mV)	15.65 ± 0.58	17.46 ± 0.45	16.56 ± 0.49	16.11 ± 0.53
AHP half-decay time (msec)	119.49 ± 6.15	99.46 ± 5.77	**141.4 ± 6.97 ***	109.9 ± 8.37

Values expressed as mean ± SEM, with number of neurons in parentheses. Significant effect (p<0.05) using ANOVA compared to the other groups (*) are shown.

REFERENCES

1. Adams DJ, and Cuevas J. Electrophysiological properties of intrinsic cardiac neurons. In: Basic and Clinical Neurocardiology, edited by Armour JA, and Ardell JL. New York: Oxford University Press, 2004, p. 1-60.
2. Ajijola OA, Vaseghi M, Zhou W, Yamakawa K, Benharash P, Hadaya J, Lux RL, Mahajan A, and Shivkumar K. Functional differences between junctional and extrajunctional adrenergic receptor activation in mammalian ventricle. Am J Physiol Heart Circ Physiol 304: H579-588, 2013.
3. Ajijola OA, Yagishita D, Reddy NK, Yamakawa K, Vaseghi M, Downs AM, Hoover DB, Ardell JL, and Shivkumar K. Remodeling of stellate ganglion neurons after spatially targeted myocardial infarction: Neuropeptide and morphologic changes. Heart Rhythm 12: 1027-1035, 2015.
4. Allen TG, and Burnstock G. M1 and M2 muscarinic receptors mediate excitation and inhibition of guinea-pig intracardiac neurones in culture. J Physiol 422: 463-480, 1990.
5. Andresen MC, Kunze DL, and Mendelowitz D. Central Nervous System Regulation of the Heart. In: Basic and Clincial Neurocardiology, edited by Armour JA, and Ardell JL. New York: Oxford University Press, 2004, p. 187-219.
6. Ardell JL. Intrathoracic neuronal regulation of cardiac function In: Basic and Clinical Neurocardiology, edited by Armour JA, and Ardell JL. New York: Oxford University Press, 2004, p. 118-152.
7. Ardell JL, Cardinal R, Vermeulen M, and Armour JA. Dorsal spinal cord stimulation obtunds the capacity of intrathoracic extracardiac neurons to transduce myocardial ischemia. Am J Physiol Regul Integr Comp Physiol 297: R470-477, 2009.
8. Ardell JL, Rajendran PS, Nier HA, KenKnight BH, and Armour JA. Central-peripheral neural network interactions evoked by vagus nerve stimulation: functional consequences on control of cardiac function. Am J Physiol Heart Circ Physiol 309: H1740-1752, 2015.
9. Ardell JL, and Randall WC. Selective vagal innervation of sinoatrial and atrioventricular nodes in canine heart. Am J Physiol 251: H764-773, 1986.
10. Ardell JL, Randall WC, Cannon WJ, Schmacht DC, and Tasdemiroglu E. Differential sympathetic regulation of automatic, conductile, and contractile tissue in dog heart. Am J Physiol 255: H1050-1059, 1988.
11. Armour JA. Potential clinical relevance of the 'little brain' on the mammalian heart. Exp Physiol 93: 165-176, 2008.

12. Armour JA, and Ardell JL. Basic and Clinical Neurocardiology. New York: Oxford University Press, 2004.
13. Armour JA, and Kember G. Cardiac sensory neurons. In: Basic and Clinical Neurocardiology, edited by Armour JA, and Ardell JL. New York: Oxford University Press, 2004, p. 79-117.
14. Beaumont E, Salavatian S, Southerland EM, Vinet A, Jacquemet V, Armour JA, and Ardell JL. Network interactions within the canine intrinsic cardiac nervous system: implications for reflex control of regional cardiac function. J Physiol 591: 4515-4533, 2013.
15. Beaumont E, Southerland EM, Hardwick JC, Wright GL, Ryan S, Li Y, KenKnight BH, Armour JA, and Ardell JL. Vagus nerve stimulation mitigates intrinsic cardiac neuronal and adverse myocyte remodeling postmyocardial infarction. Am J Physiol Heart Circ Physiol 309: H1198-1206, 2015.
16. Beker F, Weber M, Fink RH, and Adams DJ. Muscarinic and nicotinic ACh receptor activation differentially mobilize Ca2+ in rat intracardiac ganglion neurons. J Neurophysiol 90: 1956-1964, 2003.
17. Bibevski S, and Dunlap ME. Evidence for impaired vagus nerve activity in heart failure. Heart Fail Rev 16: 129-135, 2011.
18. Bonaz B, Picq C, Sinniger V, Mayol JF, and Clarencon D. Vagus nerve stimulation: from epilepsy to the cholinergic anti-inflammatory pathway. Neurogastroenterol Motil 25: 208-221, 2013.
19. Buckley U, Shivkumar K, and Ardell JL. Autonomic Regulation Therapy in Heart Failure. Curr Heart Fail Rep 12: 284-293, 2015.
20. Cardinal R, Page P, Vermeulen M, Ardell JL, and Armour JA. Spatially divergent cardiac responses to nicotinic stimulation of ganglionated plexus neurons in the canine heart. Auton Neurosci 145: 55-62, 2009.
21. Chatterjee NA, and Singh JP. Novel Interventional Therapies to Modulate the Autonomic Tone in Heart Failure. JACC Heart Fail 2015.
22. Coote JH. Myths and realities of the cardiac vagus. J Physiol 591: 4073-4085, 2013.
23. De Ferrari GM, Crijns HJ, Borggrefe M, Milasinovic G, Smid J, Zabel M, Gavazzi A, Sanzo A, Dennert R, Kuschyk J, Raspopovic S, Klein H, Swedberg K, Schwartz PJ, and CardioFit Multicenter Trial I. Chronic vagus nerve stimulation: a new and promising therapeutic approach for chronic heart failure. Eur Heart J 32: 847-855, 2011.

24. Dell'Italia LJ. Translational success stories: angiotensin receptor 1 antagonists in heart failure. Circ Res 109: 437-452, 2011.
25. Florea VG, and Cohn JN. The autonomic nervous system and heart failure. Circ Res 114: 1815-1826, 2014.
26. Foreman RD, Linderoth B, Ardell JL, Barron KW, Chandler MJ, Hull SS, Jr., TerHorst GJ, DeJongste MJ, and Armour JA. Modulation of intrinsic cardiac neurons by spinal cord stimulation: implications for its therapeutic use in angina pectoris. Cardiovasc Res 47: 367-375, 2000.
27. Fukuda K, Kanazawa H, Aizawa Y, Ardell JL, and Shivkumar K. Cardiac innervation and sudden cardiac death. Circ Res 116: 2005-2019, 2015.
28. Furukawa Y, Hoyano Y, and Chiba S. Parasympathetic inhibition of sympathetic effects on sinus rate in anesthetized dogs. Am J Physiol 271: H44-50, 1996.
29. Gladden JD, Linke WA, and Redfield MM. Heart failure with preserved ejection fraction. Pflugers Arch 466: 1037-1053, 2014.
30. Hardwick JC, Baran CN, Southerland EM, and Ardell JL. Remodeling of the guinea pig intrinsic cardiac plexus with chronic pressure overload. Am J Physiol Regul Integr Comp Physiol 297: R859-866, 2009.
31. Hardwick JC, Mawe GM, and Parsons RL. Evidence for afferent fiber innervation of parasympathetic neurons of the guinea-pig cardiac ganglion. J Auton Nerv Syst 53: 166-174, 1995.
32. Hardwick JC, Ryan SE, Beaumont E, Ardell JL, and Southerland EM. Dynamic remodeling of the guinea pig intrinsic cardiac plexus induced by chronic myocardial infarction. Auton Neurosci 181: 4-12, 2014.
33. Hardwick JC, Ryan SE, Powers EN, Southerland EM, and Ardell JL. Angiotensin receptors alter myocardial infarction-induced remodeling of the guinea pig cardiac plexus. Am J Physiol Regul Integr Comp Physiol 309: R179-188, 2015.
34. Hardwick JC, Southerland EM, Girasole AE, Ryan SE, Negrotto S, and Ardell JL. Remodeling of intrinsic cardiac neurons: effects of beta-adrenergic receptor blockade in guinea pig models of chronic heart disease. Am J Physiol Regul Integr Comp Physiol 303: R950-958, 2012.
35. Harper RM, Kumar R, Macey PM, Ogren JA, and Richardson HL. Functional neuroanatomy and sleep-disordered breathing: implications for autonomic regulation. Anat Rec (Hoboken) 295: 1385-1395, 2012.

36. Hoover DB, Isaacs ER, Jacques F, Hoard JL, Page P, and Armour JA. Localization of multiple neurotransmitters in surgically derived specimens of human atrial ganglia. Neuroscience 164: 1170-1179, 2009.
37. Hopkins DA, Macdonald SE, Murphy DA, and Armour JA. Pathology of intrinsic cardiac neurons from ischemic human hearts. Anat Rec 259: 424-436, 2000.
38. Houser SR, Margulies KB, Murphy AM, Spinale FG, Francis GS, Prabhu SD, Rockman HA, Kass DA, Molkentin JD, Sussman MA, Koch WJ, American Heart Association Council on Basic Cardiovascular Sciences CoCC, Council on Functional G, and Translational B. Animal models of heart failure: a scientific statement from the American Heart Association. Circ Res 111: 131-150, 2012.
39. Kember G, Armour JA, and Zamir M. Dynamic neural networking as a basis for plasticity in the control of heart rate. J Theor Biol 317: 39-46, 2013.
40. Kember G, Armour JA, and Zamir M. Neural control hierarchy of the heart has not evolved to deal with myocardial ischemia. Physiol Genomics 45: 638-644, 2013.
41. Kember G, Armour JA, and Zamir M. Neural control of heart rate: the role of neuronal networking. J Theor Biol 277: 41-47, 2011.
42. Kumar R, Nguyen HD, Ogren JA, Macey PM, Thompson PM, Fonarow GC, Hamilton MA, Harper RM, and Woo MA. Global and regional putamen volume loss in patients with heart failure. Eur J Heart Fail 13: 651-655, 2011.
43. Levy MN. Sympathetic-parasympathetic interactions in the heart. Circ Res 29: 437-445, 1971.
44. Levy MN, and Martin PJ. Neural control of the heart. In: Handbook of Physiology: Section 2: The Cardiovascular System, Volume 1: The Heart, edited by Berne RM. Bethesda: The American Physiological Society, 1979, p. 581-620.
45. Matsui T, Nagoshi T, and Rosenzweig A. Akt and PI 3-kinase signaling in cardiomyocyte hypertrophy and survival. Cell Cycle 2: 220-223, 2003.
46. McGuirt AS, Schmacht DC, and Ardell JL. Autonomic interactions for control of atrial rate are maintained after SA nodal parasympathectomy. Am J Physiol 272: H2525-2533, 1997.
47. Nonogaki K. New insights into sympathetic regulation of glucose and fat metabolism. Diabetologia 43: 533-549, 2000.
48. Parsons RL. Mammalian cardiac ganglia as local integration centers: histochemical and electrophysiological evidence. In: Neural Mechanisms in Cardiovascular Regulation,

edited by Dun NJ, Machado BH, and Pilowsky PM. Boston: Kluwer Academic Publishers, 2004, p. 335-356.

49. Premchand RK, Sharma K, Mittal S, Monteiro R, Dixit S, Libbus I, DiCarlo LA, Ardell JL, Rector TS, Amurthur B, KenKnight BH, and Anand IS. Extended Follow-Up of Patients with Heart Failure Receiving Autonomic Regulation Therapy in the ANTHEM-HF Study. J Card Fail 2015.
50. Rajendran PS, Nakamura K, Ajijola OA, Vaseghi M, Armour JA, Ardell JL, and Shivkumar K. Myocardial infarction induces structural and functional remodelling of the intrinsic cardiac nervous system. J Physiol 594: 321-341, 2016.
51. Randall DC, Brown DR, McGuirt AS, Thompson GW, Armour JA, and Ardell JL. Interactions within the intrinsic cardiac nervous system contribute to chronotropic regulation. Am J Physiol Regul Integr Comp Physiol 285: R1066-1075, 2003.
52. Shimazu T. Innervation of the liver and glucoregulation: roles of the hypothalamus and autonomic nerves. Nutrition 12: 65-66, 1996.
53. Shinlapawittayatorn K, Chinda K, Palee S, Surinkaew S, Thunsiri K, Weerateerangkul P, Chattipakorn S, KenKnight BH, and Chattipakorn N. Low-amplitude, left vagus nerve stimulation significantly attenuates ventricular dysfunction and infarct size through prevention of mitochondrial dysfunction during acute ischemia-reperfusion injury. Heart Rhythm 10: 1700-1707, 2013.
54. Stanley WC, Recchia FA, and Lopaschuk GD. Myocardial substrate metabolism in the normal and failing heart. Physiol Rev 85: 1093-1129, 2005.
55. Thompson GW, Collier K, Ardell JL, Kember G, and Armour JA. Functional interdependence of neurons in a single canine intrinsic cardiac ganglionated plexus. J Physiol 528: 561-571, 2000.
56. Vaseghi M, Gima J, Kanaan C, Ajijola OA, Marmureanu A, Mahajan A, and Shivkumar K. Cardiac sympathetic denervation in patients with refractory ventricular arrhythmias or electrical storm: intermediate and long-term follow-up. Heart Rhythm 11: 360-366, 2014.
57. Waldmann M, Thompson GW, Kember GC, Ardell JL, and Armour JA. Stochastic behavior of atrial and ventricular intrinsic cardiac neurons. J Appl Physiol 101: 413-419, 2006.
58. Wang HJ, Wang W, Cornish KG, Rozanski GJ, and Zucker IH. Cardiac sympathetic afferent denervation attenuates cardiac remodeling and improves cardiovascular dysfunction in rats with heart failure. Hypertension 64: 745-755, 2014.

59. Yamakawa K, Rajendran PS, Takamiya T, Yagishita D, So EL, Mahajan A, Shivkumar K, and Vaseghi M. Vagal nerve stimulation activates vagal afferent fibers that reduce cardiac efferent parasympathetic effects. Am J Physiol Heart Circ Physiol 309: H1579-1590, 2015.
60. Yamakawa K, So EL, Rajendran PS, Hoang JD, Makkar N, Mahajan A, Shivkumar K, and Vaseghi M. Electrophysiological effects of right and left vagal nerve stimulation on the ventricular myocardium. Am J Physiol Heart Circ Physiol 307: H722-731, 2014.
61. Zipes DP. Antiarrhythmic therapy in 2014: Contemporary approaches to treating arrhythmias. Nat Rev Cardiol 12: 68-69, 2015.
62. Zucker IH, Patel KP, and Schultz HD. Neurohumoral stimulation. Heart Fail Clin 8: 87-99, 2012.

CHAPTER 3:

BIOELECTRIC NEUROMODULATION OF THE PARAVERTEBRAL CARDIAC EFFERENT SYMPATHETIC OUTFLOW AND ITS EFFECT ON VENTRICULAR ELECTRICAL INDICES

INTRODUCTION

Sudden cardiac death, as a result of ventricular arrhythmias, is often the first presenting sign of structural heart disease (12). Autonomic dysregulation secondary to cardiac pathology is central to the development of heart failure and ventricular arrhythmias (3, 17). Surgical removal of the T1-T4 paravertebral chain reduces ventricular arrhythmia burden, by removing excessive sympathetic input to the cardiac myocytes (9, 32). Although effective, by decentralizing peripheral cardiac sympathetic control from the central nervous system, surgically removing a section of the sympathetic paravertebral ganglia (T1-T4) evoked off-target side effects including thoracic hyperalgesia and/or compensatory abdominal hyperhidrosis in patients (32).

In managing transient episodic autonomic imbalances, an alternative way of targeting the cardiac nervous system would be technologies that allow for on-demand suppression of cardiac sympathetic activity in a reversible manner. This can be accomplished through a bioelectronic therapy called axonal modulation therapy (AMT). One iteration of AMT is symmetric, voltage controlled kilohertz frequency alternating current (KHFAC) (23). This technology uses electrical current to directly inhibit the local conduction of action potentials (23). KHFAC, as applied to somatic nerves, produces rapid block of nerve conduction that is quickly reversible (8, 23). However, one confounding effect with KHFAC is that an onset response, reflective of excitation before block, accompanies current initiation (8, 23). The utility of KHFAC to dynamically manage cardiac control via the autonomic nervous system has not been evaluated.

Sympathetic control of the heart reflects the dynamic interplay between central and intrathoracic aspects of the cardiac nervous system (3, 17, 29). To control sympathetic outflow to the heart it is critical to target primary nexus (convergence) points where pre and/or post-ganglionic projections run together prior to their divergence to atrial and ventricular tissues via branches of the thoracic vagosympathetic nerve trunk; the T1-T2 segment of the paravertebral chain is a nexus point for sympathetic control of the heart (11, 24). By surgically removing T1-T2 we are able to block sympathetic efferent control of ventricular activation recovery intervals (11). The upper thoracic aspects of the paravertebral chain are readily accessible in pigs and man (6, 9, 20); well suited as future targets for chronic AMT.

The primary objective of this study was to evaluate the efficacy of KHFAC, when applied to T1-T2 paravertebral chain, to mitigate sympathetic outflow to the heart in a reversible manner. By reversibly inhibiting the nerve conduction in the paravertebral chain, one could scale the level of sympathetic efferent inputs to the heart, limit the potential for off target effects

(as in the case of surgical decentralization (32)) and can switch back on full cardiac sympathetic control as required.

METHODS

The study protocol was approved by the University of California Los Angeles Institutional Animal Care and Use Committee and conforms to the National Institutes of Health Guide for the Care and Use of Laboratory Animals (Eighth Edition, 2011).

Surgical preparation

Yorkshire pigs (n=12) were sedated with tiletamine-zolazepam (4-8mg/kg, intramuscular) and anesthetized with isoflurane (1-5%, INH). After endotracheal insertion the animals were ventilated and general anaesthesia was maintained with inhaled isoflurane (1-2%) and boluses of fentanyl (20-30ug/kg, intravenous (IV)) as required during surgery. The depth of anesthesia was assessed throughout the experiments by monitoring corneal reflexes, jaw tone, and hemodynamic indices. Once the surgical preparation was completed, the anaesthesia was switched to α-chloralose bolus (50mg/kg over 30 minutes, titrated based on hemodynamic response and depth of anesthesia) and subsequent maintenance infusion (20-35mg/kg/hr IV). The femoral artery and vein were cannulated for monitoring of systemic pressure and infusion of fluids or medications respectively. A posterior 12 lead electrocardiogram was placed and end tidal carbon dioxide monitoring maintained between 35-45mmHg. Arterial blood gas sampling was assessed on a 1-2 hourly basis and adjustments to tidal volume, respiratory rate or doses of sodium bicarbonate performed to maintain adequate oxygenation and homeostasis.

A midline sternotomy was performed to expose the heart and paravertebral sympathetic ganglia from T1-T4. The cervical vagi were isolated and transected bilaterally (n=9). In a subset of animals (n=3), paravertebral stimulation and KHFAC were applied in animals with intact vagi and with pre-treatment with atropine (1mg/kg). After the surgical preparation there was a 1 hour stabilization period. On completion of the experiment, the animals were euthanized by administration of sodium pentobarbital (100mg/kg, iv) with potassium chloride (1-2mEq/Kg, iv) under high dose isoflurane (5% inhaled).

Hemodynamic measurements

A 5 French Millar pressure catheter (SPR-350) was inserted into the left ventricle via the left carotid artery. This was connected to the MVPS Ultra Pressure Volume Loop System (Millar Instruments, Houston, Texas). From this measurement of left ventricular (LV) pressure, cardiac contractility (dP/dt), and heart rate were derived. A lead II ECG, LV pressure and system pressure were input to a Cambridge Electronics Design (model 1401) data acquisition system for continuous monitoring of hemodynamic status.

Activation recovery index recording and analysis

A custom made 56-electrode epicardial sock was placed over both ventricles to provide regional unipolar electrograms for the ventricular epicardium. This data was collected via a Prucka CardioLab system (GE Healthcare, Fairfield, CT) and analysed using customized software (ScalDyn M, University of Utah, Salt Lake City, UT). ARI was assessed similarly to previous published work by our group (11, 33). In brief, the activation time was measured from the beginning of the first derivative of the derived voltage (dV/dt) in the depolarization wave of the intrinsic deflection of voltage. The recovery time was the maximum dV/dt to time of the peak of repolarization (T wave). The ARI is the recovery time minus the activation time. ARI has been shown to correlate with regional ventricular action potential duration (19).

Sympathetic electrical stimulations of the stellate and T3 paravertebral ganglion

The stellate and T3 paravertebral ganglia were stimulated using bipolar needle electrodes with and without KHFAC. The bipolar electrodes were interfaced with Grass S88 stimulators (Grass Co., Warwick, RI) via SIU6 constant current stimulus isolation units. Electrical stimulation of the stellate and T3 ganglia were titrated at 4Hz to achieve a 10% increase in left ventricular end systolic pressure, heart rate, dP/dt max or decrease in activation recovery interval (ARI). After threshold was identified, the stimulus intensity used thereafter was 1.5 times threshold, applied for 30 second periods. Between sequential nerve stimulations there was a waiting period of 10 minutes to allow for all parameters to return to baseline.

KHFAC

A bipolar Ag electrode was placed around the paravertebral sympathetic axons between T1 and T2 (figure 1). This electrode interface was then connected to a charge-balanced, voltage controlled, square wave, KHFAC waveform function generator (Stanford Research System, Sunnyvale, CA) with varying frequency and voltages assessed from 5-20 kHz and 5-20 Volts. A capacitor was placed in series on each output line of the waveform generator to

prevent direct current contamination of the signal. A symmetric KHFAC implies a zero net charge.

Protocol for assessing block induced by KHFAC

Baseline ventricular epicardial ARI, LV contractility (dP/dt), and heart rate were assessed. They were then evaluated with (T1) stellate ganglion and T3 stimulations with and without KHFAC. T3 electrical stimulation was performed 10 min after each KHFAC to ensure complete recovery of nerve function. During KHFAC T1 stimulation was performed to assess whether KHFAC had an effect on nerve conduction proximal to the electrode. Between stimuli there was a waiting period of ten minutes to ensure complete recovery of hemodynamic and electrical indices to baseline. KHFAC stimulation resulted in a transient activation of the sympathetic nervous system prior to blocking nerve conduction. Therefore, there was a waiting period of at least two minutes or until the hemodynamic and electrical indices return to baseline parameters before blocking efficacy was assessed by T3 stimulation. If after 5 minutes of KHFAC the cardiac hemodynamic indices did not return to baseline then KHFAC was discontinued and frequency or intensity re-adjusted to mitigate the onset response.

Protocol for assessing the onset response to KHFAC

Baseline ventricular epicardial activation recovery intervals, LV contractility, and heart rate were assessed. KHFAC was applied 15 seconds and the change in hemodynamic and electrical indices from baseline assessed. The range of frequencies and voltages tested was from 5 to 20 kHz and 5-20 volts. At least 5 min separated sequential KHFAC challenges.

Statistical analysis

Statistical analysis was done using Sigma Stat (SigmaStat Software, San Jose, CA) with one-way repeated ANOVA of variance for comparing hemodynamic and regional ventricular indices with and without KHFAC. Paired Student t test and Wilcoxon rank sum were also performed for comparison of continuous variables. Data was considered statistically significant where the $P<0.05$. Data are presented as a mean ± SE.

RESULTS:

KHFAC block assessment

Chronotropic, dromotropic and inotropic responses to baseline stimulations

In 9 porcine subjects (5 male, 4 female), weighing on average 41±3kg, paravertebral KHFAC applications were assessed. T1 (stellate) and T3 stimulations were titrated to produce equivalent changes in heart rate and ventricular ARI. At 4Hz, stimulation parameters of 2.2±0.3mA for RT1, 3.3±0.8mA for RT3, 3.2±0.9mA LT1, and 9.3±5.7mA LT3 produced at least a 10% increase in LVSP, heart rate or shortening of ARI and were defined as threshold. Subsequent T1 and T3 stimulations were done at 4Hz, 1.5x threshold.

Baseline T3 stimulations resulted in a change in ARI on 51±15ms on the right sympathetic paravertebral ganglia and 26±10ms for the left ($p<0.05$). T3 stimulation also resulted in a heart rate change of (34±11bpm right; 6±8bpm left) and LVSP change of (22±5mmHg right; 22±7mmHg left). The maximum dP/dt was augmented with T3 stimulation by (657±38mmHg/s right; 689±176mmHg/s left). Repeated T3 stimulations resulted in a consistent response throughout the experiment.

Chronotropic, dromotropic and inotropic responses to KHFAC

Figure 2 shows a representative cardiac hemodynamic onset response to initiation of KHFAC, the blunted cardiac response to subsequent RT3 stimulation when delivered during KHFAC and the full reversibility of this block in the recovery phase (RT3 Post). Note that the efficacy of block was manifest for heart rate, LV dp/dt and LV pressure. Note also that at 15 kHz and 15 volts KHFAC the onset response had extinguished within 1 minute of initiation.

Figure 3 shows a polar map indicating regional ventricular ARI in response to RT3 stimulation prior to and during KHFAC (15 kHz, 15 volts). The pattern of ARI shortening evoked at the onset of KHFAC (panel D) paralleled that with RT3 stimulation (panel B), but rapidly returned towards but not all the way back to baseline control (panel E). The positive dromotropic effect evoked by RT3 stimulation (panel B) was mitigated by KHFAC (panel F) with no aberrant conduction pathways evident.

Figure 4 summarizes the average evoked cardiac hemodynamic response to T3 stimulation prior to, during and following KHFAC (15±0.8 kHz, 15±1.3 volts). The evoked cardiac response to T3 stimulation repeated in the presence of KHFAC were significantly reduced for ventricular ARI (-14.8±2.8% vs -5.2±3.1%), heart rate (36.5±7% vs 11.0±5.1%), LV +dp/dt (57.7±18.7% vs 16.1±7.7%) and LVSP (20.2±3.0% vs 10.3±3.1%). Equivalent levels of cardiac hemodynamic responses were evoked prior to and following KHFAC; indicative of the reversible nature of short duration block imposed by high-frequency alternating current applied to the paravertebral chain. For example, percentage change in ARI pre (15±7%) and post (18 ±11%) KHFAC were evoked with right-sided T3 stimulation.

Figure 5 illustrates the cardiac hemodynamic response evoked in response to stellate ganglia (RT1) stimulation prior to and in the presence of KHFAC. This stimulation point is upstream from the block location and demonstrates the focal nature of the current blocking at the T1-T2 level that does not interfere with ganglia processing capabilities of the stellate.

KHFAC onset response

KHFAC resulted in an onset response at the start of current delivery indicative of the initial activation phase evoked on underlying axons prior to establishment of blockade. Figure 2 shows a representative onset response to 15 kHz, 15 volt charge-balanced AC current. Onset responses varied with the characteristics of the stimulus waveform. In a separate subset of experiments (n=3), the onset response and blocking efficacy of KHFAC were maintained in animals with intact cervical vagi and with pre-emptive atropine (data not shown). Figure 6 illustrates the 3D response surfaces for the maximal onset response for heart rate (panel A), LV +dp/dt (panel B) and ventricular ARI (panel C) with the drive variable being frequency and intensity of KHFAC (n=9). Note that for all parameters, lower frequencies and higher intensities are associated with larger onset responses. This in turn is reflective of higher degrees of onset evoked sympatho-excitation. In the case of high level onset responses, often they had not extinguished by the end of the 5 min test period and T3 evaluations were aborted. The overall objective for KHFAC, or any form of AMT, is to optimize interfaces and stimulus protocols to minimize the onset response while maintaining flexibility to scale the degree of block during sustained current delivery.

DISCUSSION

Neuromodulation utilizing bioelectronics methodologies have the potential to regulate nerve traffic and ganglionic processing within the cardiac nervous system. While KHFAC has been assessed in many peripheral nerve preparations (8, 23), this is the first proof-of-concept use of KHFAC on the cardiac sympathetic nervous system. The main conclusions from this paper are: i) KHFAC applied to the T1-T2 region of the paravertebral chain inhibits/modulates functional sympathetic efferent projections to the heart in a scalable and reversible manner; ii) An onset augmenting response precedes the axonal blocking during KHFAC; iii) the onset response can be mitigated by adjusting KHFAC parameters; and iv) KHFAC, when deployed, can be activated on demand to counteract endogenous excessive sympatho-excitation.

Structure/function of the cardiac nervous system is a critical aspect for rational neuromodulation based therapy (3). Control of cardiac function involves the dynamic interplay

between neural networks contained on the heart (intrinsic cardiac ganglionated plexus), extracardiac intrathoracic ganglia, spinal cord, brainstem and higher centers of the central nervous system (3). For sympathetic control, descending projections from the brainstem innervate preganglionic soma located in the intermediolateral cell column (C7-T4 spinal levels) (3, 15). Preganglionic soma project axons via the paravertebral chain to post-ganglionic soma located in the stellate, middle cervical, mediastinal ganglia and intrinsic cardiac ganglia (3, 11, 24). Each of these ganglia contains a complex network of afferent, efferent and local circuit neurons that interdependently work as a distributed neural network sub-serving cardio-cardiac reflexes (3). Disruptions in reflex processing between central and peripheral aspects of the cardiac nervous system is a major contributing cause to arrhythmia formation (17, 21) and the progression of heart failure (13, 35). Neuromodulation based therapies targeted to mitigate this central/peripheral imbalance are of obvious clinical importance.

Patients with intractable ventricular arrhythmias can be effectively treated with surgical procedures that include removing the paravertebral chain from T4 up to and including the lower third of the stellate ganglia (9). While such surgical approaches have documented anti-arrhythmic effects (9, 32), these patients frequently experience off-target adverse effects including upper thoracic and limb hyperhidrosis and hyperalgesia (32). We have recently demonstrated that cardiac-related preganglionic fibers arising from the thoracic cord traverse up the paravertebral chain through the T1-T2 region (11), some making synaptic contact with post-ganglionic neurons in the stellate with others projecting through the ansae subclavia to more distal intrathoracic ganglia (middle cervical, mediastinal and intrinsic) (5, 7). As such, the ansae subclavia and the T1-T2 region of paravertebral chain are critical nexus points for sympathetic nerve traffic to and afferent projections from the heart (3, 11). Based on structure/function considerations both sites are potential targets for axonal modulation therapy.

KHFAC has been applied to the cervical vagus, the sciatic nerve, the tibial and common peroneal nerve and the dorsal region of the thoracic spinal cord (14, 23, 25). KHFAC refers to AC in the range of 1-100 KHz and without DC offset (23). It is being used for a variety of pathological neural activity including limb and back pain management (14, 31). High frequency bioelectronic nerve block mediates its effects by producing a reversible local conduction block (23). The mechanism of conduction block is most likely via sodium channel inactivation (23). Studies by Kilgore and others suggest that that KHFAC results in increased inward sodium current compared to the outward potassium current (1, 10, 22). This depolarization resulted in activation of about 90% of the sodium channels in the node directly under the electrode (1). Neurotransmitter depletion as opposed to true nerve conduction block (22) is not the

mechanism as confirmed herein by a local conduction block at and distal to the KHFAC but not proximal to the KHFAC with stellate ganglion stimulation. As demonstrated in peripheral (8, 23) and now sympathetic nerves, the local conduction block reverses rapidly and can be applied multiple times without degradation in the underlying nerve processes.

Clinical Perspectives:

Sudden cardiac death secondary to ventricular arrhythmias is a major clinical problem (30). Cardiac pathologies such as ischemic heart disease disrupt the autonomic nervous system (12, 17, 29). Ventricular electrical storm has been treated with medications (26), thoracic epidural anesthesia (9), and in the case of refractory ventricular arrhythmias surgical resection (9, 28, 32). Surgical resection of the sympathetic paravertebral ganglia, while effective, results in adverse side-effects for patients (32). Axonal modulation therapy poses a rapid and reversible way to target the sympathetic nervous system and thereby control the level of functional efferent input to the heart. Electrical currents applied to nerves at high frequency can directly inhibit conduction of action potentials (8, 23). Based on anatomical considerations (11, 20), the preferred site for control of sympathetic input to heart in humans is to deploy the KHFAC electrodes to the T1-T2 region of the paravertebral chain, an area readily accessible by video-assisted thoracic surgery as routinely done for cardiac sympathetomy (9). It should also be considered that the initial application of KHFAC results in a transient axonal activation termed the onset response (8, 23). While the onset response can be mitigated by modifications in stimulation protocol and characteristics of the electrode/nerve interface such as contact size/spacing (23), future studies may involve development of hybrid technologies that include of KHFAC and DC current (16). It can be envisioned that AMT can be implemented as part of an on-demand system to mitigate periods of central/peripheral imbalances in leading to sympatho-excitation.

Limitations:

These experiments were done in anesthetized pig with no underlying pathology. They were also done with vagotomy to minimize confounding influences evoked from vagal afferents and efferents in reflex response to imposed stressors (4). Blocking functional parasympathetic efferent effects with atropine in animals with intact vagi did not interfere with the onset or blocking response to T1-T2 paravertebral KHFAC. Future studies should consider the effects of neural remodelling in cardiac disease (2, 18, 27) on the efficacy of axonal modulation therapy.

It should also be considered that T1-T2 region of the paravertebral chain as well as the ansae subclavia are mixed nerves containing both afferent and efferent projecting fibers (3). While future studies should consider the potential contributions of afferent vs efferent control (34), it is clear from the current study that KHFAC of mixed sympathetic nerve does not evoke aberrant cardiac conduction, at least in normal animals. The transient axonal activation as a result of KHFAC, in the case of the sympathetic nervous system and the presence of structural heart disease, could potentially result in lethal ventricular arrhythmias if the onset response is not adequately controlled. The onset response may be mitigated by adjusting KHFAC parameters (23). Finally, these studies only assessed the effects of relatively short-term KHFAC. Future studies should consider the effects (plasticity and memory) of longer-term and chronic KHFAC on integrated control of the cardiac nervous system.

Author contributions:

*Authors UB and RWC contributed equally to the design, execution and data analysis of study. PSR, TV contributed in experiments and in technology development. KS and JLA contributed to conceptual design and analytics. UB drafted the manuscript. All authors edited the manuscript. All authors approved the final version of the manuscript.

Acknowledgment:

The authors acknowledge the inputs from Drs. Kevin Kilgore and Niloy Bhadra (Case Western Reserve University) in their review of the manuscript and in sharing their recognized experience in bioelectronic technologies of KHFAC nerve block. The authors acknowledge Dr. Arun Sridhar (Glaxo Smith Kline) in concept development.

FIGURES

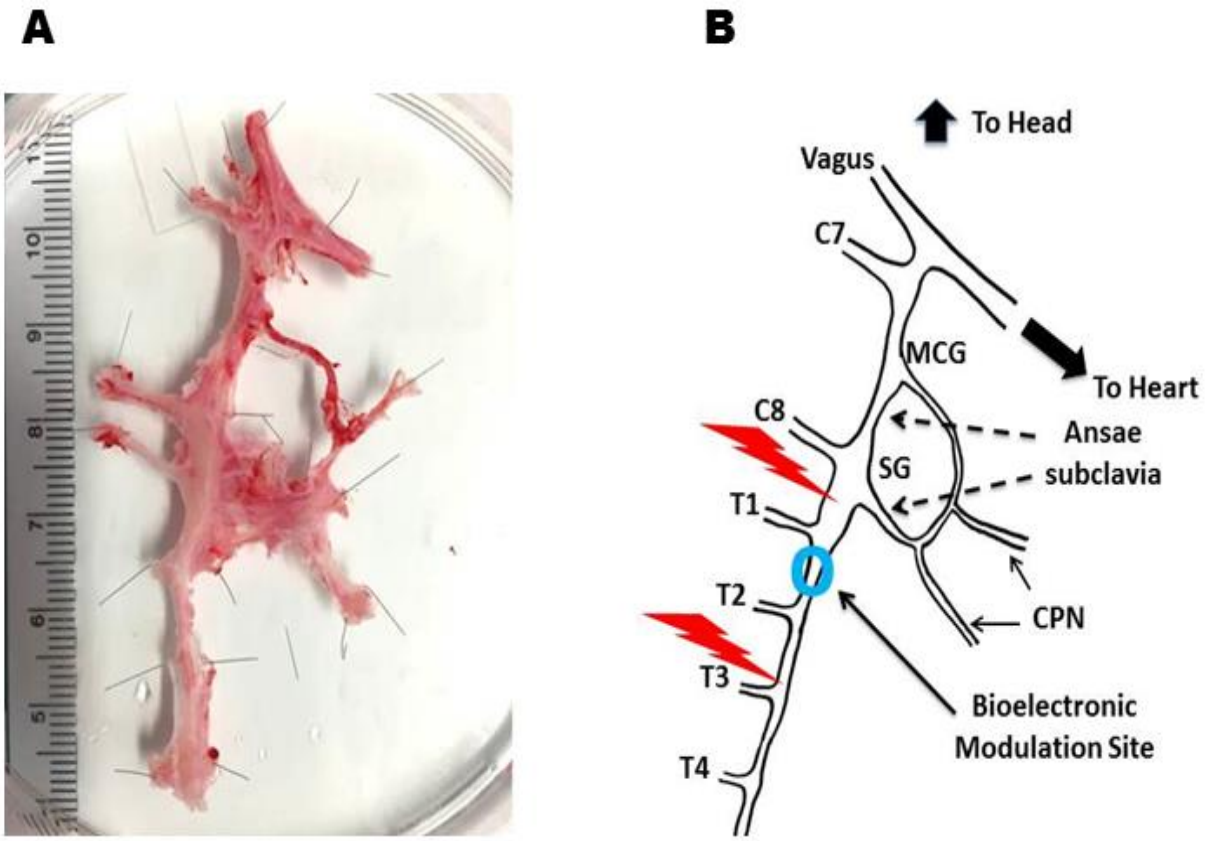

Figure 1: Anatomy of the paravertebral sympathetic ganglia. Panel A: Dissected specimen from a porcine model showing the paravertebral chain (c7-T4), stellate ganglia (SG) and interconnections to middle cervical ganglia (MCG). Panel B: Stylized image demonstrates two nexus points for axonal modulation therapy for cardiac sympathetic control, the ansae subclavia and between T1-T2 of the paravertebral sympathetic ganglia. Stim, stimulation; CPN, cardiopulmonary nerve.

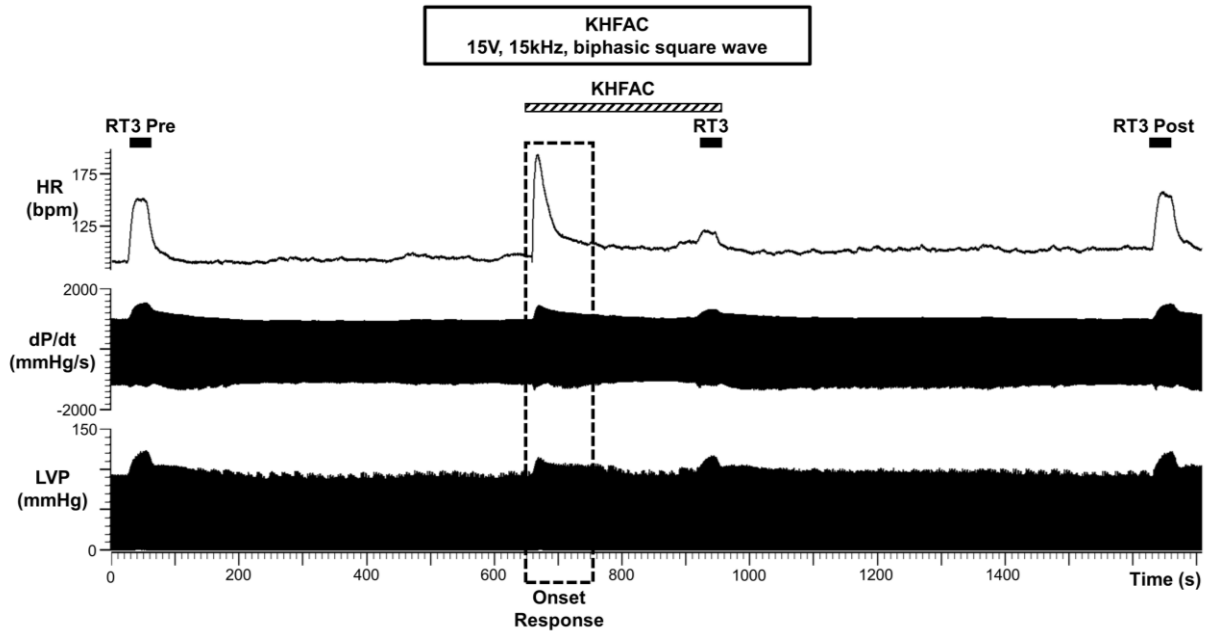

Figure 2: An example of the cardiac hemodynamic response to paravertebral chain stimulation at the T3 level prior to (pre), during KHFAC (15KHz, 15Volts) and in the recovery phase (post). Shown are induced changes in heart rate (HR), LV dp/dt and LV Pressure (LVP). Note also the cardiac response at KFHAC onset reflective of transient activation of underlying sympathetic axons, the "onset" response. The ~80% block of functional sympathetic control of the heart during KHFAC was readily reversible as indicated the T3 stimulation in the recovery phase (RT3 post).

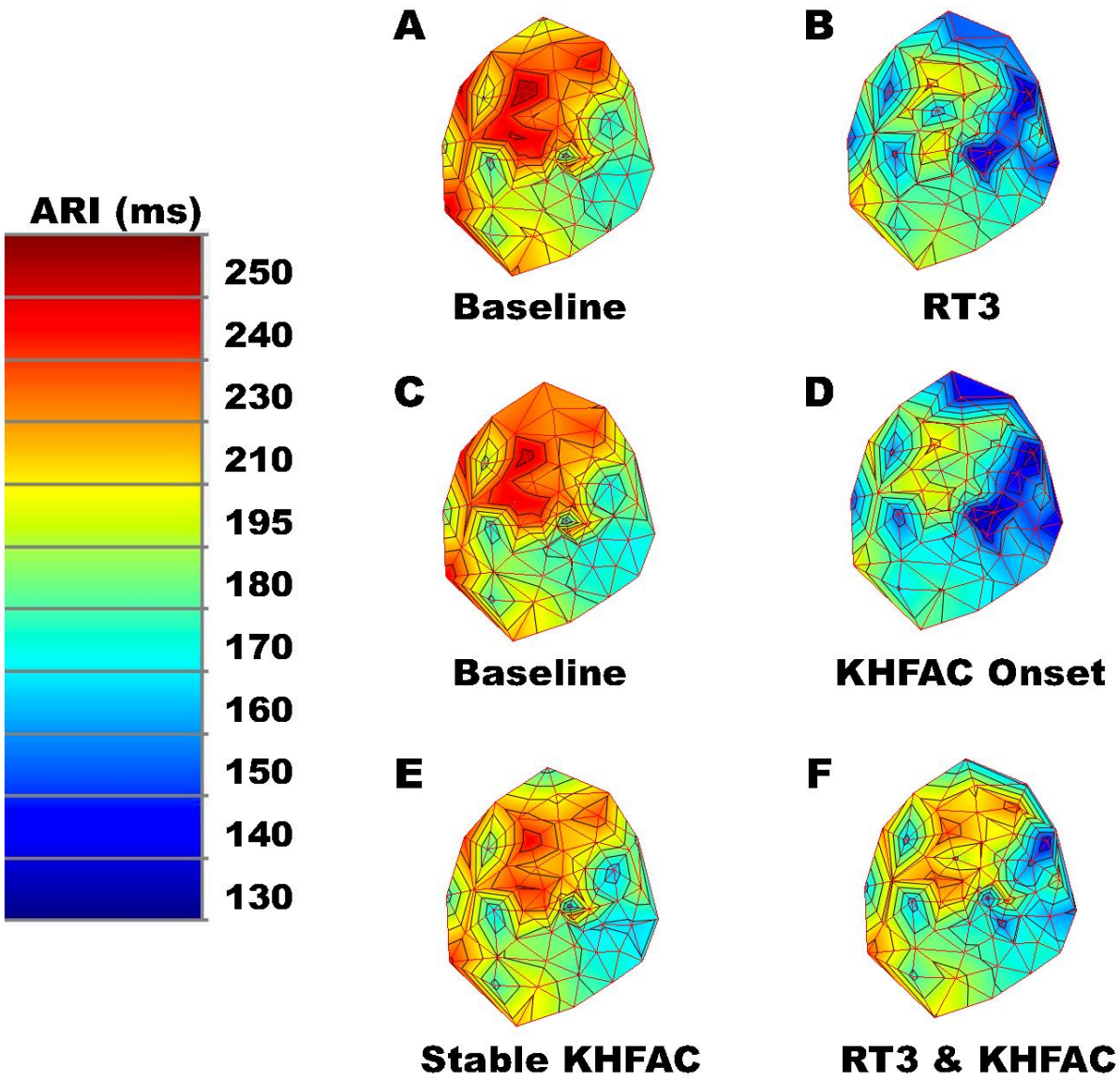

Figure 3: Representative polar map of ARI (ms) in one animal comparing baseline intact (panels A and C) conditions, with right T3 ganglion stimulation (RT3) (panel B), during the onset (panel D) and stable phase of KHFAC (panel E) and with RT3 applied during the stable phase of KHFAC (panel F). The pattern of ARI shortening was similar between RT3 stimulation and onset of KHFAC as applied to T1-T2 region of paravertebral chain. In the stable phase of KHFAC, ARI returned towards baseline, but remained shortened. KHFAC mitigated the ARI shortening associated with RT3 stimulation.

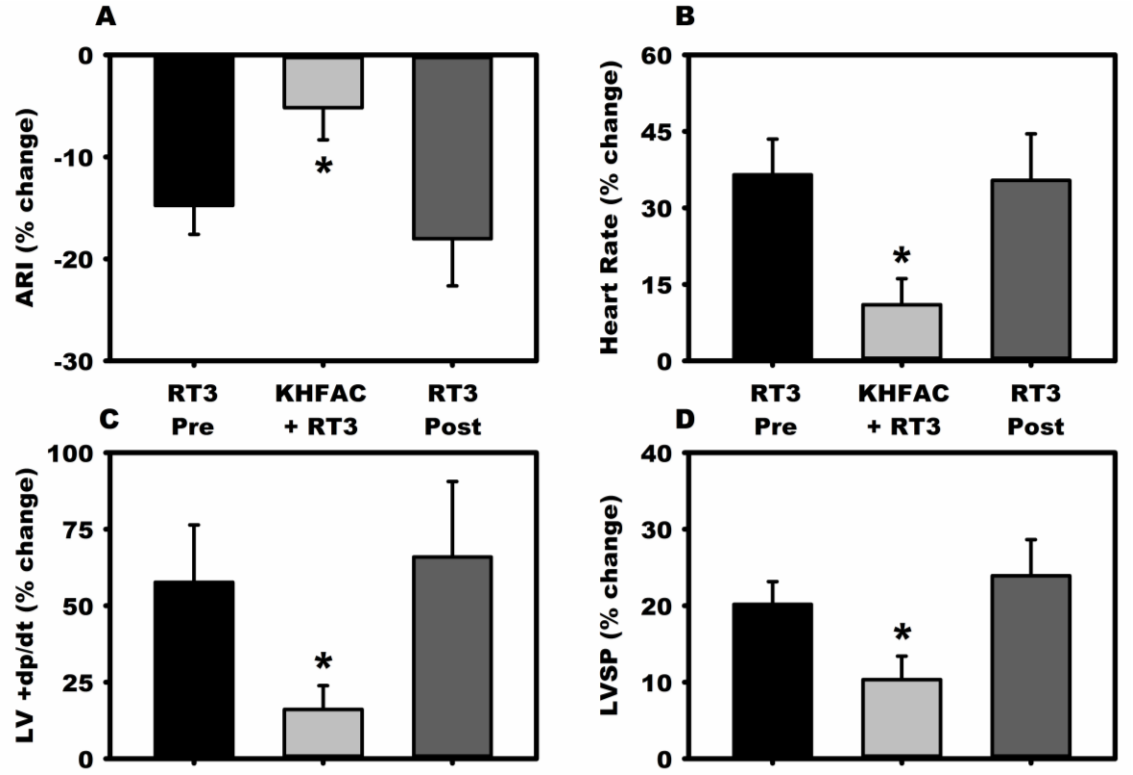

Figure 4: The percentage change in ventricular ARI (panel A), heart rate (panel B), LV dp/dt (panel C) and LVSP (panel D) in response to T3 stimulation prior to (RT3 pre), during KHFAC (KHFAC+RT3) and in the recovery phase after bioelectric blockade (RT3 post). * = $p<0.05$

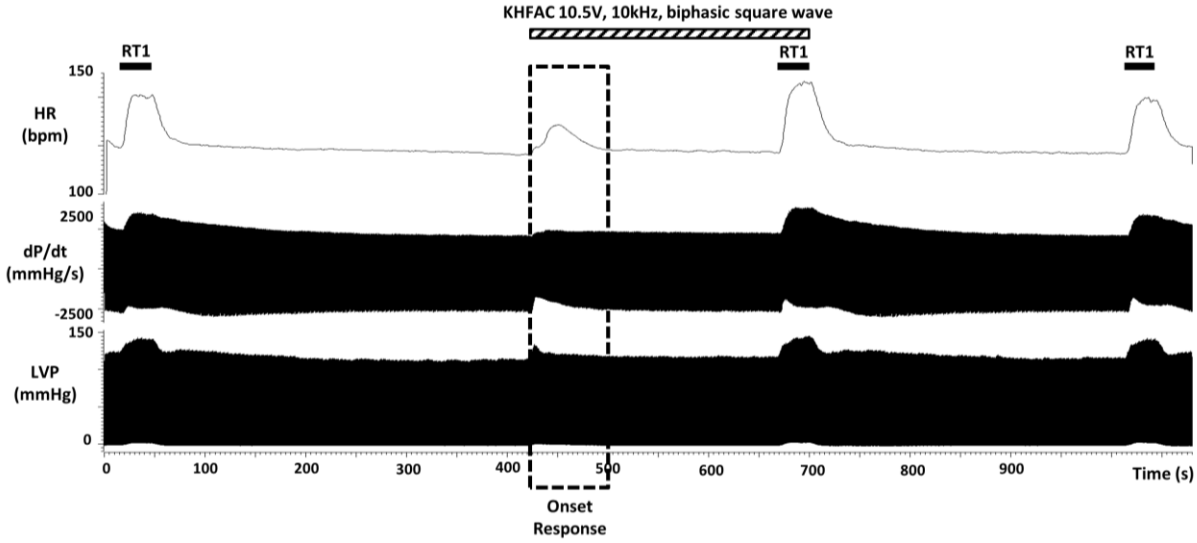

Figure 5: Response to T1 stimulation prior to and during T1-T2 KHFAC. Note the maintained response in heart rate, LV +dp/dt and LVSP during blocking currents applied caudal to stellate stimulation.

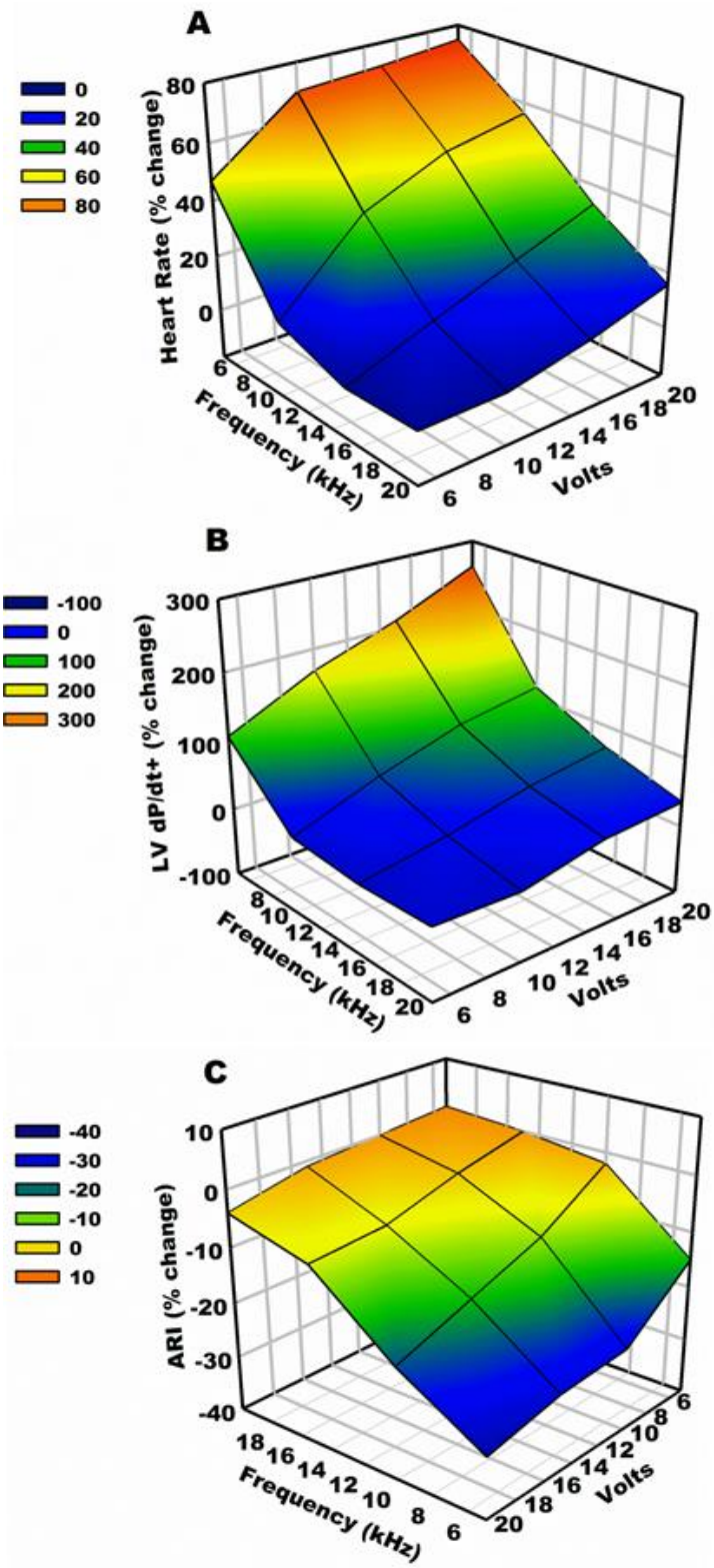

Figure 6: Effects on KHFAC frequency and intensity on magnitude of the onset response for heart rate (panel A), LV dP/dt+ (panel B), and ARI (panel C – note frequency and voltage axis values are reversed relative to panel A and B). Lower frequency and higher voltage resulted in a greater onset response.

REFERENCES

1. Ackermann DM, Bhadra N, Gerges M, and Thomas PJ. Dynamics and sensitivity analysis of high-frequency conduction block. J Neur Eng 8: 065007, 2011.
2. Ajijola OA, Yagishita D, Reddy NK, Yamakawa K, Vaseghi M, Downs AM, Hoover DB, Ardell JL, and Shivkumar K. Remodeling of stellate ganglion neurons after spatially targeted myocardial infarction: Neuropeptide and morphologic changes. Heart Rhythm 12: 1027-1035, 2015.
3. Ardell JL, Andresen MC, Armour JA, Billman GE, Chen PS, Foreman RD, Herring N, O'Leary DS, Sabbah HN, Schultz HD, Sunagawa K, and Zucker IH. Translational neurocardiology: preclinical models and cardioneural integrative aspects. J Physiol 594: 3877-3909, 2016.
4. Ardell JL, Rajendran PS, Nier HA, KenKnight BH, and Armour JA. Central-peripheral neural network interactions evoked by vagus nerve stimulation: functional consequences on control of cardiac function. Am J Physiol Heart Circ Physiol309: H1740-1752, 2015.
5. Armour JA. Potential clinical relevance of the 'little brain' on the mammalian heart. Exp Physiol 93: 165-176, 2008.
6. Arora RC, Waldmann M, Hopkins DA, and Armour JA. Porcine intrinsic cardiac ganglia. The anatomical record Part A, Discoveries in molecular, cellular, and evolutionary biology 271: 249-258, 2003.
7. Beaumont E, Salavatian S, Southerland EM, Vinet A, Jacquemet V, Armour JA, and Ardell JL. Network interactions within the canine intrinsic cardiac nervous system: implications for reflex control of regional cardiac function. J Physiol 591: 4515-4533, 2013.
8. Bhadra N and Kilgore KL. High-frequency electrical conduction block of mammalian peripheral motor nerve. Muscle Nerve 32: 782-790, 2005.
9. Bourke T, Vaseghi M, Michowitz Y, Sankhla V, Shah M, Swapna N, Boyle NG, Mahajan A, Narasimhan C, Lokhandwala Y, and Shivkumar K. Neuraxial modulation for refractory ventricular arrhythmias: value of thoracic epidural anesthesia and surgical left cardiac sympathetic denervation. Circulation 121: 2255-2262, 2010.
10. Bromm B. Spike frequency of the nodal membrane generated by high-frequency alternating current. Pflugers Archiv 353: 1-19, 1975.

11. Buckley U, Yamakawa K, Takamiya T, Andrew Armour J, Shivkumar K, and Ardell JL. Targeted stellate decentralization: Implications for sympathetic control of ventricular electrophysiology. Heart Rhythm 13: 282-288, 2016.
12. Chugh SS, Reinier K, Teodorescu C, Evanado A, Kehr E, Al Samara M, Mariani R, Gunson K, and Jui J. Epidemiology of sudden cardiac death: clinical and research implications. Prog Cardiovasc Dis 51: 213-228, 2008.
13. Florea VG and Cohn JN. The autonomic nervous system and heart failure. Circ Res 114: 1815-1826, 2014.
14. Foreman RD and Linderoth B. Neural mechanisms of spinal cord stimulation. Int Rev Neurobiol 107: 87-119, 2012.
15. Foreman RDD, M.J.L.; Linderoth, B. Integrative control of cardiac function by cervical and thoracic spinal neurons. In: Basic and Clinical Neurocardiology, edited by Armour JA and Ardell JL. New York: Oxford University Press, 2004, p. 153-186.
16. Franke M, Vrabec T, Wainright J, Bhadra N, Bhadra N, and Kilgore K. Combined KHFAC + DC nerve block without onset or reduced nerve conductivity after block. J Neur Eng 11: 056012, 2014.
17. Fukuda K, Kanazawa H, Aizawa Y, Ardell JL, and Shivkumar K. Cardiac innervation and sudden cardiac death. Circ Res 116: 2005-2019, 2015.
18. Hardwick JC, Ryan SE, Beaumont E, Ardell JL, and Southerland EM. Dynamic remodeling of the guinea pig intrinsic cardiac plexus induced by chronic myocardial infarction. Auton Neurosci 181: 4-12, 2014.
19. Haws CW and Lux RL. Correlation between in vivo transmembrane action potential durations and activation-recovery intervals from electrograms. Effects of interventions that alter repolarization time. Circulation 81: 281-288, 1990.
20. Janes RD, Brandys JC, Hopkins DA, Johnstone DE, Murphy DA, and Armour JA. Anatomy of human extrinsic cardiac nerves and ganglia. Am J Cardiol 57: 299-309, 1986.
21. Kember G, Armour JA, and Zamir M. Neural control hierarchy of the heart has not evolved to deal with myocardial ischemia. Physiol Genom 45: 638-644, 2013.
22. Kilgore KL and Bhadra N. Nerve conduction block utilising high-frequency alternating current. Med Biol Eng Comp 42: 394-406, 2004.
23. Kilgore KL and Bhadra N. Reversible nerve conduction block using kilohertz frequency alternating current. Neuromodulation 17: 242-254; discussion 254-245, 2014.

24. Norris JE, Foreman RD, and Wurster RK. Responses of the canine heart to stimulation of the first five ventral thoracic roots. Am J Physiol 227: 9-12, 1974.
25. Patel YA, Saxena T, Bellamkonda RV, and Butera RJ. Kilohertz frequency nerve block enhances anti-inflammatory effects of vagus nerve stimulation. Sci Rep 7: 39810, 2017.
26. Priori SG, Blomstrom-Lundqvist C, Mazzanti A, Blom N, Borggrefe M, Camm J, Elliott PM, Fitzsimons D, Hatala R, Hindricks G, Kirchhof P, Kjeldsen K, Kuck KH, Hernandez-Madrid A, Nikolaou N, Norekval TM, Spaulding C, and Van Veldhuisen DJ. 2015 ESC Guidelines for the management of patients with ventricular arrhythmias and the prevention of sudden cardiac death: The Task Force for the Management of Patients with Ventricular Arrhythmias and the Prevention of Sudden Cardiac Death of the European Society of Cardiology (ESC). Endorsed by: Association for European Paediatric and Congenital Cardiology (AEPC). Eur Heart J 36: 2793-2867, 2015.
27. Rajendran PS, Nakamura K, Ajijola OA, Vaseghi M, Armour JA, Ardell JL, and Shivkumar K. Myocardial infarction induces structural and functional remodelling of the intrinsic cardiac nervous system. J Physiol 594: 321-341, 2016.
28. Schwartz PJ. Cardiac sympathetic denervation to prevent life-threatening arrhythmias. Nat Rev Cardiol 11: 346-353, 2014.
29. Shen MJ and Zipes DP. Role of the autonomic nervous system in modulating cardiac arrhythmias. Circ Res 114: 1004-1021, 2014.
30. Stecker EC, Reinier K, Marijon E, Narayanan K, Teodorescu C, Uy-Evanado A, Gunson K, Jui J, and Chugh SS. Public health burden of sudden cardiac death in the United States. Circ Arrhyth Electrophysiol 7: 212-217, 2014.
31. Van Buyten JP, Al-Kaisy A, Smet I, Palmisani S, and Smith T. High-frequency spinal cord stimulation for the treatment of chronic back pain patients: results of a prospective multicenter European clinical study. Neuromodulation 16: 59-65; discussion 65-56, 2013.
32. Vaseghi M, Gima J, Kanaan C, Ajijola OA, Marmureanu A, Mahajan A, and Shivkumar K. Cardiac sympathetic denervation in patients with refractory ventricular arrhythmias or electrical storm: intermediate and long-term follow-up. Heart Rhythm 11: 360-366, 2014.
33. Vaseghi M, Zhou W, Shi J, Ajijola OA, Hadaya J, Shivkumar K, and Mahajan A. Sympathetic innervation of the anterior left ventricular wall by the right and left stellate ganglia. Heart Rhythm 9: 1303-1309, 2012.
34. Yamakawa K, Howard-Quijano K, Zhou W, Rajendran P, Yagishita D, Vaseghi M, Ajijola OA, Armour JA, Shivkumar K, Ardell JL, and Mahajan A. Central vs. peripheral neuraxial

sympathetic control of porcine ventricular electrophysiology. Am J Physiol Reg Integr Comp Physiol 310: R414-421, 2016.

35. Zucker IH, Patel KP, and Schultz HD. Neurohumoral stimulation. Heart Fail Clin 8: 87-99, 2012.

CHAPTER 4:

BIOELECTRONIC BLOCK OF PARAVERTEBRAL SYMPATHETIC NERVES MITIGATES POST-MYOCARDIAL INFARCTION VENTRICULAR ARRHYTHMIAS

INTRODUCTION

Sudden cardiac death occurs as a result of ventricular tachyarrhythmias (VTs) in patients with coronary artery disease and heart failure (11). Medication can reduce arrhythmias, but can also be pro-arrhythmic, especially when there is ischemia (23). Implantable cardioverter defibrillators reactively treat VT but do not prevent them (23). Catheter ablation is an effective treatment in patients with VT, but subsets of individuals remain unresponsive to conventional therapeutic approaches (29). For these patients, bilateral cardiac stellate decentralization (BCSD) has shown efficacy for reducing arrhythmia events (30). While efficacious in VT management (30), BCSD is permanent and often accompanied by off-target effects including hyperalgesia and hyperhidrosis (12). Thus, a major unmet need is to impact neural control of cardiac function with a targeted, rapid, reversible and scalable modality that is safe for autonomic nerves and, ultimately, can be deployed chronically.

Bioelectronic therapies utilize electrical current to impact tissue/organ function. Depending on the target, electrode/tissue interface and stimulation protocol, such therapy can stimulate or suppress action potential propagation along nerves and alter neural network function (3, 16, 32, 33). Two primary bioelectronic protocols for blocking of action potential propagation are kilo-hertz frequency alternating current (KHFAC)(16) and direct current (DC) (32, 33). DC has the capability to block nerve conduction and, when delivered in a charge-balance (CBDC) mode, can do so repeatedly and safely (32, 33). With CBDC there is a cathodic current delivery phase that is fundamental to nerve block, followed by a recharge anodic current delivery (33), the net current delivery during each cycle being ~0 mA. To prevent nerve activation in transition phases (baseline-block-recharge-baseline), current ramps are used instead of step changes (33).

CBDC for control of nerves fulfills the need for rapid onset and scalability, but from a single node it is limited by duration (33). Even short-duration DC can degrade conduction due to creation of toxic reactants at the electrode interface (20). This can be mitigated in part by using interfaces with high effective surface area and by the CBDC waveform (33). This temporal design constraint can be overcome by adding CBDC nodes in series and interlacing the stimulation waveforms (32). By such approaches, the duty cycle for CBDC can be increased up to 100% and the blocking phase increased from seconds (33) to minutes (32). This approach is referred to as CBDC carousel (CBDCC).

This study had two objectives; 1) to evaluate efficacy of CBDCC to produce rapid, reversible and scalable control of sympathetic efferent inputs to the heart; and 2) to determine if CBDCC reduced the induction of VT in hearts with chronic myocardial infarction (MI) in a porcine model. To accomplish this, the electrode interface was deployed to the T1-T2 region of

the paravertebral chain, a convergence/nexus point through which sympathetic preganglionic axons project prior to synapsing with intrathoracic sympathetic ganglia (8). Our data indicates that CBDCC meets all the constraints necessary to functionally blunt sympathetic efferent projections to the heart such that the potential for arrhythmias can be reduced, even in the setting of a heterogeneous cardiac electrophysiological substrate.

MATERIAL AND METHODS

Animal care was performed in accordance with guidelines set by the *NIH Guide for the Care and Use of Laboratory Animals* (8th Edition, 2011). The experimental protocols were approved by the UCLA Animal Research Committee. A two-tier experimental design was used: Phase 1, in acute porcine models, consisted of interface and stimulation parameters optimization to achieve focal, graded and reversible nerve block of cardiac-related sympathetic axons traversing the T1-T2 region of the paravertebral chain; Phase 2 evaluated the efficacy of CBDCC applied to the T1-T2 region of the paravertebral chain to stabilize ventricular electrical function in a porcine model with chronic MI.

Electrode design, Waveform and Power Sources:

Multi-contact J-cuff electrodes were fabricated using the design detailed in Vrabec et al. (32) (Figure 1B). The CBDCC waveform used has a zero net charge and consisted of a linear ramp (2 s) to a plateau amplitude (4 s), and then a linear ramp (2 s) back to zero (Figure 1C). The recharge phase consists of a ramp, followed by a 16 second plateau at 34% of cathodic current (charge-balance the first phase of the waveform) and a return to zero. This waveform is generated successively on four channels with seven seconds between each channel as shown in Figure 1D and detailed in Vrabec et al (32). By such timing, by the time node 4 has completed its plateau phase, node 1 has completed recharge and is available for re-stimulation. Waveforms were generated by custom LabView software, outputting through a National Instruments DAQ (NI USB-6229 M Series BNC, Austin, TX). Each node was powered by individual current sources (Abcase LLC, Strongsville, OH). All four current sources used a common ground that was connected to an electrode placed subcutaneously on the animal's chest. The electrode was deployed to the right-side paravertebral chain between the T1-T2 paravertebral ganglia (Figure 1A).

Animal Model:

Two groups of animals (Yorkshire pigs) were used in the study. Phase 1 were acute studies to optimize interface and stimulation parameters for CBDCC (n=7 animals, 36 ± 5 kg) and phase 2 animals with healed anteroapical MI (n=7 animals, 88 ± 19 kg) to assess the efficacy of CBDCC to stabilize cardiac electrical function.

MI Induction:

MI was created as previously described (22). Briefly, animals were sedated (telazol, 8mg/kg, IM), intubated, ventilated and general anesthesia maintained with isoflurane (1-2%, INH). From femoral vascular access an Amplatz Guidewire with J-Tip (Boston Scientific, Marlborough, MA) was used to guide the Amplatz (AL2, Boston Scientific, Marlborough, MA) coronary guide catheter under fluoroscopy to the left anterior descending coronary artery (LAD). A balanced middle weight wire (Abbott Vascular, Temecula, CA) was directed into the LAD and a 3.0x20 mm 135 mm internal diameter over the wire angioplasty balloon (FoxCross PTA Catheter; Abbot Vascular, Temecula, CA) positioned after the first diagonal. The angioplasty balloon was inflated and 3-5 mL of polystyrene microspheres suspended in saline (Polybead, 90 μm diameter; Polysciences Inc., Warrington, PA) were injected through the lumen of the angioplasty balloon catheter. Occlusion of the artery was confirmed by contrast angiography, and acute myocardial ischemia confirmed by the presence of ST-segment elevations. Terminal studies were 8-16 weeks post infarct.

Terminal Surgical Preparation:

Animals were sedated with telazol (8 mg/kg, IM), intubated, ventilated and general anesthesia maintained with isoflurane (1-2%, INH). After fentanyl (20-30 μg/kg, IV), a sternotomy was performed to expose the heart and paravertebral chain. A femoral vein was used for saline administration and femoral artery for monitoring arterial pressure. Left ventricular pressure (LVP) was recorded using a Millar catheter (SPR-350, Millar Instruments, Houston, TX) placed into the left ventricle (LV) via the left carotid artery. In acute animals, to eliminate potential competing effects mediated by vagal reflexes during T1/T2 sympathetic stimulation, the vagosympathetic nerve trunks were isolated and cut. Vagosympathetic nerve trunks remained intact in the chronic MI models. For terminal procedures, ECG along with LV and arterial pressures were input to Power1401 data acquisition system (Cambridge Electrical Design Ltd, Cambridge, UK).

Following completion of surgery, general anesthesia was transitioned to α-chloralose (50 mg/kg IV bolus with maintenance at 25 mg/kg/hr; Sigma-Aldrich, St. Louis, MO). Body

temperature was maintained using heating pads. Acid-base balance was monitored and adjusted by changing respiratory parameters and/or bicarbonate infusion. At experiment completion, animals were euthanized by sodium pentobarbital (100 mg/kg, IV).

T1/T2 Stimulations and Electrode Placement:

The right paravertebral chain was exposed from the T1 to T2 ganglia and bipolar needle electrodes were inserted into each ganglion. The electrodes were interfaced with Grass S88 stimulators (Grass Co., Warwick, RI) via SIU6 constant current stimulus isolation units. The CBDCC electrode was placed under the chain, between T1 and T2 ganglia (Figure 1A). Electrical stimulation of the T1 and T2 ganglia were titrated at 4Hz to achieve a 20% increase in LVP, heart rate, dP/dt max or decrease in activation recovery interval. After threshold was identified, the stimulus intensity used thereafter was 1.5 times threshold, applied for 30 second periods. Between sequential nerve stimulations there was a waiting period of 10 min to allow for all parameters to return to baseline.

CBDCC:

For control animals, T2 ganglion stimulations were conducted with and without graded CBDCC block. The same current was applied to all nodes of the CBDCC electrode. Current to the electrode was sequentially ramped (0.1 – 0.5 mA steps) until no further suppression of cardiac indices in response to T2 stimulation was observed or to a maximum of 4mA was achieved. The maximal current limit was below the water window based on the average Q for these electrodes.(33) For terminal studies involving MI animals, a current was applied to the CBDCC electrode sufficient to decrease the T2-induced sympathetic augmentation in cardiac (chronotropic, inotropic and dromotropic) function by > 66%. For these studies, VT inducibility was assessed prior to and during CBDCC.

Activation Recovery Interval (ARI) Recordings:

ARIs are reliable surrogates for activation potential duration (1, 21) and can be utilized to assess indices of regional and global cardiac electrophysiological function (31). A 56-electrode sock array was placed over the ventricular epicardium to concurrently record unipolar cardiac electrograms (EGM). The data was acquired with a Prucka CardioLab system (GE Healthcare, Pasadena, CA). Using custom software to generate the first derivative of recorded unipolar EGMs, ARI is the difference between repolarization and activation time, as measured from the

minimum dV/dt (in the QRS complex) to the maximal dV/dt (near peak of T wave) (1, 31). Mean global ARI is the average from all 56 electrodes.

Cardiac Electrical Stability Assessment:

A bipolar pacing catheter (St Jude, St Paul, MN) was inserted into the right ventricular apex and connected to the Prucka and Micropace systems (EPS320; Micropace, Canterbury, New South Wales, Australia). Pacing threshold was established and pacing output set as 2x threshold. Programmed ventricular stimulation was performed with an 8-beat drive train at two different cycle lengths (600 ms; 400 ms), at 2 different sites (right ventricular endocardium and LV epicardium), with up to 3 extra-stimuli, to the effective refractory period or a minimum of 200 milliseconds, or until sustained VT or ventricular fibrillation was induced. The inter-train pause was 3 seconds. Ventricular effective refractory period (VERP) was defined as the longest coupling interval for which a premature impulse fails to propagate through that tissue. Inducibility was defined as VT that lasted greater than 30 seconds or that degenerated into ventricular fibrillation requiring direct cardioversion. This test was performed at baseline and under CBDCC block, with a minimum 1 hour recovery in between. If necessary, sustained arrhythmias were terminated with a 15 J epicardial shock from a defibrillator (Lifepak; Physio-Control, Redmond, WA) to restore sinus rhythm. Without therapeutic interventions, VT assessments using this methodology are stable over time (9, 10, 25).

Statistical Analyses:

Data are reported as mean ± standard error of the mean (SEM). Statistical comparisons for block efficacy and changes in basal cardiac function were done using a one-way repeated measure ANOVA. If the p-value using ANOVA was significant ($p \leq 0.05$), post-hoc multiple comparisons were done using the Tukey Test. A Chi-square test was used to assess inducibility of VT before and after CBDCC application. Statistical analyses were performed using SigmaPlot 12 (Systat Software Inc., San Jose, CA).

RESULTS

Validation of CBDCC Block (Phase 1)

Stimulation currents were established for right (RT1) and right paravertebral ganglia (RT2) to evoke equivalent increases in heart rate, LVP and the first derivative of LV developed pressure (dP/dt). These currents averaged 1.9±0.4 mA for RT1 and 8.6±1.5 mA for RT2 (n=7). Figure 2 shows a representative response to RT2 and RT1 stimulation delivered prior to and during 5 cycles of CBDCC and an RT2 stimulus challenge delivered 5 min after termination of the CBDCC. CBDCC did not impact the cardiac augmenting response to RT1 (upstream) stimulation. In contrast, note the suppression in RT2-evoked changes in heart rate, LVP and LV dP/dt during CBDCC, a response that had fully recovered 5 min after block termination.

Figure 3 illustrates the scaling capabilities of CBDCC as manifest against the background sympatho-excitation evoked by T2 stimulation. Note the progressive attenuation of T2-induced ARI shortening as CBDCC current is increased from 0.7 to 1.0 mA. Across all animals, there was an approximate curvilinear relationship of current intensity to block of T2-evoked positive chronotopic (panel 4B), inotropic (panel 4C) and dromotropic (panel 4D) function. RT1 and RT2 stimulation responses without block were stable over the course of the experiment (data not shown). CBDCC exerted minimal effects on basal cardiac function (Figure 4A).

Chronic MI (Phase 2)

Chronic MI animals were terminated 8-16 weeks following MI induction. VT was induced at baseline in all animals (n=7). The VT cycle length ranged from 200 – 300 milliseconds and all were initially sustained monomorphic VT with 2/7 degenerating into polymorphic VT. One animal died after the baseline induction. Evoked cardiac augmenting responses, using T2 stimulation, were first characterized (Figure 5); the currents required were equivalent in chronic MI model (7.4±4.9 mA) vrs normal animals (8.6±1.5 mA). A level of CBDCC current (2.3±0.6 mA) was then established that created an average block of at least 66% of assessed cardiac hemodynamic variables. This CBDCC current produced an average decrease of 66% for heart rate, 75% of LV dP/dt and 81% for ventricular ARI in the T2-evoked cardiac response (Figure 5). This block was fully reversible on block termination (Figure 5, dark gray bars).

Of the 6 animals that survived VT inducibility tests, only one was re-inducible for VT during CBDCC application (Figures 6A) ($p<0.002$). The VERP was also assessed under baseline and CBDCC conditions. At baseline in the chronic MI animals, VERP averaged 271±32 milliseconds, increasing to 323±26 milliseconds during CBDCC ($p<0.05$) (Figure 6B).

DISCUSSION

This is the first study demonstrating that reversible bioelectronic modulation of intrathoracic cardiac-related sympathetic nerve projections significantly reduces arrhythmia inducibility. The

primary findings are: i) The T1-T2 region is a well-suited nexus point for bioelectronic control of sympathetic efferent projections to the heart; ii) CBDCC waveforms did not impact basal cardiac indices; iii) there is a cathodic current-dependent relationship allowing for scalable and functional reduction in evoked-sympathetic efferent inputs to the heart; iv) repeated short term application of CBDCC waveforms did not affect nerve conduction or downstream intrathoracic ganglia function; and v) partial (66%) CBDCC unilateral block of the right T1-T2 region of the paravertebral chain significantly reduces the arrhythmia burden following MI; and vi) CBDCC increases cardiac electrical stability, mediated in part by a prolonged VERP.

Axonal Modulation therapy

The ability to safely mitigate cardiac-related sympathetic efferent nerve inputs to the heart in a rapid, scalable and reversible fashion is a fundamental design constraint for evolving axonal modulation therapeutics for clinical applications. KHFAC block has been shown to be highly efficacious in preclinical models to reduce afferent and efferent nerve activity (16); however its use is complicated by a transient “onset response” (16). For heart-related therapeutics, this sympatho-excitation at onset could prove highly detrimental to the patient (7, 11). CBDC block represents an alternative form of axonal modulation therapy with potential autonomic control indications (33).

We demonstrate that CBDCC applied under axons traversing the T1-T2 region of the paravertebral chain can block sympathetic pre-ganglionic efferent nerve projections to the heart in a safe, reproducible and scalable manner. Evoked changes in sympathetic control of the heart can be mitigated by CBDCC without interfering with intrathoracic ganglia function or altering basal cardiac function. A memory function to applied CBDCC may exist, but it would be less than 5 min in response to short-duration DC block applied herein. This anti-arrhythmic effect is manifest even when applied to right-sided stellate sympathetic control, a region where cooling or ablation has been reported to lower the threshold for VT induction (26). Recent work from patients with intractable VT has demonstrated that bilateral stellectomy confers a greater protection against spontaneous VT episodes that left stellectomy alone(30) indicating that either stellate is a viable target for neuromodulation therapy.

CBDCC can prevent arrhythmia induction

VTs evolving in the setting of chronic MI result from numerous factors, including changes in ionic balance (14), altered ion channel expression (14), substrate heterogeneity(14) and

adverse remodeling of the cardiac reflex control networks (2, 3, 24). Fundamental to the adverse neural remodeling is an afferent-mediated remodeling of intrinsic cardiac (24), intrathoracic (2) and central (17) aspects for cardiac autonomic control with resultant sympathetic overdrive and withdrawal of parasympathetic tone (3, 6). Amplification of sympatho-excitation by central aspects for cardiac control is a major factor in arrhythmia induction (11, 15). Approaches such as spinal cord stimulation (18, 27, 34), thoracic epidural anesthesia (11) and stellectomy (30) have leveraged this concept. The common theme of these approaches is that they target major convergence points for sympathetic control (e.g., thoracic cord and preganglionic projections traveling within T1-T4 aspects of the paravertebral chain destined for the intrathoracic cardiac-related sympathetic ganglia) (8). CBDCC blunting of sympathetic reflex function is a major contributor to functional cardiac stability. CBDCC likewise prolongs the VERP with minimal changes in overall ventricular ARI. The prolongation in global effective refractory period has anti-arrhythmic effects (11).

Clinical implications and future directions

Axonal modulation therapy, in this case with CBDCC, reflects a major advancement in the control of sympathetic projections to the heart. First, it is scalable, something that spinal cord stimulation is only marginally capable of (19, 28). Second, control is essentially instantaneous, occurring within 2 seconds as opposed to the minutes required for spinal cord stimulation (4, 13, 18, 28, 34). Third, it is readily reversible, with full control of sympathetic function restored within 5 minutes of CBDCC offset. This is in contrast to the 30 minute carryover effects of spinal cord stimulation (4, 5). Fourth, its sphere of influence for cardiac control is well defined (8). Finally, whereas implantable cardioverter defibrillators are a reactive therapy, axonal modulation therapy has the potential to target the underlying conflicts between central and peripheral aspects of the cardiac nervous system and reverse remodel the disease process itself.

Limitations:

While only efferent projections were evaluated in this study, the functional response to CBDCC may involve both efferent and afferent arms of the autonomic neuraxis. Depending on the site of block application, ganglia may be interspaced between the block site and the heart(8) and neural network processing could be impacted (4, 5, 34). While CBDCC protocols were optimized with vagi transected to minimize the potential for competing reflex influences during T2 stimulation, block efficacy was achieved at similar stimulus intensities when evaluated in the intact condition, indicating minimal involvement of vagal efferent or afferents in mediating the

effects of CBDCC applied to the paravertebral chain. Finally, these experiments were done in anesthetized animals, which can potentially impact autonomic control mechanisms.

Author contributions:

* RWC and UB contributed equally to the design, execution and data analysis of study. PSR and TV contributed in experiments and technology development. KS and JLA contributed to conceptual design and analytics. RWC and UB drafted the manuscript. All authors approved the final version of the manuscript.

Acknowledgment:

The authors acknowledge the inputs from Drs. Kevin Kilgore and Niloy Bhadra (Case Western Reserve University) in their review of the manuscript and in sharing their recognized experience in bioelectronic technologies of CBDC nerve block. The authors acknowledge Dr. Arun Sridhar (Glaxo Smith Kline) in concept development.

FIGURES

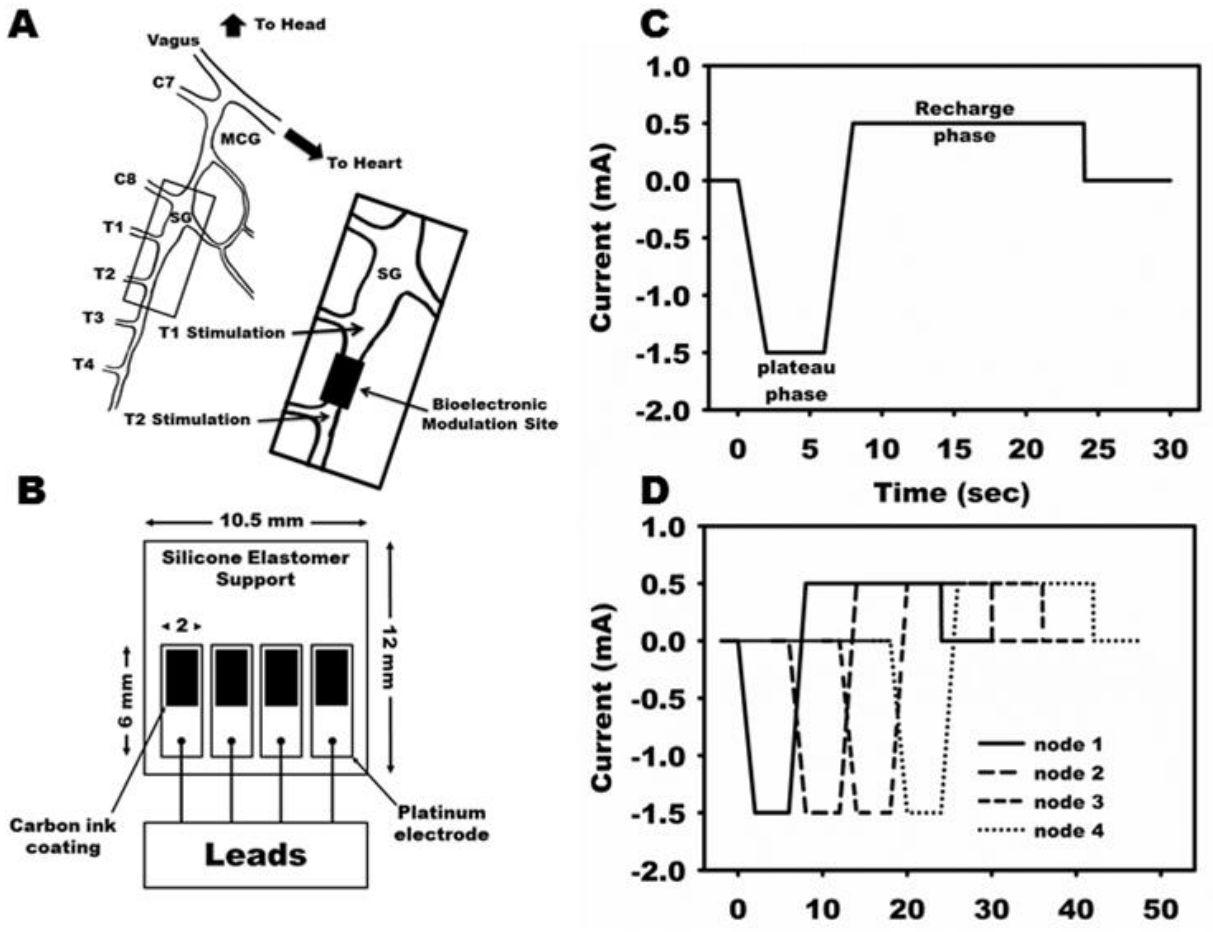

Figure 1: Implementation of bioelectronic nerve modulation for peripheral control of sympathetic inputs to the heart. Panel A: CBDC electrode is inserted between T1-T2 ganglia of the paravertebral chain with bipolar stimulating electrodes placed cranial (T1) or caudal (T2) to modulation site to assess block efficacy. Panel B: CBDC carousel consists of 4 nodes (2 mm width), evenly spaced 1.0 mm apart. Panel C: Charge-balanced waveform for single node showing ramp transitions between plateau (cathode blocking) and recharge (anode current) phase. Panel D: Interlaced stimulation protocol for charge-balanced waveforms delivered in sequence to nodes 1 to 4 of CBDC electrode.

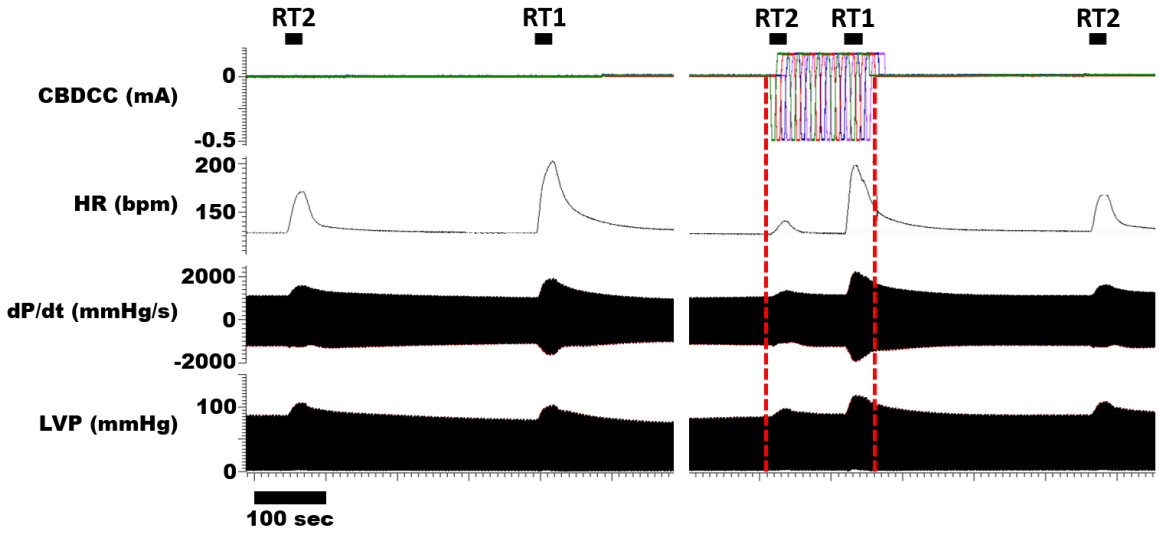

Figure 2: Cardiac hemodynamic response to stimulation of right stellate (RT1) or T2 (RT2) paravertebral ganglia with and without CBDCC. From top to bottom, figure shows time course of CBDCC (5 cycles through carousel), heart rate, left ventricular (LV) dP/dt and LV pressure. CBDCC delivered between the T1-T2 paravertebral ganglia mitigated the RT2 evoked sympathetic effects on the heart without interfering with RT1 evoked responses. Note the mitigation of the RT2 response was rapid at onset of block and readily reversible following termination of the DC current (right most RT2 stimulation).

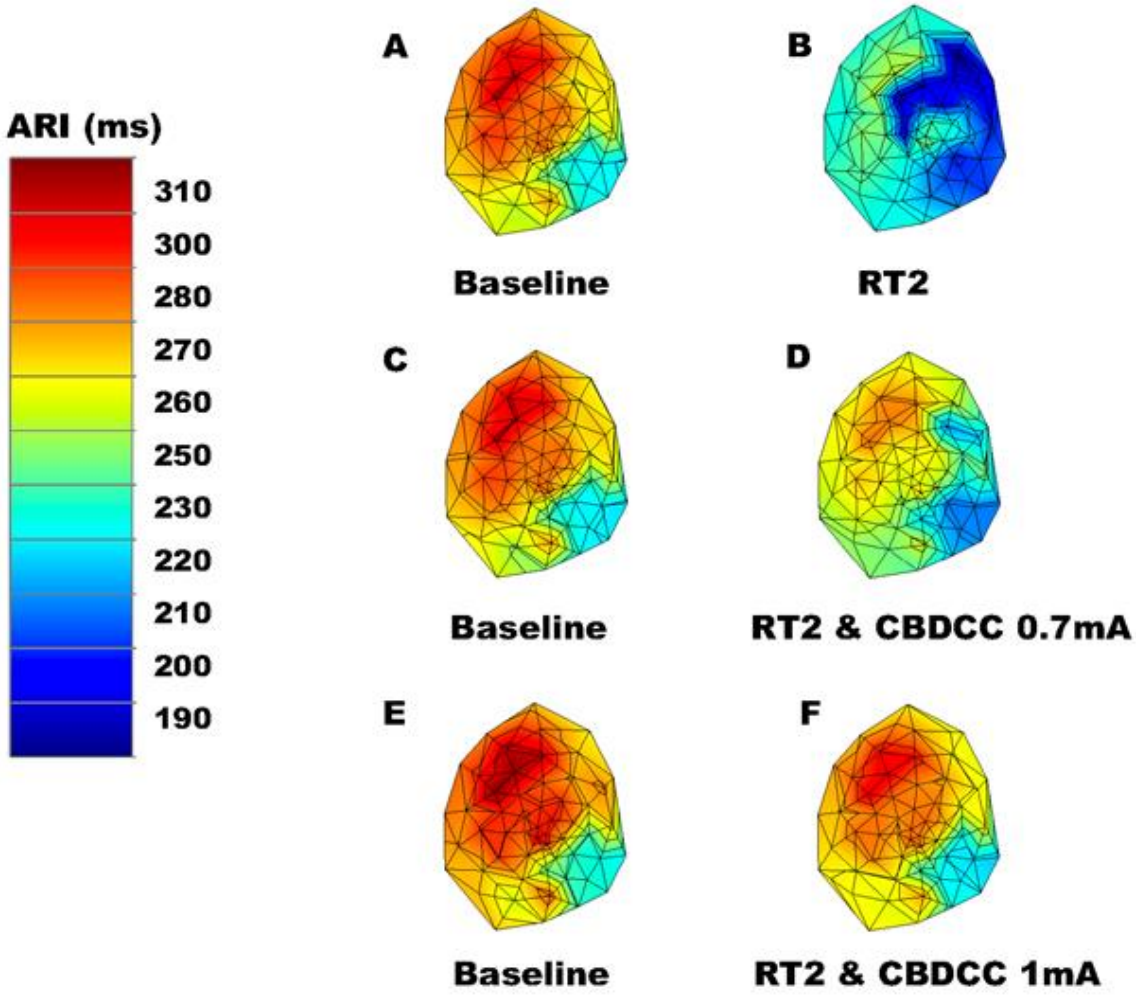

Figure 3: Representative polar maps of activation recovery intervals (ARI) (ms) in one animal comparing baseline intact (panels A, C and E) conditions, with right T2 paravertebral ganglion stimulation (RT2) alone (panel B), and RT2 stimulation during low (panel D) vs. higher (panel F) level CBDCC blockade. Note the relationship between CBDCC intensity and mitigation of the sympathetic mediated positive dromotropic response.

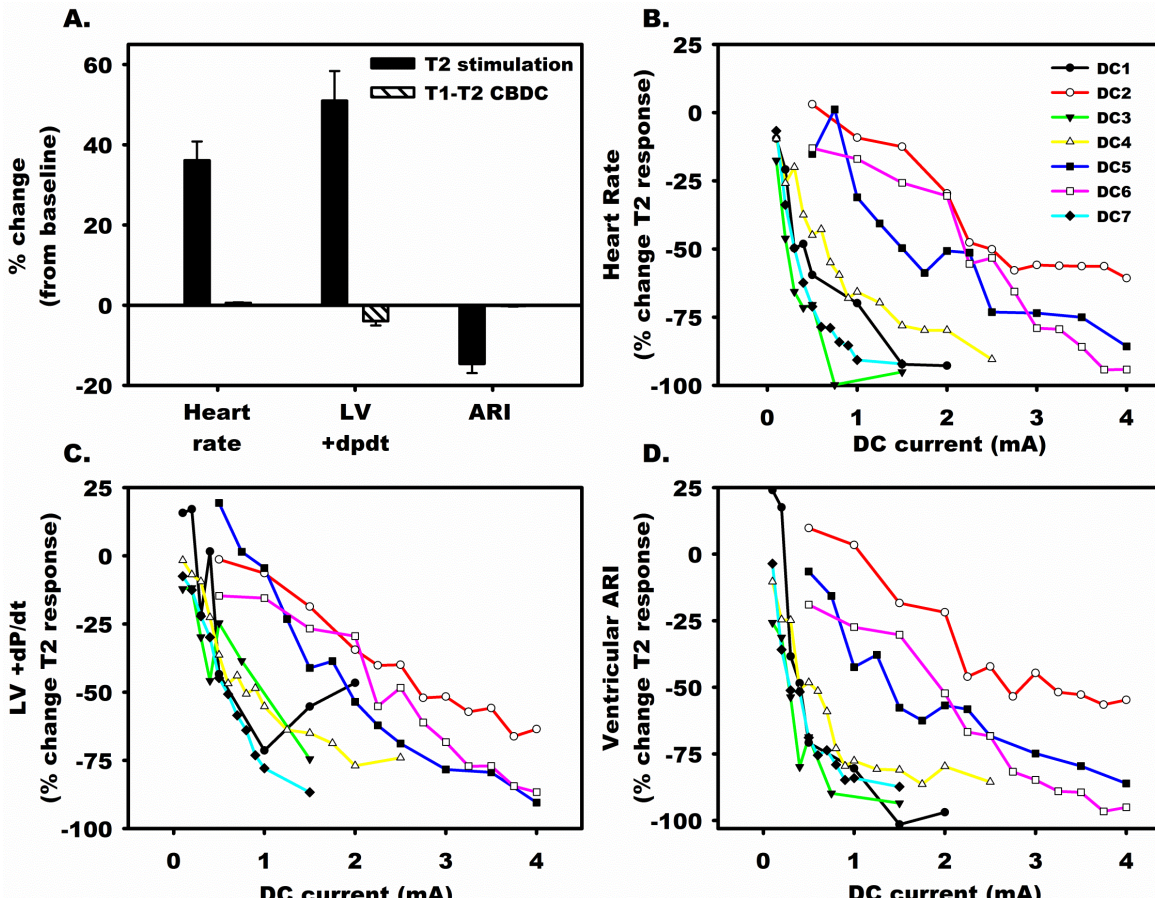

Figure 4: CBDCC induces scalable block of evoked sympathetic drive to heart without interfering with basal cardiac function. Panel A: Evoked changes in chronotropic (heart rate), inotropic (LV +dP/dt) and dromotropic (ventricular ARI) function in response to T2 stimulation (filled bars) or CBDCC (cross-hatched) bars. Percentage change of T2 evoked response in heart rate (panel B), LV +dP/dt (panel C) and LV ARI (panel D) in relation to intensity of current delivery during plateau (cathode) phase of CBDCC. The same current was applied sequentially across all four nodes. Evoked responses evaluated in 7 (DC1 to DC7) acute anesthetized animals.

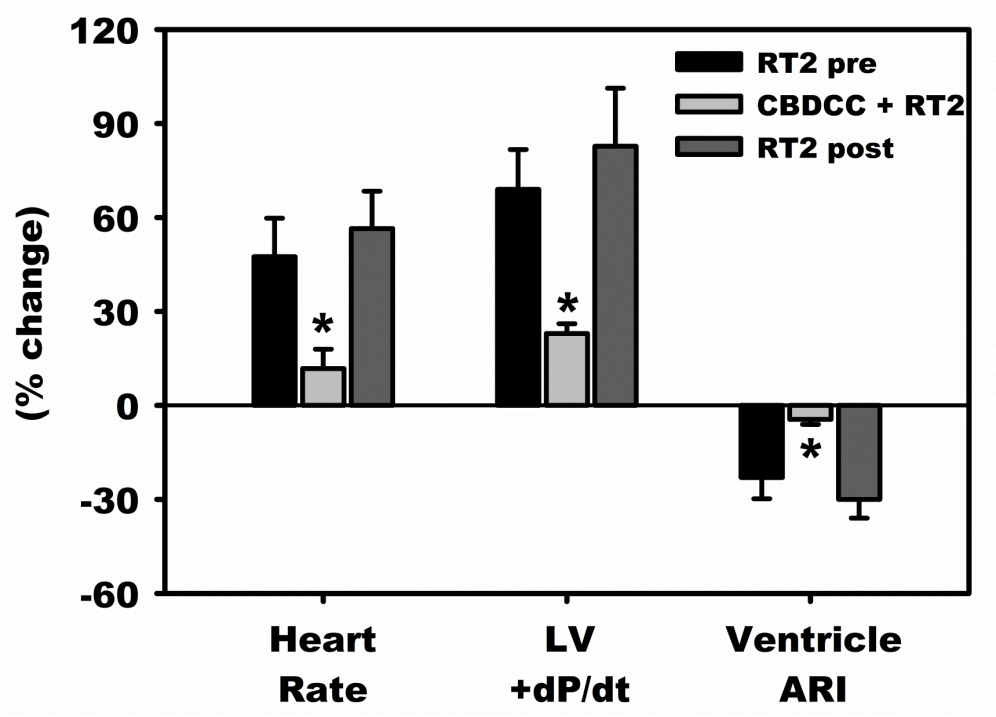

Figure 5: Implementation of CBDCC block in porcine models with chronic MI. Shown is average cardiac hemodynamics in response to RT2 stimulation prior to, during and following CBDCC. * $p<0.05$ from RT2 delivered without CBDCC (pre or post).

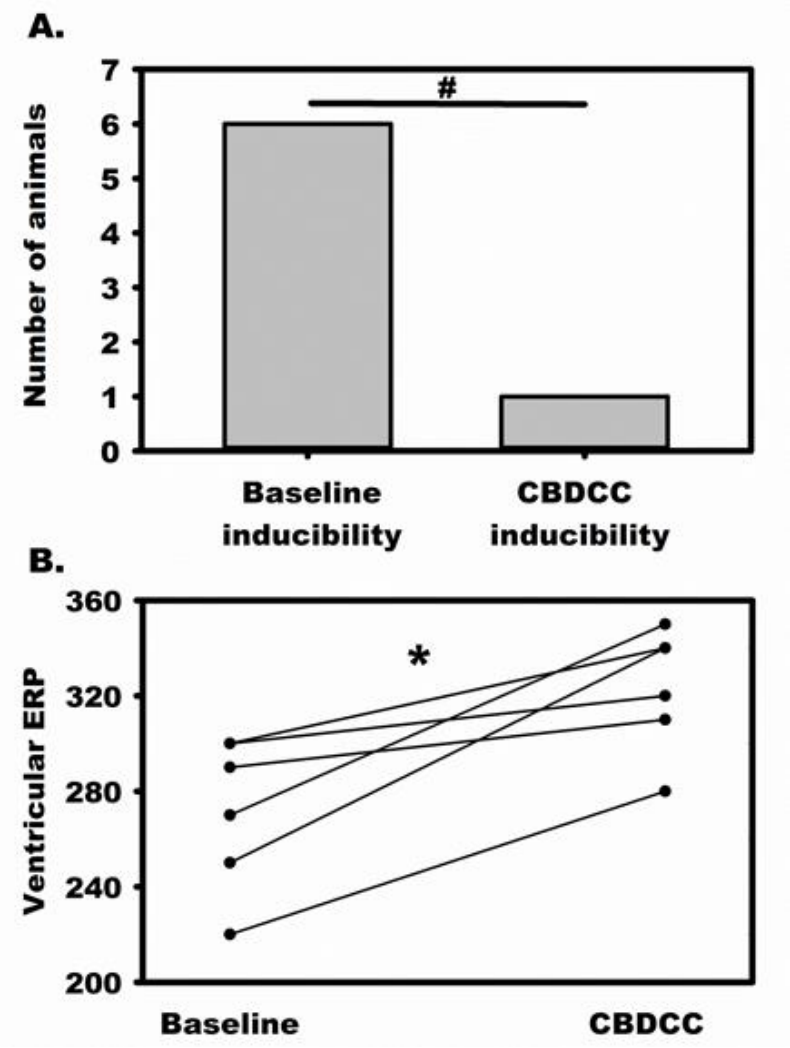

Figure 6: CBDCC applied to the T1-T2 region of the paravertebral chain improves electrical stability in chronic infarcted porcine hearts. Ventricular arrhythmias were inducible in all animals at baseline, but only one under CBDCC block (panel A). Decrease in arrhythmia induction was mediated by a significantly increased VERP with CBDCC (panel B). Each line represents an individual animal. # $p<0.002$,* $p<0.05$.

REFERENCES

1. Ajijola OA, Yagishita D, Patel KJ, Vaseghi M, Zhou W, Yamakawa K, So E, Lux RL, Mahajan A, and Shivkumar K. Focal myocardial infarction induces global remodeling of cardiac sympathetic innervation: neural remodeling in a spatial context. Am J Physiol Heart Circ Physiol 305: H1031-1040, 2013.
2. Ajijola OA, Yagishita D, Reddy NK, Yamakawa K, Vaseghi M, Downs AM, Hoover DB, Ardell JL, and Shivkumar K. Remodeling of stellate ganglion neurons after spatially targeted myocardial infarction: Neuropeptide and morphologic changes. Heart Rhythm 12: 1027-1035, 2015.
3. Ardell JL, Andresen MC, Armour JA, Billman GE, Chen PS, Foreman RD, Herring N, O'Leary DS, Sabbah HN, Schultz HD, Sunagawa K, and Zucker IH. Translational neurocardiology: preclinical models and cardioneural integrative aspects. J Physiol 594: 3877-3909, 2016.
4. Ardell JL, Cardinal R, Vermeulen M, and Armour JA. Dorsal spinal cord stimulation obtunds the capacity of intrathoracic extracardiac neurons to transduce myocardial ischemia. Am J Physiol Reg Integr Comp Physiol 297: R470-477, 2009.
5. Armour JA, Linderoth B, Arora RC, DeJongste MJ, Ardell JL, Kingma JG, Jr., Hill M, and Foreman RD. Long-term modulation of the intrinsic cardiac nervous system by spinal cord neurons in normal and ischaemic hearts. Autonomic neuroscience : basic & clinical 95: 71-79, 2002.
6. Billman GE. A comprehensive review and analysis of 25 years of data from an in vivo canine model of sudden cardiac death: implications for future anti-arrhythmic drug development. Pharmacol Ther 111: 808-835, 2006.
7. Buckley U, Chui RW, Rajendran PS, Vrabec T, Shivkumar K, and Ardell JL. Bioelectronic neuromodulation of the paravertebral cardiac efferent sympathetic outflow and its effect on ventricular electrical indices. Heart Rhythm, 2017 (in press).
8. Buckley U, Yamakawa K, Takamiya T, Andrew Armour J, Shivkumar K, and Ardell JL. Targeted stellate decentralization: Implications for sympathetic control of ventricular electrophysiology. Heart Rhythm 13: 282-288, 2016.
9. Cooper MJ, Koo CC, Skinner MP, Mortensen PT, Hunt LJ, Richards DA, Uther JB, and Ross DL. Comparison of immediate versus day to day variability of ventricular tachycardia induction by programmed stimulation. J Am Coll Cardiol 13: 1599-1607, 1989.

10. de Buitleir M, Morady F, DiCarlo LA, Jr., Baerman JM, and Krol RB. Immediate reproducibility of clinical and nonclinical forms of induced ventricular tachycardia. Am J Cardiol 58: 279-282, 1986.
11. Fukuda K, Kanazawa H, Aizawa Y, Ardell JL, and Shivkumar K. Cardiac innervation and sudden cardiac death. Circ Res 116: 2005-2019, 2015.
12. Gossot D, Kabiri H, Caliandro R, Debrosse D, Girard P, and Grunenwald D. Early complications of thoracic endoscopic sympathectomy: a prospective study of 940 procedures. Ann Thorac Surg 71: 1116-1119, 2001.
13. Issa ZF, Zhou X, Ujhelyi MR, Rosenberger J, Bhakta D, Groh WJ, Miller JM, and Zipes DP. Thoracic spinal cord stimulation reduces the risk of ischemic ventricular arrhythmias in a postinfarction heart failure canine model. Circulation 111: 3217-3220, 2005.
14. Janse MJ and Wit AL. Electrophysiological mechanisms of ventricular arrhythmias resulting from myocardial ischemia and infarction. Physiol Rev 69: 1049-1169, 1989.
15. Kember G, Armour JA, and Zamir M. Neural control hierarchy of the heart has not evolved to deal with myocardial ischemia. Physiol Genom 45: 638-644, 2013.
16. Kilgore KL and Bhadra N. Reversible nerve conduction block using kilohertz frequency alternating current. Neuromodulation 17: 242-254; discussion 254-245, 2014.
17. Kumar R, Nguyen HD, Ogren JA, Macey PM, Thompson PM, Fonarow GC, Hamilton MA, Harper RM, and Woo MA. Global and regional putamen volume loss in patients with heart failure. Eur J Heart Fail 13: 651-655, 2011.
18. Lopshire JC, Zhou X, Dusa C, Ueyama T, Rosenberger J, Courtney N, Ujhelyi M, Mullen T, Das M, and Zipes DP. Spinal cord stimulation improves ventricular function and reduces ventricular arrhythmias in a canine postinfarction heart failure model. Circulation 120: 286-294, 2009.
19. Lopshire JC and Zipes DP. Spinal cord stimulation for heart failure: preclinical studies to determine optimal stimulation parameters for clinical efficacy. J Cardiovasc Transl Res 7: 321-329, 2014.
20. McCreery DB, Agnew WF, Yuen TG, and Bullara LA. Comparison of neural damage induced by electrical stimulation with faradaic and capacitor electrodes. Ann Biomed Eng 16: 463-481, 1988.
21. Millar CK, Kralios FA, and Lux RL. Correlation between refractory periods and activation-recovery intervals from electrograms: effects of rate and adrenergic interventions. Circulation 72: 1372-1379, 1985.

22. Nakahara S, Vaseghi M, Ramirez RJ, Fonseca CG, Lai CK, Finn JP, Mahajan A, Boyle NG, and Shivkumar K. Characterization of myocardial scars: electrophysiological imaging correlates in a porcine infarct model. Heart Rhythm 8: 1060-1067, 2011.
23. Priori SG, Blomstrom-Lundqvist C, Mazzanti A, Blom N, Borggrefe M, Camm J, Elliott PM, Fitzsimons D, Hatala R, Hindricks G, Kirchhof P, Kjeldsen K, Kuck KH, Hernandez-Madrid A, Nikolaou N, Norekval TM, Spaulding C, and Van Veldhuisen DJ. 2015 ESC Guidelines for the management of patients with ventricular arrhythmias and the prevention of sudden cardiac death: The Task Force for the Management of Patients with Ventricular Arrhythmias and the Prevention of Sudden Cardiac Death of the European Society of Cardiology (ESC). Endorsed by: Association for European Paediatric and Congenital Cardiology (AEPC). Eur Heart J 36: 2793-2867, 2015.
24. Rajendran PS, Nakamura K, Ajijola OA, Vaseghi M, Armour JA, Ardell JL, and Shivkumar K. Myocardial infarction induces structural and functional remodelling of the intrinsic cardiac nervous system. J Physiol 594: 321-341, 2016.
25. Rosenbaum MS, Wilber DJ, Finkelstein D, Ruskin JN, and Garan H. Immediate reproducibility of electrically induced sustained monomorphic ventricular tachycardia before and during antiarrhythmic therapy. J Am Coll Cardiol 17: 133-138, 1991.
26. Schwartz PJ, Snebold NG, and Brown AM. Effects of unilateral cardiac sympathetic denervation on the ventricular fibrillation threshold. Am J Cardiol 37: 1034-1040, 1976.
27. Southerland EM, Gibbons DD, Smith SB, Sipe A, Williams CA, Beaumont E, Armour JA, Foreman RD, and Ardell JL. Activated cranial cervical cord neurons affect left ventricular infarct size and the potential for sudden cardiac death. Autonom neuroscience : basic & clinical 169: 34-42, 2012.
28. Southerland EM, Milhorn DM, Foreman RD, Linderoth B, DeJongste MJ, Armour JA, Subramanian V, Singh M, Singh K, and Ardell JL. Preemptive, but not reactive, spinal cord stimulation mitigates transient ischemia-induced myocardial infarction via cardiac adrenergic neurons. Am J Physiol Heart Circ Physiol 292: H311-317, 2007.
29. Tung R, Vaseghi M, Frankel DS, Vergara P, Di Biase L, Nagashima K, Yu R, Vangala S, Tseng CH, Choi EK, Khurshid S, Patel M, Mathuria N, Nakahara S, Tzou WS, Sauer WH, Vakil K, Tedrow U, Burkhardt JD, Tholakanahalli VN, Saliaris A, Dickfeld T, Weiss JP, Bunch TJ, Reddy M, Kanmanthareddy A, Callans DJ, Lakkireddy D, Natale A, Marchlinski F, Stevenson WG, Della Bella P, and Shivkumar K. Freedom from recurrent ventricular tachycardia after catheter ablation is associated with improved survival in

patients with structural heart disease: An International VT Ablation Center Collaborative Group study. Heart Rhythm 12: 1997-2007, 2015.

30. Vaseghi M, Gima J, Kanaan C, Ajijola OA, Marmureanu A, Mahajan A, and Shivkumar K. Cardiac sympathetic denervation in patients with refractory ventricular arrhythmias or electrical storm: intermediate and long-term follow-up. Heart Rhythm 11: 360-366, 2014.
31. Vaseghi M, Zhou W, Shi J, Ajijola OA, Hadaya J, Shivkumar K, and Mahajan A. Sympathetic innervation of the anterior left ventricular wall by the right and left stellate ganglia. Heart Rhythm 9: 1303-1309, 2012.
32. Vrabec T, Bhadra N, Acker G, Bhadra N, and Kilgore K. Continuous Direct Current Nerve Block Using Multi Contact High Capacitance Electrodes. IEEE Trans Neur Syst Rehab Eng, 2016 (epub).
33. Vrabec T, Bhadra N, Wainright J, Bhadra N, Franke M, and Kilgore K. Characterization of high capacitance electrodes for the application of direct current electrical nerve block. Med Biol Eng Comp 54: 191-203, 2016.
34. Wang S, Zhou X, Huang B, Wang Z, Liao K, Saren G, Lu Z, Chen M, Yu L, and Jiang H. Spinal cord stimulation protects against ventricular arrhythmias by suppressing left stellate ganglion neural activity in an acute myocardial infarction canine model. Heart Rhythm 12: 1628-1635, 2015.

CHAPTER 5

CONCLUSIONS/INTERPRETATION/FUTURE DIRECTIONS

CONCLUSIONS

The major findings of this dissertation are as follows: 1) VNS can mitigate remodeling of intrinsic cardiac neuronal function and myocardial hypertrophy associated with pressure overload, a model of heart failure with preserved ejection fraction (HFpEF); 2) in proof of concept studies, we demonstrated for the first time that either kilohertz high frequency alternating current (KHFAC) and charge-balanced direct current carousel block (CBDCC) can attenuate sympathetic drive to the heart in a normal anesthetized porcine model; and 3) CBDCC, even with unilateral application, decreases the ventricular arrhythmia (VT/VF) potential by 83% when applied acutely in the setting of chronic myocardial infarction (MI). These findings support our overall hypothesis that bioelectronic therapy can impact the abnormal central/peripheral autonomic balance that underlies cardiac disease. Furthermore, the data demonstrates the feasibility of using bioelectronic methodologies to control autonomic input into the heart. This thesis proposes a mechanism-based approach to cardiac therapy that marries the potential of bioelectronic therapy (reversible, on demand, scalable, etc.) with an intimate knowledge of cardiac neuraxis structure/function in a manner that addresses a significant unmet need for patients.

INTERPRETATION

Cardiac disease often involves central parasympathetic withdrawal and reflex-mediated sympathetic drive. While such neural reflex response results in acute compensatory benefits, long term maladaptive changes result from the altered autonomic tone with potential lethal consequences (6, 42). As such, having a detailed understanding of the structure/function of the cardiac neuraxis provides an opportunity to develop intelligent mechanism-based approaches to treat cardiac pathology that marries the benefits of bioelectronics (on-demand, reversible, scalable, etc.) while mitigating the off-target issues often associated with current standards of care (pharmacology and surgery). Specifically, by targeting the cardiac nervous system directly the evolution of cardiac pathology can be altered. This opens up a multitude of novel therapeutic opportunities for both arrhythmia management and the progression of heart failure.

Aberrant Central/Peripheral Nervous System Interactions Underlie Cardiac Disease

Physical cardiac injury (e.g. infarction, focal inflammation) results in scar formation on the heart and alterations in the network loops within the cardiac neuraxis (80, 99). Substrate level changes can result in electrophysiological changes that promote reentrant arrhythmias (5). Changes within the neuraxis can alter autonomic tone, favoring increased sympathetic drive and

reduced parasympathetic involvement (42, 57). This provides acute benefits, but chronically can be detrimental (57). Furthermore, the acute response mediates a state where there is continued abnormal afferent signaling, which is reflective of reactive and adaptive responses on the neuraxis to cardiac insult, neuronal excitability and network interconnectivity form the ICNS through to the insular cortex (17, 107). Increased sympathetic tone coupled with reduced parasympathetic tone can mediate cardiac arrhythmias and SCD by a number of different mechanisms: reducing ventricular refractory period; reducing VF threshold; and promoting triggered activity and automaticity (42).

Cardiac control by cortical and subcortical areas of the brain has been demonstrated clinically and preclinically (45, 74). Furthermore, these brain areas have also been implicated in cardiac arrhythmias (63). As such, it has been suggested that the efficacy of autonomic regulation therapy is due to reduction in conflicts between the different levels of the cardiac neuraxis (23, 58). The electrical stability seen in transplanted hearts supports the stabilizing role of the ICNS, in the absence of central drive (98).

Over the past few decades, there has been a growing appreciation for the role the ANS plays in arrhythmogenesis, as it has been demonstrated that disease-induced disruption of network loops at various levels of the cardiac neuraxis can have devastating consequences (4, 15, 21, 42, 44, 83, 84, 87, 88, 91, 105). In response to cardiac insult, maladaptive changes can occur on many different levels, including: alterations of efferent outputs to different cardiac regions (14, 57); and changes in intrinsic cardiac (40, 51) and extracardiac intrathoracic ganglia (4, 7, 14), and spinal and supraspinal reflex processing (35, 41, 65, 101, 107).

Alteration of Autonomic Imbalance = Therapeutic Approach

Modulation of Sympathetic Drive

Excessive sympathetic drive alters calcium dynamics and increases inotropy, driving increased myocardial oxygen demand (68, 102, 107), when coupled with pre-existing ischemic conditions can predispose the heart to lethal arrhythmias (64, 73). This is further exacerbated with abnormal cardiac structure, such as that found in ischemic/dilated/hypertrophic cardiomyopathies and arrhythmogenic right ventricular cardiomyopathy (38, 42). In patients post MI and those with congestive heart failure, high sympathetic activity is a negative prognostic indicator (29, 60, 62, 72). In long QT syndrome types 1 and 2, increased adrenergic drive enhances proarrhythmic potential (91).

Reduction of sympathetic drive with β-blockers has been the only effective pharmacological approach that can decrease mortality post MI or in chronic congestive HF (28,

52). However, these can also be pro-arrhythmic in the context of ischemia (76). Implantable cardioverter defibrillators (ICD) treat symptoms, but decrease quality of life, correlate with poor prognosis and increase mortality (69). Interventional procedures such as stellectomy (2, 86), thoracic epidural anesthesia (23), renal sympathetic denervation (24) and VNS (50) have come to the fore as means to reduce adrenergic drive in cardiac pathologies. These latter approaches are last line measures, when other standards of care have been exhausted. In this context, these patients have unmet medical needs that require new modalities that can demonstrate reversible, on demand, on target activity, while minimizing some of the downsides associated with the aforementioned approaches.

Bioelectronic Control of Sympathetic Drive The proof of concept studies with KHFAC and CBDCC are the first to demonstrate that bioelectronic block has the capacity to modulate efferent sympathetic drive to the heart. Furthermore, the CBDCC approach has addressed the onset sympatho-excitation observed in KHFAC, been efficacious in blocking sympathetic cardiac activity in a current-dependent manner and partial block could reduce the VT/VF potential by 83% in a porcine MI model. Furthermore, the reduction in arrhythmic potential is mediated by increasing the ventricular ERP, providing a more electrically stable substrate. This finding is particularly compelling, as it demonstrates that partial unilateral adrenergic block is sufficient to mitigate arrhythmias that may arise due to centrally-mediated sympathetic drive and can stabilize some of the autonomic imbalances/remodeling that have accumulated in response to myocardial infarction.

This has tremendous translational potential, as partial sympathetic block would permit basal efferent/afferent traffic while attenuating the hyperadrenergic drive that may potentiate cardiac arrhythmias in a highly proarrhythmic model. It should also be considered that the anti-arrhythmic effects of AMT were dramatic even when applied unilateral and to the right-sided sympathetic outflows. From a surgical perspective, since bilateral stellate stimulation is more effective in reducing the VT burden in patients with intractable VT, future studies should consider the efficacy of concurrent bilateral AMT.

Enhancement of Parasympathetic Influence

Under normal physiological conditions, parasympathetic activity reduces heart rate, inotropy and moderates calcium homeostasis. This activity is anti-arrhythmic as it can increase

the ventricular fibrillation threshold, which may be due to a nNOS/muscarinic receptor pathway (54, 71). Congestive HF patients with impaired vagal function have poor prognosis (62). Exercise can induce high vagal tone (22, 33), which is cardioprotective (30). On the other hand, vagal tone can be pro-arrhythmic in patients with SCN5A mutation causing LQT3 or Brugada Syndrome, though the exact mechanism has not been completely elucidated (91).

Parasympathetic activity mitigates sympathetic drive by inhibiting the adenylate cyclase-cyclic adenosine monophosphate (cAMP)-protein kinase A-L-type calcium current pathway. Modulation of these cellular pathways, through direct and indirect mechanisms, manifest as prolongation of action potential duration (APD), flattening of the electrical restitution curve, and reduction of spatial electrical heterogeneity (6, 70). Together, these effects will reduce the potential for aberrant conduction within the heart by altering myocyte function and electrical coupling. VNS exerts its anti-adrenergic effects by acting at the end-terminus (nerves to myocytes) and by neural network interactions mediated within the cardiac nervous system (43, 66, 77-79).

Sympathetic-Parasympathetic Interactions The intrinsic cardiac nervous system (ICNS) is primarily responsible for the coordination of regional cardiac indices (13). It consists of aggregates in ganglionated plexi composed of sensory (afferent), local circuit (LCN) and motor (adrenergic and cholinergic efferent) neurons that communicate with intrathoracic ganglia, all under the control of the central nervous system and circulating catecholamines (13). Major interactions between the sympathetic and parasympathetic nervous systems occur at the level of the ICNS and at the end termini of efferent projections to the heart (18, 43, 66, 77). The vagus innervates both ventricles extensively in large animals (10, 104), but sympathetic projections are more asymmetric (3, 11). This difference in innervation pattern between the sympathetic and parasympathetic efferent components may underscore some of the differential efficacy of right vs. left VNS on cardioneural remodeling in the pressure overload model (19). As mentioned previously, there is altered autonomic function in cardiac pathology due to remodeling of multiple levels of the cardiac neuraxis. In this context, this manifests itself as alterations in neurotransmitter interactions and synaptic processing at the level of the ICNS (20, 47-49). Reduction of sympathetic drive or enhancement of parasympathetic activity has the potential to stabilize cardiac electrophysiology.

Bioelectronic Control of the Parasympathetic Nervous System Vagal stimulation impacts multiple pathways: 1) afferent-mediated pathways (8, 103); 2) cardiac muscarinic M2 and M3

receptors and inhibition of pro-inflammatory cytokines (53, 95); and 3) NO signaling (81, 82). Vagal stimulation potentiates acetylcholine release by cholinergic postganglionic neurons that innervate the heart, mediating reductions in chronotropy, dromotropy and inotropy (68). In heart failure, abnormal alterations occur at multiple levels, from the cardiac myocardium to the cardiac neuraxis and neurohormonal control (6, 13, 34, 67, 99, 106, 107). Alterations in the cardiac neuronal hierarchy can manifest on a number of different areas. Altered intrathoracic reflex control that results from substrate and ganglion levels changes (1, 6, 12, 13, 26, 38, 42, 107). Compromised baroreflex function contributes to hyperdynamic sympathoexcitation (6, 38, 42, 107). Increased activity of skeletal muscle afferents often causes increased sympathetic activity and circulating levels of vasoactive hormones, mediating peripheral vasoconstriction, which would limit the ability to increase ventricular function (6, 31, 32, 46, 61, 94). Less well defined is the suggestion that chemoreflexes can be tonically activated in disease states that potentiates hyperdynamic adrenergic drive causing increased cardiac stress and arrhythmogenesis, among others (6). A common component to all these remodeled reflex control systems is disease induced alterations in afferent processing (101). Bioelectronic medicine has the potential to alter that afferent signaling and the neural network responses both afferent and efferent inputs (25).

Despite the increasing incidence of HFpEF, treatment options are ineffective, resulting in high all-causes mortality (90). With our data, we have demonstrated that chronic VNS therapy attenuates the negative effects of pressure overload on cardiac structure and function via direct targeting of intrinsic cardiac neurons and the neural-myocyte interface. The former can modify autonomic balance and mitigate the hyperadrenergic state induced by PO, whereas the latter induces a cardioprotective state, likely due to alterations in energetics (18, 19, 92, 93). This approach addresses a significant paucity of treatment options for HFpEF patients, in a multifactorial manner, which may be more efficacious than standard small molecule pharmacological approaches.

FUTURE DIRECTIONS

This dissertation addressed a number of questions regarding the feasibility of bioelectronic intervention in the sympathetic and parasympathetic systems, however, there are a number that remain. Addressing these questions, particularly with respect to managing sympathetic drive to the heart, will be critical to evolving these technologies to the patient. Future studies should address optimization of the electrode-nerve interface for chronic

implementation, evaluate whether duration of block affects basal cardiac parameters, miniaturization of power sources, duty cycle and degree of block, understanding degree of efferent/afferent pathways affected, unilateral vs. bilateral block, among many others.

Unilateral vs Bilateral Sympathetic Block It is unclear what impact bioelectronic sympathetic block has on the various levels of the cardiac neuraxis. Left CSD (LCSD), analogous to 100% duty cycle with complete block, has demonstrated potential for reducing arrhythmia burden (and shortening of the QTc interval in long QT syndrome) (89). This is most likely due to alterations in the autonomic tone in favor of parasympathetic drive. Long term, LCSD has proven to have diminished efficacy. This is most likely due to the possibility of contralateral remodeling (37) and anatomical variability (27, 100). The former has been shown in sheep with surgical resection of the left superior cervical ganglion (SCG) caused a compensatory 77% increase in right SCG size after 7 weeks, increasing to 215% by 12 weeks post-surgery (37). This data has driven studies evaluating bilateral CSD (BCSD) that suggest this may be a more amenable surgical anti-arrhythmic approach (2, 97). Future studies should consider the therapeutic efficacy of right vs left axonal modulation therapy and the potential cost-benefit of bilateral vs. unilateral therapy. It is likely that a hybrid approach may be required (KHFAC+transient DC) may be required if sympathetic control is required over prolonged periods of time.

Our acute data demonstrated that partial unilateral block is sufficient to have a strong anti-arrhythmic effect, however long term remodeling, as seen in surgical applications, may compromise that efficacy. However, if proven to be effective in longer term studies, this has profound implications for maintaining basal network activity, while mitigating the hyperadrenergic drive that is pro-arrhythmic – a situation that could be characterized as the “best of both worlds”.

Role of Afferent Pathways and Memory Engaging afferent pathways and memory may be advantageous in prolonging the beneficial effects of this type of therapy. For both disease and autonomic therapy, alterations of these pathways impact progression and therapeutic potential. In progressive cardiac disease, it has been demonstrated that the cardiac nervous system exhibits short-term memory (7, 16) and longer-term plasticity (42, 56, 101). For example, myocardial ischemia has been shown to affect afferents at multiple levels, impacting both peripheral and central reflex pathways (12, 65, 85, 96). Spinal cord stimulation (SCS) has been shown to affect autonomic reflexes at multiple levels of the cardiac neuroaxis to attenuate sympathetic reflex responses to stress, by altering neurotransmitter release/activity (35, 36) and

blunting reflex sympathoexcitation, as seen in transient cardiac ischemia (7, 59). Within the ICNS, SCS can blunt reflex responses to transient ischemic stress (16, 40), with the protective effects extending for up to 1 h post SCS intervention (16). This memory has profound clinical implications for disease management, as it suggests that intermittent application can be efficacious when the ANS is a willing dance partner (13, 39, 57). It remains to be determined if axonal modulation therapy exerts persistence or memory when evaluated in the context of direct control of the sympathetic (or parasympathetic) inputs to the heart and if cardiac disease alters these fundamental neural network responses.

Therapeutic Management of Heart Failure Preclinical data has demonstrated VNS efficacy in HF management, however clinical data has been less conclusive. Extended follow-up data from the ANTHEM-HF study demonstrated that: 1) both right and left VNS were feasible and safe for patients; 2) improvements in cardiac function and symptoms were seen at 6 months and maintained after 12 months of therapy (75). This study demonstrated greater therapeutic efficacy than either the INOVATE-HF or the NECTAR-HF studies. The concept of the "neural fulcrum" appears to be an important factor in clinical efficacy, as balance between afferent and efferent components of the ANS may allow effective VNS-evoked changes, without engaging reactive changes that occur with high currents and/or frequencies (9, 55). Particularly in HFpEF, the multifactorial therapeutic approach offered by VNS may offer significant upside to the current standard of care, which is ineffective.

PERSPECTIVES AND SIGNIFICANCE

Current approaches for managing cardiac pathology mainly relies on pharmacology or surgical interventions, which can be problematic or ineffective. The data within this thesis provides validation for a logical mechanism-based approach to cardiac therapy that combines the potential of bioelectronic therapy with a detailed knowledge of cardiac neuraxis structure/function, addressing a significant unmet need for patients. If validated in the clinic, these approaches open up a multitude of novel therapeutic opportunities for managing both arrhythmia burden and the progression of heart failure. The end result, of course, is the potential benefit to the patient, including mitigation of symptoms and improvement in quality/duration of life.

REFERENCES

1. Ahonen A, Harkonen M, Juntunen J, Kormano M, and Penttila A. Effects of myocardial infarction on adrenergic nerves of the rat heart muscle, a histochemical study. Acta Physiol Scand 93: 336-344, 1975.
2. Ajijola OA, Lellouche N, Bourke T, Tung R, Ahn S, Mahajan A, and Shivkumar K. Bilateral cardiac sympathetic denervation for the management of electrical storm. J Am Coll Cardiol 59: 91-92, 2012.
3. Ajijola OA, Vaseghi M, Zhou W, Yamakawa K, Benharash P, Hadaya J, Lux RL, Mahajan A, and Shivkumar K. Functional differences between junctional and extrajunctional adrenergic receptor activation in mammalian ventricle. Am J Physiol Heart Circ Physiol 304: H579-588, 2013.
4. Ajijola OA, Yagishita D, Reddy NK, Yamakawa K, Vaseghi M, Downs AM, Hoover DB, Ardell JL, and Shivkumar K. Remodeling of stellate ganglion neurons after spatially targeted myocardial infarction: Neuropeptide and morphologic changes. Heart Rhythm 12: 1027-1035, 2015.
5. Antzelevitch C and Burashnikov A. Overview of Basic Mechanisms of Cardiac Arrhythmia. Card Electrophysiol Clin 3: 23-45, 2011.
6. Ardell JL, Andresen MC, Armour JA, Billman GE, Chen PS, Foreman RD, Herring N, O'Leary DS, Sabbah HN, Schultz HD, Sunagawa K, and Zucker IH. Translational neurocardiology: preclinical models and cardioneural integrative aspects. J Physiol 594: 3877-3909, 2016.
7. Ardell JL, Cardinal R, Vermeulen M, and Armour JA. Dorsal spinal cord stimulation obtunds the capacity of intrathoracic extracardiac neurons to transduce myocardial ischemia. Am J Physiol Regul Integr Comp Physiol 297: R470-477, 2009.
8. Ardell JL, Ragendran PS, Nier HA, KenKnight BH, and Armour JA. Central-Peripheral Neural Network Interactions Evoked by Vagus Nerve Stimulation: Functional Consequences on Control of Cardiac Function. Am J Physiol Heart Circ Physiol: ajpheart.00557.02015, 2015.
9. Ardell JL, Rajendran PS, Nier HA, KenKnight BH, and Armour JA. Central-peripheral neural network interactions evoked by vagus nerve stimulation: functional consequences on control of cardiac function. Am J Physiol Heart Circ Physiol 309: H1740-1752, 2015.
10. Ardell JL and Randall WC. Selective vagal innervation of sinoatrial and atrioventricular nodes in canine heart. Am J Physiol 251: H764-773, 1986.

11. Ardell JL, Randall WC, Cannon WJ, Schmacht DC, and Tasdemiroglu E. Differential sympathetic regulation of automatic, conductile, and contractile tissue in dog heart. Am J Physiol 255: H1050-1059, 1988.
12. Armour JA. Myocardial ischaemia and the cardiac nervous system. Cardiovasc Res 41: 41-54, 1999.
13. Armour JA. Potential clinical relevance of the 'little brain' on the mammalian heart. Exp Physiol 93: 165-176, 2008.
14. Armour JA, Collier K, Kember G, and Ardell JL. Differential selectivity of cardiac neurons in separate intrathoracic autonomic ganglia. Am J Physiol 274: R939-949, 1998.
15. Armour JA, Hageman GR, and Randall WC. Arrhythmias induced by local cardiac nerve stimulation. Am J Physiol 223: 1068-1075, 1972.
16. Armour JA, Linderoth B, Arora RC, DeJongste MJ, Ardell JL, Kingma JG, Hill M, and Foreman RD. Long-term modulation of the intrinsic cardiac nervous system by spinal cord neurons in normal and ischaemic hearts. Auton Neurosci 95: 71-79, 2002.
17. Beaumont E, Salavatian S, Southerland EM, Vinet A, Jacquemet V, Armour JA, and Ardell JL. Network interactions within the canine intrinsic cardiac nervous system: implications for reflex control of regional cardiac function. J Physiol 591: 4515-4533, 2013.
18. Beaumont E, Southerland EM, Hardwick JC, Wright GL, Ryan S, Li Y, KenKnight BH, Armour JA, and Ardell JL. Vagus nerve stimulation mitigates intrinsic cardiac neuronal and adverse myocyte remodeling postmyocardial infarction. Am J Physiol Heart Circ Physiol 309: H1198-1206, 2015.
19. Beaumont E, Wright GL, Southerland EM, Li Y, Chui R, KenKnight BH, Armour JA, and Ardell JL. Vagus nerve stimulation mitigates intrinsic cardiac neuronal remodeling and cardiac hypertrophy induced by chronic pressure overload in guinea pig. Am J Physiol Heart Circ Physiol 310: H1349-1359, 2016.
20. Bibevski S and Dunlap ME. Evidence for impaired vagus nerve activity in heart failure. Heart Fail Rev 16: 129-135, 2011.
21. Billman GE. A comprehensive review and analysis of 25 years of data from an in vivo canine model of sudden cardiac death: implications for future anti-arrhythmic drug development. Pharmacol Ther 111: 808-835, 2006.
22. Billman GE. Cardiac autonomic neural remodeling and susceptibility to sudden cardiac death: effect of endurance exercise training. Am J Physiol Heart Circ Physiol 297: H1171-1193, 2009.

23. Bourke T, Vaseghi M, Michowitz Y, Sankhla V, Shah M, Swapna N, Boyle NG, Mahajan A, Narasimhan C, Lokhandwala Y, and Shivkumar K. Neuraxial modulation for refractory ventricular arrhythmias: value of thoracic epidural anesthesia and surgical left cardiac sympathetic denervation. Circulation 121: 2255-2262, 2010.
24. Bradfield JS, Vaseghi M, and Shivkumar K. Renal denervation for refractory ventricular arrhythmias. Trends Cardiovasc Med 24: 206-213, 2014.
25. Buckley U, Shivkumar K, and Ardell JL. Autonomic Regulation Therapy in Heart Failure. Curr Heart Fail Rep 12: 284-293, 2015.
26. Chen PS, Chen LS, Cao JM, Sharifi B, Karagueuzian HS, and Fishbein MC. Sympathetic nerve sprouting, electrical remodeling and the mechanisms of sudden cardiac death. Cardiovasc Res 50: 409-416, 2001.
27. Chung IH, Oh CS, Koh KS, Kim HJ, Paik HC, and Lee DY. Anatomic variations of the T2 nerve root (including the nerve of Kuntz) and their implications for sympathectomy. J Thorac Cardiovasc Surg 123: 498-501, 2002.
28. CIBIS-II. The Cardiac Insufficiency Bisoprolol Study II (CIBIS-II): a randomised trial. Lancet 353: 9-13, 1999.
29. Cohn JN, Levine TB, Olivari MT, Garberg V, Lura D, Francis GS, Simon AB, and Rector T. Plasma norepinephrine as a guide to prognosis in patients with chronic congestive heart failure. N Engl J Med 311: 819-823, 1984.
30. Cole CR, Blackstone EH, Pashkow FJ, Snader CE, and Lauer MS. Heart-rate recovery immediately after exercise as a predictor of mortality. N Engl J Med 341: 1351-1357, 1999.
31. Coutsos M, Sala-Mercado JA, Ichinose M, Li Z, Dawe EJ, and O'Leary DS. Muscle metaboreflex-induced coronary vasoconstriction limits ventricular contractility during dynamic exercise in heart failure. Am J Physiol Heart Circ Physiol 304: H1029-1037, 2013.
32. Crisafulli A, Salis E, Tocco F, Melis F, Milia R, Pittau G, Caria MA, Solinas R, Meloni L, Pagliaro P, and Concu A. Impaired central hemodynamic response and exaggerated vasoconstriction during muscle metaboreflex activation in heart failure patients. Am J Physiol Heart Circ Physiol 292: H2988-2996, 2007.
33. Danson EJ and Paterson DJ. Enhanced neuronal nitric oxide synthase expression is central to cardiac vagal phenotype in exercise-trained mice. J Physiol 546: 225-232, 2003.

34. Dell'Italia LJ. Translational success stories: angiotensin receptor 1 antagonists in heart failure. Circ Res 109: 437-452, 2011.
35. Ding X, Ardell JL, Hua F, McAuley RJ, Sutherly K, Daniel JJ, and Williams CA. Modulation of cardiac ischemia-sensitive afferent neuron signaling by preemptive C2 spinal cord stimulation: effect on substance P release from rat spinal cord. Am J Physiol Regul Integr Comp Physiol 294: R93-101, 2008.
36. Ding X, Hua F, Sutherly K, Ardell JL, and Williams CA. C2 spinal cord stimulation induces dynorphin release from rat T4 spinal cord: potential modulation of myocardial ischemia-sensitive neurons. Am J Physiol Regul Integr Comp Physiol 295: R1519-1528, 2008.
37. Fioretto ET, Rahal SC, Borges AS, Mayhew TM, Nyengaard JR, Marcondes JS, Balieiro JC, Teixeira CR, de Melo MP, Ladd FV, Ladd AA, de Lima AR, da Silva AA, and Coppi AA. Hypertrophy and neuron loss: structural changes in sheep SCG induced by unilateral sympathectomy. Int J Dev Neurosci 29: 475-481, 2011.
38. Florea VG and Cohn JN. The autonomic nervous system and heart failure. Circ Res 114: 1815-1826, 2014.
39. Foreman RD and Linderoth B. Neural mechanisms of spinal cord stimulation. Int Rev Neurobiol 107: 87-119, 2012.
40. Foreman RD, Linderoth B, Ardell JL, Barron KW, Chandler MJ, Hull SS, Jr., TerHorst GJ, DeJongste MJ, and Armour JA. Modulation of intrinsic cardiac neurons by spinal cord stimulation: implications for its therapeutic use in angina pectoris. Cardiovasc Res 47: 367-375, 2000.
41. Fu LW and Longhurst JC. Regulation of cardiac afferent excitability in ischemia. Handb Exp Pharmacol: 185-225, 2009.
42. Fukuda K, Kanazawa H, Aizawa Y, Ardell JL, and Shivkumar K. Cardiac innervation and sudden cardiac death. Circ Res 116: 2005-2019, 2015.
43. Furukawa Y, Hoyano Y, and Chiba S. Parasympathetic inhibition of sympathetic effects on sinus rate in anesthetized dogs. Am J Physiol 271: H44-50, 1996.
44. Gelband H, Rosen MR, Myerburg RJ, Bush HL, Bassett AL, and Hoffman BF. Restorative effect of epinephrine on the electrophysiologic properties of depressed human atrial tissue. J Electrocardiol 10: 313-320, 1977.
45. Gray MA, Taggart P, Sutton PM, Groves D, Holdright DR, Bradbury D, Brull D, and Critchley HD. A cortical potential reflecting cardiac function. Proc Natl Acad Sci U S A 104: 6818-6823, 2007.

46. Hammond RL, Augustyniak RA, Rossi NF, Churchill PC, Lapanowski K, and O'Leary DS. Heart failure alters the strength and mechanisms of the muscle metaboreflex. Am J Physiol Heart Circ Physiol 278: H818-828, 2000.
47. Hardwick JC, Baran CN, Southerland EM, and Ardell JL. Remodeling of the guinea pig intrinsic cardiac plexus with chronic pressure overload. Am J Physiol Regul Integr Comp Physiol 297: R859-866, 2009.
48. Hardwick JC, Ryan SE, Powers EN, Southerland EM, and Ardell JL. Angiotensin receptors alter myocardial infarction-induced remodeling of the guinea pig cardiac plexus. Am J Physiol Regul Integr Comp Physiol 309: R179-188, 2015.
49. Hardwick JC, Southerland EM, Girasole AE, Ryan SE, Negrotto S, and Ardell JL. Remodeling of intrinsic cardiac neurons: effects of β-adrenergic receptor blockade in guinea pig models of chronic heart disease. Am J Physiol Regul Integr Comp Physiol 303: R950-958, 2012.
50. Huang J, Qian J, Yao W, Wang N, Zhang Z, Cao C, and Song B. Vagus nerve stimulation reverses ventricular electrophysiological changes induced by hypersympathetic nerve activity. Exp Physiol 100: 239-248, 2015.
51. Huang MH, Ardell JL, Hanna BD, Wolf SG, and Armour JA. Effects of transient coronary artery occlusion on canine intrinsic cardiac neuronal activity. Integr Physiol Behav Sci 28: 5-21, 1993.
52. ISIS-1. Randomised trial of intravenous atenolol among 16 027 cases of suspected acute myocardial infarction: ISIS-1. First International Study of Infarct Survival Collaborative Group. Lancet 2: 57-66, 1986.
53. Janig W. Sympathetic nervous system and inflammation: a conceptual view. Auton Neurosci 182: 4-14, 2014.
54. Kalla M, Chotalia M, Coughlan C, Hao G, Crabtree MJ, Tomek J, Bub G, Paterson DJ, and Herring N. Protection against ventricular fibrillation via cholinergic receptor stimulation and the generation of nitric oxide. J Physiol 594: 3981-3992, 2016.
55. Kember G, Ardell JL, Armour JA, and Zamir M. Vagal nerve stimulation therapy: what is being stimulated? PLoS One 9: e114498, 2014.
56. Kember G, Armour JA, and Zamir M. Dynamic neural networking as a basis for plasticity in the control of heart rate. J Theor Biol 317: 39-46, 2013.
57. Kember G, Armour JA, and Zamir M. Neural control hierarchy of the heart has not evolved to deal with myocardial ischemia. Physiol Genomics 45: 638-644, 2013.

58. Khalsa SS, Shahabi L, Ajijola OA, Bystritsky A, Naliboff BD, and Shivkumar K. Synergistic application of cardiac sympathetic decentralization and comprehensive psychiatric treatment in the management of anxiety and electrical storm. Front Integr Neurosci 7: 98, 2014.
59. Kingma JG, Linderoth B, Ardell JL, Armour JA, DeJongste MJ, and Foreman RD. Neuromodulation therapy does not influence blood flow distribution or left-ventricular dynamics during acute myocardial ischemia. Auton Neurosci 91: 47-54, 2001.
60. Kleiger RE, Miller JP, Bigger JT, Jr., and Moss AJ. Decreased heart rate variability and its association with increased mortality after acute myocardial infarction. Am J Cardiol 59: 256-262, 1987.
61. Koba S, Xing J, Sinoway LI, and Li J. Sympathetic nerve responses to muscle contraction and stretch in ischemic heart failure. Am J Physiol Heart Circ Physiol 294: H311-321, 2008.
62. La Rovere MT, Bigger JT, Jr., Marcus FI, Mortara A, and Schwartz PJ. Baroreflex sensitivity and heart-rate variability in prediction of total cardiac mortality after myocardial infarction. ATRAMI (Autonomic Tone and Reflexes After Myocardial Infarction) Investigators. Lancet 351: 478-484, 1998.
63. Laowattana S, Zeger SL, Lima JA, Goodman SN, Wittstein IS, and Oppenheimer SM. Left insular stroke is associated with adverse cardiac outcome. Neurology 66: 477-483; discussion 463, 2006.
64. Lubbe WF, Podzuweit T, and Opie LH. Potential arrhythmogenic role of cyclic adenosine monophosphate (AMP) and cytosolic calcium overload: implications for prophylactic effects of beta-blockers in myocardial infarction and proarrhythmic effects of phosphodiesterase inhibitors. J Am Coll Cardiol 19: 1622-1633, 1992.
65. Malliani A and Montano N. Emerging excitatory role of cardiovascular sympathetic afferents in pathophysiological conditions. Hypertension 39: 63-68, 2002.
66. McGuirt AS, Schmacht DC, and Ardell JL. Autonomic interactions for control of atrial rate are maintained after SA nodal parasympathectomy. Am J Physiol 272: H2525-2533, 1997.
67. Mill JG, Stefanon I, dos Santos L, and Baldo MP. Remodeling in the ischemic heart: the stepwise progression for heart failure. Braz J Med Biol Res 44: 890-898, 2011.
68. MN L and PJ M. Neural control of the heart. Bethesda, MA: The American Physiological Society 1979.

69. Moss AJ, Schuger C, Beck CA, Brown MW, Cannom DS, Daubert JP, Estes NA, 3rd, Greenberg H, Hall WJ, Huang DT, Kautzner J, Klein H, McNitt S, Olshansky B, Shoda M, Wilber D, and Zareba W. Reduction in inappropriate therapy and mortality through ICD programming. N Engl J Med 367: 2275-2283, 2012.
70. Ng GA, Brack KE, and Coote JH. Effects of direct sympathetic and vagus nerve stimulation on the physiology of the whole heart--a novel model of isolated Langendorff perfused rabbit heart with intact dual autonomic innervation. Exp Physiol 86: 319-329, 2001.
71. Ng GA, Brack KE, Patel VH, and Coote JH. Autonomic modulation of electrical restitution, alternans and ventricular fibrillation initiation in the isolated heart. Cardiovasc Res 73: 750-760, 2007.
72. Nolan J, Batin PD, Andrews R, Lindsay SJ, Brooksby P, Mullen M, Baig W, Flapan AD, Cowley A, Prescott RJ, Neilson JM, and Fox KA. Prospective study of heart rate variability and mortality in chronic heart failure: results of the United Kingdom heart failure evaluation and assessment of risk trial (UK-heart). Circulation 98: 1510-1516, 1998.
73. Opie LH and Clusin WT. Cellular mechanism for ischemic ventricular arrhythmias. Annu Rev Med 41: 231-238, 1990.
74. Oppenheimer SM and Cechetto DF. Cardiac chronotropic organization of the rat insular cortex. Brain Res 533: 66-72, 1990.
75. Premchand RK, Sharma K, Mittal S, Monteiro R, Dixit S, Libbus I, DiCarlo LA, Ardell JL, Rector TS, Amurthur B, KenKnight BH, and Anand IS. Extended Follow-Up of Patients With Heart Failure Receiving Autonomic Regulation Therapy in the ANTHEM-HF Study. J Card Fail 22: 639-642, 2016.
76. Priori SG, Blomstrom-Lundqvist C, Mazzanti A, Blom N, Borggrefe M, Camm J, Elliott PM, Fitzsimons D, Hatala R, Hindricks G, Kirchhof P, Kjeldsen K, Kuck KH, Hernandez-Madrid A, Nikolaou N, Norekval TM, Spaulding C, and Van Veldhuisen DJ. 2015 ESC Guidelines for the management of patients with ventricular arrhythmias and the prevention of sudden cardiac death: The Task Force for the Management of Patients with Ventricular Arrhythmias and the Prevention of Sudden Cardiac Death of the European Society of Cardiology (ESC)Endorsed by: Association for European Paediatric and Congenital Cardiology (AEPC). Europace 17: 1601-1687, 2015.

77. Randall DC, Brown DR, McGuirt AS, Thompson GW, Armour JA, and Ardell JL. Interactions within the intrinsic cardiac nervous system contribute to chronotropic regulation. Am J Physiol Regul Integr Comp Physiol 285: R1066-1075, 2003.
78. Randall WC, Ardell JL, Calderwood D, Milosavljevic M, and Goyal SC. Parasympathetic ganglia innervating the canine atrioventricular nodal region. J Auton Nerv Syst 16: 311-323, 1986.
79. Randall WC, Milosavljevic M, Wurster RD, Geis GS, and Ardell JL. Selective vagal innervation of the heart. Ann Clin Lab Sci 16: 198-208, 1986.
80. Rubart M and Zipes DP. Mechanisms of sudden cardiac death. J Clin Invest 115: 2305-2315, 2005.
81. Sabbah HN. Electrical vagus nerve stimulation for the treatment of chronic heart failure. Cleve Clin J Med 78 Suppl 1: S24-29, 2011.
82. Sabbah HN, Ilsar I, Zaretsky A, Rastogi S, Wang M, and Gupta RC. Vagus nerve stimulation in experimental heart failure. Heart Fail Rev 16: 171-178, 2011.
83. Scherlag BJ, Patterson E, and Po SS. The neural basis of atrial fibrillation. J Electrocardiol 39: S180-183, 2006.
84. Scherlag BJ and Po S. The intrinsic cardiac nervous system and atrial fibrillation. Curr Opin Cardiol 21: 51-54, 2006.
85. Schultz HD and Ustinova EE. Cardiac vagal afferent stimulation by free radicals during ischaemia and reperfusion. Clin Exp Pharmacol Physiol 23: 700-708, 1996.
86. Schwartz PJ. Cardiac sympathetic denervation to prevent life-threatening arrhythmias. Nat Rev Cardiol 11: 346-353, 2014.
87. Schwartz PJ. QT prolongation, sudden death, and sympathetic imbalance: the pendulum swings. J Cardiovasc Electrophysiol 12: 1074-1077, 2001.
88. Schwartz PJ, Billman GE, and Stone HL. Autonomic mechanisms in ventricular fibrillation induced by myocardial ischemia during exercise in dogs with healed myocardial infarction. An experimental preparation for sudden cardiac death. Circulation 69: 790-800, 1984.
89. Schwartz PJ, Priori SG, Cerrone M, Spazzolini C, Odero A, Napolitano C, Bloise R, De Ferrari GM, Klersy C, Moss AJ, Zareba W, Robinson JL, Hall WJ, Brink PA, Toivonen L, Epstein AE, Li C, and Hu D. Left cardiac sympathetic denervation in the management of high-risk patients affected by the long-QT syndrome. Circulation 109: 1826-1833, 2004.
90. Shah SJ and Gheorghiade M. Heart failure with preserved ejection fraction: treat now by treating comorbidities. Jama 300: 431-433, 2008.

91. Shen MJ and Zipes DP. Role of the autonomic nervous system in modulating cardiac arrhythmias. Circ Res 114: 1004-1021, 2014.
92. Shinlapawittayatorn K, Chinda K, Palee S, Surinkaew S, Kumfu S, Kumphune S, Chattipakorn S, KenKnight BH, and Chattipakorn N. Vagus nerve stimulation initiated late during ischemia, but not reperfusion, exerts cardioprotection via amelioration of cardiac mitochondrial dysfunction. Heart Rhythm 11: 2278-2287, 2014.
93. Shinlapawittayatorn K, Chinda K, Palee S, Surinkaew S, Thunsiri K, Weerateerangkul P, Chattipakorn S, KenKnight BH, and Chattipakorn N. Low-amplitude, left vagus nerve stimulation significantly attenuates ventricular dysfunction and infarct size through prevention of mitochondrial dysfunction during acute ischemia-reperfusion injury. Heart Rhythm 10: 1700-1707, 2013.
94. Smith SA, Mammen PP, Mitchell JH, and Garry MG. Role of the exercise pressor reflex in rats with dilated cardiomyopathy. Circulation 108: 1126-1132, 2003.
95. Tracey KJ. Physiology and immunology of the cholinergic antiinflammatory pathway. J Clin Invest 117: 289-296, 2007.
96. Ustinova EE and Schultz HD. Activation of cardiac vagal afferents in ischemia and reperfusion. Prostaglandins versus oxygen-derived free radicals. Circ Res 74: 904-911, 1994.
97. Vaseghi M, Gima J, Kanaan C, Ajijola OA, Marmureanu A, Mahajan A, and Shivkumar K. Cardiac sympathetic denervation in patients with refractory ventricular arrhythmias or electrical storm: intermediate and long-term follow-up. Heart Rhythm 11: 360-366, 2014.
98. Vaseghi M, Lellouche N, Ritter H, Fonarow GC, Patel JK, Moriguchi J, Fishbein MC, Kobashigawa JA, and Shivkumar K. Mode and mechanisms of death after orthotopic heart transplantation. Heart Rhythm 6: 503-509, 2009.
99. Vaseghi M and Shivkumar K. The role of the autonomic nervous system in sudden cardiac death. Prog Cardiovasc Dis 50: 404-419, 2008.
100. W J. The Integrative Action of the Autonomic Nervous System: Neurobiology of Homeostasis New York: Cambridge University Press, 2006.
101. Wang HJ, Wang W, Cornish KG, Rozanski GJ, and Zucker IH. Cardiac sympathetic afferent denervation attenuates cardiac remodeling and improves cardiovascular dysfunction in rats with heart failure. Hypertension 64: 745-755, 2014.
102. WC R. Efferent sympathetic innervation of the heart. In: Neurocardiology, edited by JA A and JL A. New York: Oxford University Press, 1994, p. 77-94.

103. Yamakawa K, Howard-Quijano K, Zhou W, Rajendran P, Yagishita D, Vaseghi M, Ajijola OA, Armour JA, Shivkumar K, Ardell JL, and Mahajan A. Central vs. peripheral neuraxial sympathetic control of porcine ventricular electrophysiology. Am J Physiol Regul Integr Comp Physiol 310: R414-421, 2016.
104. Yamakawa K, So EL, Rajendran PS, Hoang JD, Makkar N, Mahajan A, Shivkumar K, and Vaseghi M. Electrophysiological effects of right and left vagal nerve stimulation on the ventricular myocardium. Am J Physiol Heart Circ Physiol 307: H722-731, 2014.
105. Zipes DP. Antiarrhythmic therapy in 2014: Contemporary approaches to treating arrhythmias. Nat Rev Cardiol 12: 68-69, 2015.
106. Zipes DP, Camm AJ, Borggrefe M, Buxton AE, Chaitman B, Fromer M, Gregoratos G, Klein G, Moss AJ, Myerburg RJ, Priori SG, Quinones MA, Roden DM, Silka MJ, Tracy C, Smith SC, Jr., Jacobs AK, Adams CD, Antman EM, Anderson JL, Hunt SA, Halperin JL, Nishimura R, Ornato JP, Page RL, Riegel B, Blanc JJ, Budaj A, Dean V, Deckers JW, Despres C, Dickstein K, Lekakis J, McGregor K, Metra M, Morais J, Osterspey A, Tamargo JL, and Zamorano JL. ACC/AHA/ESC 2006 guidelines for management of patients with ventricular arrhythmias and the prevention of sudden cardiac death: a report of the American College of Cardiology/American Heart Association Task Force and the European Society of Cardiology Committee for Practice Guidelines (Writing Committee to Develop Guidelines for Management of Patients With Ventricular Arrhythmias and the Prevention of Sudden Cardiac Death). J Am Coll Cardiol 48: e247-346, 2006.
107. Zucker IH, Patel KP, and Schultz HD. Neurohumoral stimulation. Heart Fail Clin 8: 87-99, 2012.